Discontinuous Transition to Superconducting Phase

Takumi Sato

Department of Applied Physics, Hokkaido University

February 20, 2024

Acknowledgments

Firstly, I would like to express my sincere gratitude to my supervisor Associate Prof. Yasuhiro Asano for the continuous support of my Ph.D. study. His guidance helped me in all the time and his words always encouraged me. I would like to thank Prof. Kousuke Yakubo and Associate Prof. Hideaki Obuse for giving me useful advice on my research and my presentations.

I am grateful to Dr. Shingo Kobayashi, Dr. Tetsuro Habe, Dr. Shu Suzuki, and Dr. Satoshi Ikegaya for useful discussions on the physics of superconductivity and for giving me useful advice to get a job. I also thank Dr. Dakyeong Kim and Akihiro Sasaki for daily discussions on physics.

Finally, I would like to express my appreciation for my parents, my sister, and my grandparents. Their kindness and warmness always helped me. I could finish my research on their continuous cooperation.

Contents

Chapter 1

General introduction

Superconductivity has attracted much attention of many researchers due to its anomalous electromagnetic properties and has continued to be a central topic in condenced matter physics from its discovery [1]. This phenomenon is explained well by BCS theory [2] and arises from the condensation of Cooper pairs on the order of Avogadro number $N_{\mathrm{A}} \sim 10^{23}$. A number of Cooper pairs composed of two electrons on the Fermi level condense in the same quantum state by aligning their phases and the energy gap in the single-particle spectrum opens near the Fermi level. As a result, the superconductors gain the condensation energy and acquire the phase coherence. When a weak orbital magnetic field is applied to a superconductor, it can not penetrate the object. Since the magnetic fields are perturbations that disturb the phase coherence, the superconductors gain a larger energy by expelling the magnetic fields rather than attracting them. The phenomenon known as *Meissner-Ochsenfeld effect* [3] is more fundamental than the disappearance of electric resistance. It has been widely accepted that Cooper pairs have the diamagnetic property and stabilize the superconducting states.

Electrons have internal degrees of freedom such as spin σ and spatial coordinate $\boldsymbol{r}$. Therefore, Cooper pairs can be classified by its symmetry. Cooper pairs composed of spin-1/2 electrons are represented by the pairing correlation function $\mathcal{F}_{\sigma,\sigma'}(\boldsymbol{r},\boldsymbol{r}')$ and are classified into two symmetry classes: spin-singlet even-parity symmetry class and spin-triplet odd-parity symmetry class. The former is represented by an antisymmetric function under the permutation of the spin degree of freedom and realized in superconductivity in most metals and cuprates [4]. On the other hand, the latter is represented by a symmetric function under the above permutation and realized in heavy electron systems [5–8], superfluid ^{3}He [9], and so on. Since physical phenomena strongly depend on the symmetry in general, understanding how the observable depends on the symmetry and why it does so remains a challenge in theoretical physics.

In 1974, Berezinskii proposed a new symmetry class of Cooper pair, *odd-frequency Cooper pair*, to explain the symmetry of the order realized in superfluid ^{3}He [10]. The concept is based on the idea of focusing on the relative time of two electrons forming a Cooper pair. We need to add the time degree of freedom τ to the correlation function $\mathcal{F}_{\sigma,\sigma'}(\boldsymbol{r},\tau;\boldsymbol{r}',\tau')$ to describe the new pairs. Compared with odd-frequency Cooper pairs, conventional spin-singlet even-parity pairs and spin-triplet odd-parity pairs are collectively referred to as even-frequency Cooper pairs. Although the proposal itself ended in a failure, this new concept has sparked many theoretical and experimental studies as a result [11–15]. It has been understood that odd-frequency Cooper pairs appear in local region such as at a vortex core [16], in the vicinity of a magnetic impurity [17, 18], and at the surface of a topologically nontrivial superconductor [19, 20]. Important and curious property of odd-frequency Cooper pairs is *paramagnetism* [21]. So far, phenomena in inhomogeneous systems, such as long-range proximity effects in superconductor/ferromagnet junctions [22] and anomalous proximity effects in normal metal/superconductor junctions [19, 23], have been explained well by the concept of odd-frequency Cooper pair. The reason for the dramatic change in local physical phenomena is commonly attributed to the paramagnetic property of odd-frequency Cooper pairs. The concept of odd-frequency Cooper pair is still being used to gain a unified understanding of the property of various physical phenomena in inhomogeneous superconducting systems. In other words, the formation of odd-frequency Cooper pairs is a usuful picture for understanding superconductivity in a rational way.

It has been considered that uniform odd-frequency Cooper pairs are not able to exist in the bulk since they destabilize superconductivity by disturbing phase coherence due to the paramagnetic property [24–26]. In fact, superconductivity with odd-frequency pairing order has never been reported experimentally although there are a number of theoretical studies [27–46]. On the other hand, it has been shown that uniform odd-frequency Cooper pairs are able to exist in systems where electrons near the Fermi level have large internal degrees of freedom such as band, orbital, and sublattice [47, 48]. Many superconductors such as MgB_2 [49–51], heavy fermion compounds [52, 53] iron compounds [54, 55], and $Cu_xBi_2Se_3$ [56, 57] are regarded as "multiband/orbital superconductors". Recently, the condition for a superconducting state that contains spatially uniform odd-frequency Cooper pairs has been presented [14, 58, 59]. In these superconducting states, odd-frequency Cooper pairs exist as subdominant pairing correlations apart from even-frequency Cooper pairs which are linked to the superconducting order parameter. In fact, Bogoliubov quasiparticles [60, 61] forming the Fermi surfaces, which is known as one of the characteristics of superconductors with large internal degrees of freedom [62–64] and odd-frequency Cooper pairs coexist [65, 66]. It is also shown that

the magnetic response of such uniform odd-frequency Cooper pairs is paramagnetic and then they suppress the superconducting transition temperature T_c [67]. However, this fact has made its characteristic physical phenomena extremely obscure. Only when the amplitude of the odd-frequency pairs become dominant compared with that of even-frequency pairs, physical phenomena unique to odd-frequency Cooper pairs are expected to occur. Unfortunately, odd-frequency Cooper pairs, which are paramagnetic, are thermodynamically unstable and cannot be dominant pair correlations. Therefore, the effect of uniform odd-frequency Cooper pairs on physical phenomena was unclear. The purpose of this study is to fill the gaps in knowledge on the physical phenomena unique to uniform odd-frequency Cooper pairs.

In this thesis, we focus on the stability of the multiband/orbital superconductivity against thermal fluctuations and disorder, which has been known to exhibit anomalous characteristics: discontinuous transition to the superconducting phase and suppression of T_c due to nonmagnetic impurities. Even seemingly obvious properties for most superconductors such as the second-order transition and the robustness of s-wave superconducting order against disorder [68, 69] do not hold true in multiband/orbital systems [70, 71]. Unfortunately, there had been no comprehensive understandings of these anomalous phenomena. We show that the paramagnetic odd-frequency Cooper pairs play a key role to understand the underlying physics. We expand the Ginzburg-Landau (GL) free energy in a multiband/orbital superconductor by using the anomalous Green's function and discuss the relationships between the existence of the uniform odd-frequency Cooper pairs and the thermodynamic stability of the superconducting phase. We demonstrate that odd-frequency pairing correlation functions change the sign of the coefficient of the Δ^4 term in the GL free-energy and cause the discontinuous transition to the superconducting phase. We also show a potential for the discontinuous transition is a common feature of superconductors that accommodate odd-frequency Cooper pairs. In addition, we discuss the effects of potential disorder on T_c in a multiorbital s-wave superconductor. We demonstrate that the uniform odd-frequency Cooper pairs in the clean limit play an important role to discuss the robustness.

This thesis is organized as follows. In Chapter. 2, we present the classification of Cooper pairs by its symmetry and discuss how odd-frequency Cooper pairs emerge in some superconducting systems. A brief review of the magnetic properties of odd-frequency Cooper pairs are also presented. In Chapter. 3, we discuss the instability of uniform superconducting state caused by subdominant odd-frequency Cooper pairs. We demonstrate the transition to the superconducting phase with changing the temperature becomes discontinuous. We discuss the mechanism of the phenomenon in terms of odd-frequency Cooper pairs. In Chapter. 4, we study the effect of potential

disorder in a multiorbital superconductor using the effective model of $Cu_xBi_2Se_3$. We show the robustness of the multiorbital s-wave superconducting order highly depends on its parity with respect to the orbital degree of freedom. The effect of odd-frequency Cooper pairs are also discussed. Finally, the summary of this thesis is presented in Chapter. 5.

Chapter 2

Paramagnetic odd-frequency Cooper pair

In this chapter, we introduce odd-frequency Cooper pairs and briefly review their properties. Firstly, we present the symmetry classification of Cooper pairs including the relative time degree of freedom of two electrons. Next, we discuss how the symmetry of Cooper pair affects the magnetic property of a superconductor. We show both non-uniform and uniform odd-frequency Cooper pairs exhibit a paramagnetic response to external magnetic fields.

2.1 Symmetry classification of Cooper pair

In the mean-field theory of superconductivity, the presence of Cooper pair in superconductors is represented by the pairing correlation function:

$$\mathcal{F}_{\sigma,\sigma'}(\boldsymbol{r},\boldsymbol{r}') = -\langle\psi_\sigma(\boldsymbol{r})\psi_{\sigma'}(\boldsymbol{r}')\rangle, \tag{2.1}$$

where σ, σ' represents the spin degree of freedom of an electron and $\boldsymbol{r}$, $\boldsymbol{r}'$ represents the spatial coordinate. $\psi_\sigma(\boldsymbol{r})$ is the annihilation operator of an electron at $\boldsymbol{r}$ with spin σ and satisfies the following anticommutation relation:

$$\{\psi_\sigma(\boldsymbol{r}),\, \psi_{\sigma'}(\boldsymbol{r}')\} = 0, \tag{2.2}$$

since the electron is a fermion. Therefore the correlation function must be antisymmetric under the permutation of the two electrons:

$$\mathcal{F}_{\sigma,\sigma'}(\boldsymbol{r},\boldsymbol{r}') = -\mathcal{F}_{\sigma',\sigma}(\boldsymbol{r}',\boldsymbol{r}). \tag{2.3}$$

This antisymmetry is carried by the spin or coordinate degree of freedom of the electron. Therefore, the Cooper pairs are classified into two symmetry classes. One is spin-singlet even-parity (s-wave, d-wave, $\cdots$) symmetry class. The relation

$$\mathcal{F}_{\sigma,\sigma'}(\boldsymbol{r},\boldsymbol{r}') = -\mathcal{F}_{\sigma',\sigma}(\boldsymbol{r},\boldsymbol{r}') \tag{2.4}$$

$$= +\mathcal{F}_{\sigma,\sigma'}(\boldsymbol{r}',\boldsymbol{r}), \tag{2.5}$$

holds true among the correlation functions belonging to this symmetry class. In this class, the spin degree of freedom carry the antisymmetry. The other is spin-triplet odd-parity (p-wave, f-wave, $\cdots$) symmetry class represented as

$$\mathcal{F}_{\sigma,\sigma'}(\boldsymbol{r},\boldsymbol{r}') = +\mathcal{F}_{\sigma',\sigma}(\boldsymbol{r},\boldsymbol{r}') \tag{2.6}$$

$$= -\mathcal{F}_{\sigma,\sigma'}(\boldsymbol{r}',\boldsymbol{r}). \tag{2.7}$$

The coordinate degree of freedom carry the antisymmetry in this symmetry class. Spin-singlet s-wave Cooper pairs are known to be realized in most metalic superconductors such as Al and Pb while spin-singlet d-wave Cooper pairs exist in cuprates. Materials realizing spin-triplet Cooper pairs are limited, but superfluid ^{3}He and superconductivity in heavy fermion compounds are the examples. When we assume the internal degrees of freedom of the electron are only spin and coordinate, above classification of Cooper pair is completely exhaustive. We summarized this "conventional" classification of Cooper pairs in Table. 2.1.

Table 2.1: Classification of Cooper pairs. In this classification, the spin and coordinate degrees of freedom are took into account. Parity below originates from the coordinate degree of freedom. The two symmetry classes below satisfy the antisymmetric relation in Eq. (2.3).

	Spin	Parity
1	Singlet	Even
2	Triplet	Odd

Above arguments are based on the assumption that two electrons form a Cooper pair at the same time. In addition to the spin and coordinate degrees of freedom, electrons naturally have the "time" degree of freedom derived from the equations of motion. It is not necessary for two electrons to form a Cooper pair at the same time. To include the time degree of freedom to our arguments, it is useful to define the following

pairing correlation function:

$$\begin{aligned}\mathcal{F}_{\sigma,\sigma'}(\boldsymbol{r},\tau;\boldsymbol{r}',\tau') =& -\langle T_\tau \psi_\sigma(\boldsymbol{r},\tau)\psi_{\sigma'}(\boldsymbol{r}',\tau')\rangle \\ =& -\theta(\tau-\tau')\langle\psi_\sigma(\boldsymbol{r},\tau)\psi_{\sigma'}(\boldsymbol{r}',\tau')\rangle \\ &+\theta(\tau'-\tau)\langle\psi_{\sigma'}(\boldsymbol{r}',\tau')\psi_\sigma(\boldsymbol{r},\tau)\rangle, \end{aligned} \tag{2.8}$$

where τ is the imaginary time of the electron, T_τ represents imaginary time-ordering operator, and $\psi_\sigma(\boldsymbol{r},\tau) = e^{\tau\mathcal{H}}\psi_\sigma(\boldsymbol{r})e^{-\tau\mathcal{H}}$ represents imaginary time Heisenberg represenation of the annihilation operator as commonly employed in quantum field theory at finite temperature [69, 72, 73]. This correlation function is referred to as anomalous Green's function in the Gor'kov's formalism and depends only on the relative time between two electrons $\tau - \tau'$ when we assume uniformity of the time. The anomalous Green's function in Eq. (2.8) also satisfies the relation

$$\mathcal{F}_{\sigma,\sigma'}(\boldsymbol{r},\tau;\boldsymbol{r}',\tau') = -\mathcal{F}_{\sigma',\sigma}(\boldsymbol{r}',\tau';\boldsymbol{r},\tau), \tag{2.9}$$

due to the antisymmetric property of electrons. Strictly speaking, this property is considered through the time-ordering since the anticommutation relation of fermions including the time degree of freedom is not defined in quantum mechanics. This extention enables us to consider the odd function with respect to the relative time as

$$\mathcal{F}_{\sigma,\sigma'}(\boldsymbol{r},\tau;\boldsymbol{r}',\tau') = -\mathcal{F}_{\sigma,\sigma'}(\boldsymbol{r},\tau';\boldsymbol{r}',\tau). \tag{2.10}$$

The symmetry of Cooper pairs including the time degree of freedom are usually discussed in terms of the Matsubara frequency ω_n. Cooper pairs that satisfy Eq. (2.10) are called "odd-frequency Cooper pairs" since the relation

$$\mathcal{F}_{\sigma,\sigma'}(\boldsymbol{r},\boldsymbol{r}',i\omega_n) = -\mathcal{F}_{\sigma,\sigma'}(\boldsymbol{r},\boldsymbol{r}',-i\omega_n), \tag{2.11}$$

$$\mathcal{F}_{\sigma,\sigma'}(\boldsymbol{r},\boldsymbol{r}',i\omega_n) = \int_0^{1/T} d(\tau-\tau')\mathcal{F}_{\sigma,\sigma'}(\boldsymbol{r},\tau;\boldsymbol{r}',\tau')e^{i\omega_n(\tau-\tau')}, \tag{2.12}$$

holds true. In Table. 2.2, we present a complete classification of Cooper pairs including the time (frequency) degree of freedom. Cooper pairs are classified into the four symmetry classes:

1. even-frequency spin-singlet even-parity symmetry class (ESE class).
2. even-frequency spin-triplet odd-parity symmetry class (ETO class).
3. odd-frequency spin-singlet odd-parity symmetry class (OSO class).

Table 2.2: Classification of Cooper pairs including the time degree of freedom in addition to the spin and coordinate. The four symmetry classes below satisfy the antisymmetric relation in Eq. (2.9).

	Frequency	Spin	Parity
ESE class	Even	Singlet	Even
ETO class	Even	Triplet	Odd
OSO class	Odd	Singlet	Odd
OTE class	Odd	Triplet	Even

4. odd-frequency spin-triplet even-parity symmetry class (OTE class).

Spin-singlet even-parity and spin-triplet odd-parity Cooper pairs in Table. 2.1 can be regarded as Cooper pairs belonging to ESE class and ETO class in Table. 2.1, respectively. On the other hand, Cooper pairs belonging to OSO class or OTE class emerge only when we consider the relative time degree of freedom.

The concept of odd-frequency Cooper pair was introduced by Berezinskii to explain the superfluidity in ^{3}He [10]. Although there has been much theoretical work on odd-frequency superconducting states in bulk systems since 1990s [27–46] experimental evidence is still lacking. The spatially uniform odd-frequency superconducting order was shown to be impossible in single-band metals [26]. However, it turns out that the subdominant odd-frequency Cooper pairs are allowed to exist in some systems. For instance, the odd-frequency spin-triplet s-wave state can be realized as an induced subdominant pairing correlation in a rather conventional system consisting of a spin-singlet s-wave superconductor and a ferromagnet [22]. Induced odd-frequency pairing correlations have been discussed in connection with a subgap quasiparticle appearing at a surface of unconventional superconductors [12, 74–77], a vortex core [16, 78], an edge of a Majorana nanowire [20], and around a magnetic impurity/cluster [17, 18, 79, 80]. Superconductors having internal degrees of freedom (e.g., band, orbital, sublattice) could also be a platform for realizing subdominant odd-frequency Cooper pairs [47, 48]. A quasiparticle on the Bogoliubov Fermi surface [62] in such multiband/orbital superconductors [63, 64] also accompanies an odd-frequency Cooper pair [65, 66].

2.2 Paramagnetic Cooper pairs

The most important property of odd-frequency Cooper pairs is that they exhibit a paramagnetic response to an external magnetic field [21, 67, 81, 82]. To discuss the effects of paramagnetic Cooper pairs, we present a phenomenological argument about

the energy of the superconducting condensate.

The superconducting condensate can be described phenomenologically by the macroscopic wave function

$$\psi(\boldsymbol{r}) = \sqrt{n_{\rm S}(\boldsymbol{r})}\, e^{i\theta(\boldsymbol{r})}, \tag{2.13}$$

where $n_{\rm S}$ is the density of Cooper pairs and θ is the phase of the condensate. The flux quantization is derived from the single-valuedness of this wave function. The Josephson effect is explained as the tunnel effect between two superconductors characterized by such wave functions. The energy of the condensate can be calculated in terms of the macroscopic wave function,

$$\begin{aligned} E &= \int d\boldsymbol{r}\, \frac{\hbar^2}{2m} \left\{ \left(\nabla + i\frac{e}{\hbar c}\boldsymbol{A} \right) \psi^\dagger(\boldsymbol{r}) \right\} \left\{ \left(\nabla - i\frac{e}{\hbar c}\boldsymbol{A} \right) \psi(\boldsymbol{r}) \right\} \\ &= \int d\boldsymbol{r}\, \frac{\hbar^2}{2m} \left\{ \frac{(\nabla n_{\rm S})^2}{4n_{\rm S}} + n_{\rm S} \left(\nabla\theta - \frac{e}{\hbar c}\boldsymbol{A} \right)^2 \right\}. \end{aligned} \tag{2.14}$$

The first term in Eq. (2.14) represents the kinetic energy of the condensate, and the second term means the elastic energy of the superconducting phase. Since $n_{\rm S} > 0$, both the spatial gradient of the density and the spatial gradient of the phase increase the energy of the condensate, which describes the rigidity of the superconducting state. Therefore, both the pair density and the phase are uniform at the ground state in the absence of a magnetic field. The electric current can be described by

$$\begin{aligned} \boldsymbol{j} &= \frac{e\,\hbar}{2im} \left[\psi^\dagger(\boldsymbol{r}) \left(\nabla - i\frac{e}{\hbar c}\boldsymbol{A} \right) \psi(\boldsymbol{r}) - \left(\nabla + i\frac{e}{\hbar c}\boldsymbol{A} \right) \psi^\dagger(\boldsymbol{r})\, \psi(\boldsymbol{r}) \right] \\ &= \frac{e\,\hbar\, n_{\rm S}}{m} \nabla\theta - \frac{n_{\rm S}\, e^2}{mc} \boldsymbol{A}. \end{aligned} \tag{2.15}$$

Together with the Maxwell equation $\nabla \times \boldsymbol{H} = \frac{4\pi}{c}\boldsymbol{j}$, we obtain the equation for a magnetic field in a superconductor,

$$\nabla^2 \boldsymbol{H} - \frac{4\pi\, n_{\rm S} e^2}{m\, c^2}\, \boldsymbol{H} = \boldsymbol{0}. \tag{2.16}$$

London's length $\lambda_{\rm L} = \sqrt{m\, c^2 / 4\pi\, n_{\rm S}\, e^2}$ characterizes the spatial variation of a magnetic field. Equation (2.16) represents the Meissner screening effect of a magnetic field. The dumping of a magnetic field into a superconductor is described by the negative sign at the second term on the last line in Eq. (2.15). The argument above is valid when the pair density $n_{\rm S}$ is positive everywhere in a superconductor.

Let us assume that the pair density is negative locally at a finite area around $\boldsymbol{r} = \boldsymbol{r}_0$ and let us discuss the physical consequence of $n_{\rm S}(\boldsymbol{r}_0) < 0$. The second term in Eq. (2.14) suggests that a large gradient of the phase and the penetration of a magnetic field are necessary to decrease the energy of the condensate. Namely, the condensate with the "negative pair density" is paramagnetic. Eq. (2.16) with negative $n_{\rm S}$ suggests also that a magnetic field can penetrate into such a paramagnetic superconductor [21, 81]. Such a local area around $\boldsymbol{r}_0$ may no longer be superconductive because the phase θ fluctuates easily from a constant value. Thus the pair density $n_{\rm S}$ must be positive to realize the stable homogeneous superconducting ground state both electromagnetically and thermodynamically. However, the "pair density" can be negative locally in the presence of an inhomogeneous odd-frequency pair. When the amplitude of an odd-frequency pair is dominant at some place in the inhomogeneous superconductor, the spatial gradient in the superconducting phase decreases the free-energy there. The magnetic response of a small unconventional superconductor was also shown to be paramagnetic at low temperature [82]. Furthermore, for uniform odd-frequency Cooper pairs in multiband/orbital superconductors, they suppress the transition temperature and tend to destabilize the superconducting state by disturbing the phase coherence [67]. The reason is also explained by the paramagnetic property. In such cases, the even-frequency component of the pairing correlation functions are dominant and the total pair density is always positive. The uniform superconducting order with subdominant odd-frequency Cooper pairs is stabilized by diamagnetic even-frequency Cooper pairs as well as conventional uniform superconductors. In the following, we briefly review the emergence and the magnetic property of odd-frequency Cooper pairs in both an inhomogeneous superconductor and a homogeneous multiband/orbital superconductor.

2.3 Local odd-frequency Cooper pairs in inhomogeneous superconductors

The surface of a superconductor breaks inversion symmetry locally. As a result of breaking inversion symmetry, odd-parity (even-parity) pairing correlations appear at the surface of even-parity (odd-parity) superconductor. Such induced pairing correlations belong to an odd-frequency symmetry class because the surface does not change the spin of a Cooper pair. In what follows, we demonstrate that the pair density can be

negative at such a surface by using an analytical solution of the Eilenberger equation,

$$\hbar v_F \hat{\boldsymbol{k}} \cdot \nabla \hat{g} + [H, \hat{g}] = 0, \tag{2.17}$$

$$H = \begin{bmatrix} \omega_n & \Delta(\boldsymbol{r}, \hat{\boldsymbol{k}}) \\ -s_s \underset{\sim}{\Delta}(\boldsymbol{r}, \hat{\boldsymbol{k}}) & -\omega_n \end{bmatrix}, \tag{2.18}$$

$$\hat{g}(\boldsymbol{r}, \hat{\boldsymbol{k}}, \omega_n) = \begin{bmatrix} g(\boldsymbol{r}, \hat{\boldsymbol{k}}, \omega_n) & f(\boldsymbol{r}, \hat{\boldsymbol{k}}, \omega_n) \\ -s_s \underset{\sim}{f}(\boldsymbol{r}, \hat{\boldsymbol{k}}, \omega_n) & -g(\boldsymbol{r}, \hat{\boldsymbol{k}}, \omega_n) \end{bmatrix}. \tag{2.19}$$

Here we have reduced to 2×2 particle-hole space by extracting one spin sector of the Bogoliubov-de Gennes (BdG) Hamiltonian. The pair potential obeys the symmetry relation

$$\Delta(\boldsymbol{r}, -\hat{\boldsymbol{k}}) = \begin{cases} \Delta(\boldsymbol{r}, \hat{\boldsymbol{k}}) & \text{singlet } s_s = -1, \\ -\Delta(\boldsymbol{r}, \hat{\boldsymbol{k}}) & \text{triplet } s_s = 1, \end{cases} \tag{2.20}$$

which is drived from the Fermi-Dirac statistics of electrons. The Eilenberger equation can be decomposed into three equations [25],

$$v_F \hat{\boldsymbol{k}} \cdot \nabla g = 2\Delta\, f_S, \quad v_F \hat{\boldsymbol{k}} \cdot \nabla f_B = -2\omega_n\, f_S, \quad v_F \hat{\boldsymbol{k}} \cdot \nabla f_S = 2(\Delta\, g - \omega_n\, f_B), \tag{2.21}$$

with

$$f_B = \frac{1}{2}(f - s_s \underset{\sim}{f}), \quad f_S = \frac{1}{2}(f + s_s \underset{\sim}{f}). \tag{2.22}$$

The quasiclassical Green's functions satisfy the normalization condition

$$g^2 - s_s \underset{\sim}{f}\, f = g^2 + f_B^2 - f_S^2 = 1. \tag{2.23}$$

In a homogeneous superconductor, we obtain the solution as

$$g = \frac{\omega_n}{\Omega}, \quad f_B = \frac{\Delta(\hat{\boldsymbol{k}})}{\Omega}, \quad f_S = 0, \quad \Omega = \sqrt{\omega_n^2 + \Delta^2(\hat{\boldsymbol{k}})}. \tag{2.24}$$

Thus f_B is interpreted as a bulk component of pairing correlation, which contributes to the pair potential through the gap equation

$$\Delta(\boldsymbol{r}, \hat{\boldsymbol{k}}) = T \sum_{\omega_n} \int \frac{d\hat{\boldsymbol{k}}'}{S_d} \lambda(\hat{\boldsymbol{k}}, \hat{\boldsymbol{k}}') f(\boldsymbol{r}, \hat{\boldsymbol{k}}', \omega_n), \tag{2.25}$$

where λ represents an attractive interaction between two electrons. The second equation in Eq. (2.21) represents the symmetry relationship between f_B and f_S. Since $\hat{\boldsymbol{k}}$ is an odd-parity function and ω_n is an odd in Matsubara frequency, f_S belongs to the opposite parity and opposite frequency symmetry class to f_B. Therefore, f_S is considered as an induced pairing component due to the spatial gradient of f_B. Although the anomalous Green's function f in Eq. (2.25) consists of both f_B and f_S, only the bulk component f_B contributes to the pair potential. Since f_S is an odd-function of ω_n, the summation of f_S over ω_n vanishes. The Meissner kernel for the quasiclassical Green's function is described as [83]

$$j_\mu = -\frac{2ne^2}{mc}\mathcal{Q}_{\mu,\nu}A_\nu, \tag{2.26}$$

$$\begin{aligned}\mathcal{Q}_{\mu,\nu} &= d\pi T\sum_{\omega_n}\int\frac{d\hat{\boldsymbol{k}}}{S_d}\hat{k}_\mu\,\hat{k}_\nu\,\partial_{\omega_n}g(\boldsymbol{r},\hat{\boldsymbol{k}},\omega_n)\\ &= d\pi T\sum_{\omega_n>0}\int\frac{d\hat{\boldsymbol{k}}}{S_d}\hat{k}_\mu\,\hat{k}_\nu\,(f_B^2-f_S^2)\,\partial_{\omega_n}\log\frac{1+g}{1-g}.\end{aligned} \tag{2.27}$$

The last expression suggests that the odd-frequency pairing correlation decreases $\mathcal{Q}_{\mu,\nu}$. By putting the results in Eq. (2.24) for a spin-singlet s-wave superconductor into $\mathcal{Q}$, it is possible to recover the results of [69]

$$\mathcal{Q}_{\mu,\nu} = \pi\,T\sum_{\omega_n}\frac{\Delta^2}{(\omega_n^2+\Delta^2)^{3/2}}\delta_{\mu,\nu}. \tag{2.28}$$

The product of $n\,\mathcal{Q}_{\mu,\mu}$ is often referred to as pair density.

As an example of inhomogeneous superconducting states, we consider the condensate near the surface of a two-dimensional p-wave superconductor. The pair potential is described as

$$\Delta(x) = \Delta\cos\theta\tanh\left(\frac{x}{\xi_0}\right),\quad \hat{k}_x=\cos\theta,\quad \hat{k}_y=\sin\theta,\quad \xi_0=\frac{v_F}{\Delta\cos\theta}, \tag{2.29}$$

where we assume that a surface is at $x=0$ and a p-wave superconductor occupies $x>0$, the superconducting state is uniform in the y direction, and ξ_0 is the coherence

length. The solution of Eq. (2.21) can be obtained as [84]

$$g(x,\theta,\omega_n) = \frac{\omega_n}{\Omega_\theta} + \frac{\Delta^2\cos^2\theta}{2\omega_n\Omega_\theta}\cosh^{-2}\left(\frac{x}{\xi_0}\right), \quad f_B(x,\theta,\omega_n) = \frac{\Delta\cos\theta}{\Omega_\theta}\tanh\left(\frac{x}{\xi_0}\right), \tag{2.30}$$

$$f_S(x,\theta,\omega_n) = -\frac{\Delta^2\cos^2\theta}{2\omega_n\Omega_\theta}\cosh^{-2}\left(\frac{x}{\xi_0}\right), \quad \Omega_\theta = \sqrt{\omega_n^2 + \Delta^2\cos^2\theta}. \tag{2.31}$$

The bulk component $f_B(x,\theta+\pi,\omega_n) = -f_B(x,\theta,\omega_n)$ is odd-parity, whereas the surface component f_S is even-parity because of $\cos^2(\theta+\pi) = \cos^2\theta$. The gap equation in Eq. (2.25) is described as

$$\Delta(x) = T\sum_{\omega_n}\int_0^{2\pi}\frac{d\theta'}{2\pi}(2\lambda\,\cos\theta\,\cos\theta')\left[f_B(x,\theta',\omega_n) + f_S(x,\theta',\omega_n)\right], \tag{2.32}$$

$$= \Delta\,\cos\theta\,\tanh\left(\frac{x}{\xi_0}\right)\lambda T\sum_{\omega_n}\frac{1}{\sqrt{\omega_n^2+\Delta^2}}. \tag{2.33}$$

On the way to the second line, we approximately neglect the θ dependence of Ω_θ and that of ξ_0 in $f_{\rm B}$. The amplitude of f_S increases with the decrease of ω_n at its denominator and can be larger than the amplitude of f_B for $\omega_n \ll \Delta$. The resulting response kernel,

$$\mathcal{Q}_{\mu,\nu} \approx \delta_{\mu,\nu}\,\pi T\sum_{\omega_n}\int_0^{2\pi}\frac{d\theta}{2\pi}\frac{\Delta^2\cos^2\theta}{(\omega_n^2+\Delta^2\cos^2\theta)^{3/2}}\left[1 - \frac{\Delta^2\cos^2\theta}{2\omega_n^2}\cosh^{-2}\left(\frac{x}{\xi_0}\right)\right], \tag{2.34}$$

can be negative for a low temperature $T \ll T_c$ near the surface $0 < x < \xi_0$. The paramagnetic response at the surface of an unconventional superconductor was pointed out for a *d*-wave superconductor [85, 86]. To make clear the details of the paramagnetic effect theoretically, analysis beyond the linear response is necessary. In Refs. [82, 87], the pair potential and a magnetic field are determined self-consistently with each other in a small unconventional superconductor. A small *p*-wave superconducting disk shows a paramagnetic response to a magnetic field at a low temperature. Even-frequency pairs stabilize *p*-wave superconductivity in the bulk, and odd-frequency pairs exhibit the paramagnetic response at the surface.

2.4 Uniform odd-frequency Cooper pairs in multiband superconductors

The realization of uniform odd-frequency Cooper pairs in the bulk has been considered to be difficult thermodynamically because of their paramagnetic property. However, contrary to such conventional knowledge, Black-Schaffer and Balatsky demonstrated that uniform odd-frequency Cooper pairs could exist as subdominant pairing correlations in multiband/orbital superconductors [47, 48]. They consider the band/orbital degree of freedom explicitly to describe the superconductivity. The anomalous Green's function including the band/orbital degree of freedom are difined by

$$\mathcal{F}_{\lambda\sigma,\lambda'\sigma'}(\boldsymbol{r},\tau;\boldsymbol{r}',\tau') = -\langle T_\tau \psi_{\lambda\sigma}(\boldsymbol{r},\tau)\psi_{\lambda'\sigma'}(\boldsymbol{r}',\tau')\rangle \tag{2.35}$$

$$= -\mathcal{F}_{\lambda'\sigma',\lambda\sigma}(\boldsymbol{r}',\tau';\boldsymbol{r},\tau), \tag{2.36}$$

where λ, λ' represents the band/orbital index, $\psi_{\lambda\sigma}(\boldsymbol{r})$ is the annihilation operator of an electron at $\boldsymbol{r}$ with spin σ in band/orbital λ, and $\psi_{\lambda\sigma}(\boldsymbol{r},\tau) = e^{\tau\mathcal{H}}\psi_{\lambda\sigma}(\boldsymbol{r})e^{-\tau\mathcal{H}}$ is imaginary time Heisenberg representation of the annihilation operator. The relation in the second line of Eq. (2.36) holds true due to the antisymmetry of electrons. Originally, the coordinate degree of freedom and the band degree of freedom cannot be separated because both originates from the spatial degree of freedom. However, we separate the spatial degree of freedom into the degree of freedom of lattice points and that within the lattice points (e.g., the degree of freedom of atomic orbitals). We refer to the symmetry regarding the former as "momentum parity" and that regarding the latter as "band parity". In this case, the number of the symmetry class of the Cooper pairs doubles. In Table. 2.3, we show the classification of Cooper pairs in multiband/orbital superconductors. The consideration of the additional degrees of freedom leads to the emergence of Cooper pairs belonging to various symmetry classes. Therefore, the uniform pairing correlations belonging to odd-frequency symmetry classes emerge in the bulk. In the following, we present an example of uniform superconductivity that include subdominant odd-frequency Cooper pairs and discuss the magnetic response of Cooper pairs in multiband/orbital superconductors [67].

The mean-field Hamiltonian describing the uniform electronic states of a time-

Table 2.3: Classification of Cooper pairs in multiband/orbital systems. The eight symmetry classes below satisfy the antisymmetry relation in Eq. (2.36). The momentum parity in the fourth column represents the parity with respect to the momentum $\boldsymbol{k}$ of the anomalous Green's function while the band parity in the fifth column represents the parity regarding the exchange of the band index.

	Frequency	Spin	Momentum parity	Band parity
ESEE class	Even	Singlet	Even	Even
ESOO class	Even	Singlet	Odd	Odd
ETOE class	Even	Triplet	Odd	Even
ETEO class	Even	Triplet	Even	Odd
OSOE class	Odd	Singlet	Odd	Even
OSEO class	Odd	Singlet	Even	Odd
OTEE class	Odd	Triplet	Even	Even
OTOO class	Odd	Triplet	Odd	Odd

reversal two-band superconductor is represented as

$$\mathcal{H} = \sum_{\boldsymbol{k}} \vec{\Psi}^{\dagger}_{\boldsymbol{k}} H(\boldsymbol{k}) \vec{\Psi}_{\boldsymbol{k}}, \quad H(\boldsymbol{k}) = \begin{bmatrix} H_{\mathrm{N}}(\boldsymbol{k}) & \Delta(\boldsymbol{k}) \\ -\Delta^{*}(-\boldsymbol{k}) & -H^{*}_{\mathrm{N}}(-\boldsymbol{k}) \end{bmatrix}, \tag{2.37}$$

$$\vec{\Psi}_{\boldsymbol{k}} = \left[\vec{\psi}^{\mathrm{T}}_{\boldsymbol{k}}, \vec{\psi}^{\dagger}_{-\boldsymbol{k}}\right]^{\mathrm{T}}, \quad \vec{\psi}_{\boldsymbol{k}} = \left[\psi_{\boldsymbol{k},1,\uparrow}, \psi_{\boldsymbol{k},1,\downarrow}, \psi_{\boldsymbol{k},2,\uparrow}, \psi_{\boldsymbol{k},2,\downarrow}\right]^{\mathrm{T}}, \tag{2.38}$$

$$H_{\mathrm{N}}(\boldsymbol{k}) = \begin{bmatrix} \xi_1 & 0 & V_0 + V_3 & V_1 - iV_2 \\ 0 & \xi_1 & V_1 + iV_2 & V_0 - V_3 \\ V_0^{*} + V_3 & V_1 - iV_2 & \xi_2 & 0 \\ V_1 + iV_2 & V_0^{*} - V_3 & 0 & \xi_2 \end{bmatrix}, \tag{2.39}$$

$$\Delta(\boldsymbol{k}) = \begin{bmatrix} 0 & \Delta_1 & 0 & \Delta_{12} \\ -\Delta_1 & 0 & s_{\mathrm{spin}}\Delta_{12} & 0 \\ 0 & -s_{\mathrm{spin}}\Delta_{12} & 0 & \Delta_2 \\ -\Delta_{12} & 0 & -\Delta_2 & 0 \end{bmatrix} \tag{2.40}$$

where $\psi_{\lambda,\sigma}(\boldsymbol{k})$ is the annihilation operator of an electron in band λ (1 or 2) with spin σ ($\uparrow$ or $\downarrow$) at a momentum $\boldsymbol{k}$ and $\xi_{\lambda,\boldsymbol{k}} = \frac{\boldsymbol{k}^2}{2m_\lambda} - \mu_\lambda$. In the normal state Hamiltonian $H_{\mathrm{N}}(\boldsymbol{k})$, the hybridization potential expressed by V_0 does not depend on the spin. The hybridization caused by the spin-orbit interaction is also took into account by $\boldsymbol{V} = (V_1, V_2, V_3)$ and $\boldsymbol{V}(\boldsymbol{k}) = -\boldsymbol{V}(-\boldsymbol{k})$ holds true. In $\Delta(\boldsymbol{k})$, the pair potentials consisting of two electrons with opposite spin are considered. $s_{\mathrm{spin}} = 1$ represents spin-triplet symmetry belonging to the ETEO class while $s_{\mathrm{spin}} = -1$ represents spin-singlet symmetry belonging to ESEE class.

Here, we assume that only the intraband pair potential Δ_1, Δ_2 is finite and the spin-flip hybridization is absent (i.e., $\Delta_{12} = V_1 = V_2 = 0$) for simplicity. Even in other cases, the discussion can proceed straightforwardly as well. In this case, the Hamiltonian in Eq. (2.37) can be block diagonalized and the reduced Hamiltonian is represented by

$$H(\boldsymbol{k}) = \begin{bmatrix} \xi_1 & V_0 + sV_3 & s\Delta_1 & 0 \\ V_0^* + sV_3 & \xi_2 & 0 & s\Delta_2 \\ s\Delta_1^* & 0 & -\xi_1 & -V_0^* - sV_3 \\ 0 & s\Delta_2^* & -V_0 - sV_3 & -\xi_2 \end{bmatrix}. \tag{2.41}$$

The anomalous Green's function is calculated as [67]

$$\begin{aligned} \mathcal{F}(\boldsymbol{k}, i\omega_n) = \frac{s}{2Z} \big[&\left\{ (-X + v_2^2)\Delta_+ + (K + iv_1v_2)\Delta_- \right\} \rho_0 \\ &+ \left\{ v_1(\xi_+\Delta_+ - \xi_-\Delta_-) - iv_2(\xi_+\Delta_- - \xi_-\Delta_+) \right\} \rho_1 \\ &+ \omega_n(v_1\Delta_- - iv_2\Delta_+)\rho_2 \\ &+ \left\{ (-X + v_1^2)\Delta_- + (K - iv_1v_2)\Delta_+ \right\} \rho_3 \big], \end{aligned} \tag{2.42}$$

with

$$\xi_\pm = \frac{\xi_1 \pm \xi_2}{2}, \quad \Delta_\pm = \frac{\Delta_1 \pm \Delta_2}{2}, \quad V_0 = v_1 + iv_2. \tag{2.43}$$

ρ_j for $\mathrm{j} = 1 - 3$ are Pauli matrices in the two-band space. Z, X, and K are even function with respect to both the momentum and the Matsubara frequency. The detailed expression of these functions is presented in Sec. IIIA of Ref. [67]. The third line of Eq. (2.42) represents the existence of uniform odd-frequency Cooper pairs induced by the band hybridization V_0.

General magnetic property of the uniform odd-frequency Cooper pairs can be examined by using some symmetries of the Bogoliubov-de Gennes Hamiltonian. We consider a general Bogoliubov-de Gennes Hamiltonian describing electronic states of a uniform superconductor:

$$H(\boldsymbol{k}) = \begin{bmatrix} H_\mathrm{N}(\boldsymbol{k}) & \Delta(\boldsymbol{k}) \\ -\underset{\sim}{\Delta}(\boldsymbol{k}) & -\underset{\sim}{H}_\mathrm{N}(\boldsymbol{k}) \end{bmatrix}, \tag{2.44}$$

where $\underset{\sim}{X}(\boldsymbol{k}, i\omega_n) = X^*(-\boldsymbol{k}, i\omega_n)$ represents particle-hole conjugation. We assume $H(\boldsymbol{k})$ is a $2M \times 2M$ matrix with M being a positive integer. $H(\boldsymbol{k})$ has particle-hole symmetry

described as

$$CH(-\boldsymbol{k})C^{-1} = -H(\boldsymbol{k}), \quad C = \tau_1 \mathcal{K}, \tag{2.45}$$

where C represents charge-conjugation operator and $\hat{\tau}_j$ for $j = 1-3$ are Pauli matrices in the particle-hole space. When we examine a response of superconductors to external perturbations within the linear response theory, we often need to compute a correlation function of this form:

$$\Pi = T \sum_{\omega_n} \frac{1}{V_{\rm vol}} \sum_{\boldsymbol{k}} A^2 \mathrm{Tr}\left[\mathcal{G}\mathcal{G} + \underline{\mathcal{F}}\mathcal{F}\right]_{(\boldsymbol{k}, i\omega_n)}, \tag{2.46}$$

where A represents a vertex in a corresponding correlation function (e.g., current operator in a current-current correlation function). $\mathcal{G}$ ($\mathcal{F}$) is normal (anomalous) Green's function and is calculated by the Gor'kov equation,

$$[i\omega_n - H(\boldsymbol{k})] \begin{bmatrix} \mathcal{G}(\boldsymbol{k}, i\omega_n) & \mathcal{F}(\boldsymbol{k}, i\omega_n) \\ \underline{\mathcal{F}}(\boldsymbol{k}, i\omega_n) & \underline{\mathcal{G}}(\boldsymbol{k}, i\omega_n) \end{bmatrix} = 1. \tag{2.47}$$

The relations

$$\underline{\mathcal{G}}(\boldsymbol{k}, i\omega_n) = -\underset{\sim}{\mathcal{G}}(\boldsymbol{k}, i\omega_n), \tag{2.48}$$

$$\underline{\mathcal{F}}(\boldsymbol{k}, i\omega_n) = -\underset{\sim}{\mathcal{F}}(\boldsymbol{k}, i\omega_n), \tag{2.49}$$

$$\mathcal{F}^{\mathrm{T}}(-\boldsymbol{k}, -i\omega_n) = -\mathcal{F}(\boldsymbol{k}, i\omega_n), \tag{2.50}$$

hold true by the particle-hole symmetry of the BdG Hamiltonian and the Fermi-Dirac statistics of electrons. The contribution of the anomalous Green's function to the correlation function is calculated to be

$$\begin{aligned} \Pi^{\mathcal{F}} &= T \sum_{\omega_n} \frac{1}{V_{\rm vol}} \sum_{\boldsymbol{k}} A^2 \mathrm{Tr}\left[\underline{\mathcal{F}}(\boldsymbol{k}, i\omega_n)\mathcal{F}(\boldsymbol{k}, i\omega_n)\right] \\ &= T \sum_{\omega_n} \frac{1}{V_{\rm vol}} \sum_{\boldsymbol{k}} A^2 \sum_{\alpha\beta} \mathcal{F}^*_{\beta\alpha}(\boldsymbol{k}, -i\omega_n)\mathcal{F}_{\beta\alpha}(\boldsymbol{k}, i\omega_n) \\ &= T \sum_{\omega_n} \frac{1}{V_{\rm vol}} \sum_{\boldsymbol{k}} A^2 \sum_{\alpha\beta} \left(|f^{\rm e}_{\beta\alpha}(\boldsymbol{k}, i\omega_n)|^2 - |f^{\rm o}_{\beta\alpha}(\boldsymbol{k}, i\omega_n)|^2\right), \end{aligned} \tag{2.51}$$

where we used the relations in Eqs. (2.49) and (2.50) to reach the second line. $\mathcal{F}_{\beta\alpha}$

represents (β, α)-component of the $M \times M$ matrix $\mathcal{F}$ and

$$f^{\mathrm{e/o}}_{\beta\alpha}(\boldsymbol{k}, i\omega_n) = \frac{\mathcal{F}_{\beta\alpha}(\boldsymbol{k}, i\omega_n) \pm \mathcal{F}_{\beta\alpha}(\boldsymbol{k}, -i\omega_n)}{2}, \tag{2.52}$$

represents even-/odd-frequency components of $\mathcal{F}_{\beta\alpha}$. Eq. (2.51) clearly shows the anomalous properties of odd-frequency Cooper pairs by the negative sign of the second term. When we consider a linear response to a static transverse vector potential, the second term indicates that odd-frequency pairing correlations always have negative contributions to the Meissner kernel. In other words, odd-frequency Cooper pairs exhibit a paramagnetic response to external magnetic fields and then destabilize superconductivity by disturbing phase coherence. Actually, above arguments are not valid when the corresponding vertex can not be factorized like Eq. (2.46). It has been shown that diamagnetic odd-frequency Cooper pairs can exist in some special systems [88, 89]. But the odd-frequency Cooper pairs in most multiband/orbital superconductors show paramagnetic response [67] and we do not consider such exceptional cases here.

2.5 Summary and scope of this thesis

We have presented the symmetry classifications of Cooper pairs and have introduced odd-frequency Cooper pairs. We have also reviewed the emergence of the odd-frequency Cooper pairs and their magnetic properties in both inhomogeneous and homogeneous superconductors. There are various studies on the inhomogeneous superconductors and the concept of odd-frequency Cooper pairs comprehensively explains the physics in such superconductors. However, our kowledge about the effects of uniform odd-frequency Cooper pairs on the physical phenomena has been still lacking. The purpose of this study is to fill the gaps in knowledge. In the following chaper, we discuss the thermodynamic stability and robustness against potential disorder of uniform superconductivity that include subdominant odd-frequency Cooper pairs.

Chapter 3

Discontinuous transition

3.1 Abstract

We discuss the instability of uniform superconducting states that contain the pairing correlations belonging to the odd-frequency symmetry class. The instability originates from the paramagnetic response of odd-frequency Cooper pairs and is considerable at finite temperatures. As a result, the pair potential varies discontinuously at the transition temperature when the amplitude of the odd-frequency pairing correlation functions is sufficiently large. The discontinuous transition to the superconducting phase is a general feature among superconductors having a large amplitude of odd-frequency pairing correlation functions.

3.2 Introduction

There are two types of perturbations that act on uniform superconducting states. One does not change the thermal properties, while the other does. Spin-orbit interactions and Zeeman fields correspond to the examples of such perturbations in a spin-singlet superconductor. Spin-orbit interactions do not change any thermal properties of a superconductor such as the transition temperature T_c or the dependence of order parameter Δ on temperatures T [90]. On the other hand, uniform Zeeman fields decrease T_c. Moreover, the transition to the superconducting phase by decreasing the temperature changes to a first-order transition in sufficiently strong Zeeman fields [91, 92]. Namely, the superconducting state is thermally unstable under Zeeman fields. A recent study [70] has reported that $j = 3/2$ superconductors also exhibit very similar instabilities. Although such discontinuous transition has been observed in spin-singlet superconductors under Zeeman fields [93–95], there has been no comprehensive expla-

nation for why the superconducting transition changes to a first-order transition and what distinguishes the two types of perturbations. We address these issues in this study.

To the best of our knowledge, odd-frequency Cooper pairs [10–15] tend to cause thermal instability in superconducting states. This consideration is supported by the following findings for odd-frequency pairs localized various places in a superconductor such as at a vortex core [16], in the vicinity of a magnetic cluster [17, 18], and at the surface of a topologically nontrivial superconductor [19, 20]. An analysis of the free-energy density shows that the superconducting states are unstable locally around these defects [79, 82]. The paramagnetic response of odd-frequency Cooper pairs to an external magnetic field is responsible for the instability [21]. In uniform superconductors, odd-frequency Cooper pairs exist as subdominant pairing correlations when the electronic structures have extra degrees of freedom such as spins, orbitals and sublattices [48]. It has been shown that the T_c of such superconductors decreases as the amplitude of odd-frequency pairs increases [67].

The purpose of this chapter is to show that odd-frequency Cooper pairs in uniform superconducting states are responsible for the discontinuous transition to the superconducting phase. For this purpose, we analyze the way in which the odd-frequency pairing correlation functions change the coefficient of the Δ^4 term in the Ginzburg-Landau (GL) free-energy functional and the superfluid density. We find that the odd-frequency pairing correlations decrease the coefficient and the superfluid density in the same manner. The instability originates from the suppression of the superfluid density caused by odd-frequency pairs. We conclude that a potential for the discontinuous transition to the superconducting phase is a general feature of superconductors containing odd-frequency Cooper pairs since the mechanism is explained well by basic properties of uniform odd-frequency Cooper pairs. The two types of perturbations are distinguished by whether or not they induce odd-frequency Cooper pairs.

This chapter is organaized as follows. In Sec. 3.3, we explain a model of $j = 3/2$ superconductors which we mainly analyze in this chapter and show the expression of the coefficients in the GL free-energy functional in terms of the Green's function. The discontinuous transition to the superconducting phase is demonstrated numerically in Sec. 3.4. The mechanism of the discontinuous transition is discussed by analyzing the temperature dependence of the superfluid density in Sec. 3.5. In Sec. 3.6, we discuss the universality of the phenomenon by showing the discontinuous transition in a spin-singlet superconductor in Zeeman fields and that in a two-band superconductor under the band-hybridization. The conclusions are given in Sec. 3.7.

3.3 Ginzburg-Landau Free-energy

3.3.1 Multi-band superconductors

In this chapter, we mainly analyze the Hamiltonian of pseudospin-quintet states in a $j = 3/2$ superconductor for the following several reasons. The normal state Hamiltonian describes the most general multiband electronic states, which have four internal degrees of freedom and preserve both time-reversal symmetry and inversion symmetry [96]. The pair potential can be represented by a simple formula [63, 64]. Useful mathematical tools are available to calculate the Green's function analytically. The high-pseudospin electronic states stem from the strong coupling between orbitals with angular momentum $\ell = 1$ and spin with $s = 1/2$ [63, 64, 97–99]. The mean-field Hamiltonian can be expressed as

$$\mathcal{H} = \frac{1}{2}\sum_{\boldsymbol{k}} \vec{\Psi}^{\dagger}_{\boldsymbol{k}} H(\boldsymbol{k}) \vec{\Psi}_{\boldsymbol{k}} + \frac{N\Delta^2}{\tilde{g}}, \tag{3.1}$$

$$\vec{\Psi}_{\boldsymbol{k}} = \left[\vec{\psi}^{\mathrm{T}}_{\boldsymbol{k}},\, \vec{\psi}^{\dagger}_{-\boldsymbol{k}}\right]^{\mathrm{T}}, \tag{3.2}$$

$$\vec{\psi}_{\boldsymbol{k}} = \left[c_{\boldsymbol{k},3/2},\, c_{\boldsymbol{k},1/2},\, c_{\boldsymbol{k},-1/2},\, c_{\boldsymbol{k},-3/2}\right]^{\mathrm{T}}, \tag{3.3}$$

where $\tilde{g} > 0$ represents the strength of the attractive interaction, N is the number of unit cells of the underlying lattice, Δ denotes the pair potential, and $c_{\boldsymbol{k},j_z}$ is the annihilation operator of an electron at $\boldsymbol{k}$ with pseudospin j_z. The Bogoliubov-de Gennes Hamiltonian in Eq. (3.1) is,

$$H(\boldsymbol{k}) = \begin{bmatrix} H_{\mathrm{N}}(\boldsymbol{k}) & \Delta(\boldsymbol{k}) \\ -\Delta^*(-\boldsymbol{k}) & -H^*_{\mathrm{N}}(-\boldsymbol{k}) \end{bmatrix}. \tag{3.4}$$

The normal state Hamiltonian is represented by the tight-binding model on a simple cubic lattice [97] as

$$\begin{aligned} H_{\mathrm{N}}(\boldsymbol{k}) &= -2t_1 \sum_{\nu} \cos k_\nu - 2t_2 \sum_{\nu} \cos k_\nu\, J_\nu^2 \\ &\quad + 4t_3 \sum_{\nu\neq\nu'} \sin k_\nu \sin k_{\nu'}\, J_\nu J_{\nu'} + 6t_1 + \frac{15}{2} t_2 - \mu, \\ &= \xi_{\boldsymbol{k}} + \vec{\epsilon}_{\boldsymbol{k}} \cdot \vec{\gamma}, \end{aligned} \tag{3.5}$$

with μ being the chemical potential. The corresponding point group is O_h. The nearest neighbor hopping independent of (depending on) pseudospin is t_1 (t_2). The second

neighbor hopping is denoted by t_3. $\xi_{\boldsymbol{k}}$ represents kinetic energy of an electron and the five-component vector $\vec{\epsilon}_{\boldsymbol{k},\mathrm{j}}$ for $\mathrm{j} = 1-5$ determines the dependence of the normal state dispersions on pseudospins. Each is defined as

$$\xi_{\boldsymbol{k}} = \left(-2t_1 - \frac{5}{2}t_2\right)\sum_{\nu}\cos k_\nu + 6t_1 + \frac{15}{2}t_2 - \mu, \tag{3.6}$$

$$\epsilon_{\boldsymbol{k},1} = 4\sqrt{3}t_3 \sin k_x \sin k_y, \tag{3.7}$$

$$\epsilon_{\boldsymbol{k},2} = 4\sqrt{3}t_3 \sin k_y \sin k_z, \tag{3.8}$$

$$\epsilon_{\boldsymbol{k},3} = 4\sqrt{3}t_3 \sin k_z \sin k_x, \tag{3.9}$$

$$\epsilon_{\boldsymbol{k},4} = \sqrt{3}t_2(-\cos k_x + \cos k_y), \tag{3.10}$$

$$\epsilon_{\boldsymbol{k},5} = t_2(-2\cos k_z + \cos k_x + \cos k_y). \tag{3.11}$$

The spinors for the angular momenum of $j = 3/2$ are described by,

$$J_x = \frac{1}{2}\begin{bmatrix} 0 & \sqrt{3} & 0 & 0 \\ \sqrt{3} & 0 & 2 & 0 \\ 0 & 2 & 0 & \sqrt{3} \\ 0 & 0 & \sqrt{3} & 0 \end{bmatrix}, \tag{3.12}$$

$$J_y = \frac{1}{2}\begin{bmatrix} 0 & -i\sqrt{3} & 0 & 0 \\ i\sqrt{3} & 0 & -2i & 0 \\ 0 & 2i & 0 & -i\sqrt{3} \\ 0 & 0 & i\sqrt{3} & 0 \end{bmatrix}, \tag{3.13}$$

$$J_z = \frac{1}{2}\begin{bmatrix} 3 & 0 & 0 & 0 \\ 0 & 1 & 0 & 0 \\ 0 & 0 & -1 & 0 \\ 0 & 0 & 0 & -3 \end{bmatrix}. \tag{3.14}$$

The five Dirac's γ-matrices are defined in 4×4 pseudospin space as

$$\gamma^1 = \frac{1}{\sqrt{3}}(J_x J_y + J_y J_x), \quad \gamma^2 = \frac{1}{\sqrt{3}}(J_y J_z + J_z J_y), \tag{3.15}$$

$$\gamma^3 = \frac{1}{\sqrt{3}}(J_z J_x + J_x J_z), \quad \gamma^4 = \frac{1}{\sqrt{3}}(J_x^2 - J_y^2), \tag{3.16}$$

$$\gamma^5 = \frac{1}{3}(2J_z^2 - J_x^2 - J_y^2), \tag{3.17}$$

and $1_{4\times4}$ is the identity matrix. They satisfy the following relations

$$\gamma^{\mathrm{i}}\,\gamma^{\mathrm{j}}+\gamma^{\mathrm{j}}\,\gamma^{\mathrm{i}}=2\times1_{4\times4}\delta_{\mathrm{i,j}}, \tag{3.18}$$

$$\gamma^{1}\,\gamma^{2}\,\gamma^{3}\,\gamma^{4}\,\gamma^{5}=-1_{4\times4}, \tag{3.19}$$

$$\{\gamma^{\mathrm{i}}\}^{*}=\{\gamma^{\mathrm{i}}\}^{\mathrm{T}}=U_T\,\gamma^{\mathrm{i}}\,U_T^{-1},\quad U_T=\gamma^{1}\,\gamma^{2}, \tag{3.20}$$

where U_T is the unitary part of the time-reversal operation $\mathcal{T}=U_T\,\mathcal{K}$ with $\mathcal{K}$ meaning complex conjugation. Eq. (3.5) corresponds to the Luttinger-Kohn Hamiltonian [97] with cubic anisotropy when we expand the trigonometric functions up to the second order of the momentum.

The pair potential is described as

$$\Delta(\boldsymbol{k})=\Delta\,\vec{\eta}_{\boldsymbol{k}}\cdot\vec{\gamma}\,U_T, \tag{3.21}$$

$$\vec{\eta}_{\boldsymbol{k}}=(\eta_{\boldsymbol{k},1},\eta_{\boldsymbol{k},2},\eta_{\boldsymbol{k},3},\eta_{\boldsymbol{k},4},\eta_{\boldsymbol{k},5}), \tag{3.22}$$

where the five-component vector $\vec{\eta}_{\boldsymbol{k}}$ with $|\vec{\eta}_{\boldsymbol{k}}|=\sqrt{\vec{\eta}_{\boldsymbol{k}}\cdot\vec{\eta}_{\boldsymbol{k}}^{*}}=1$ represents an even-parity pseudospin-quintet pairing order.

3.3.2 Ginzburg-Landau expansion

To analyze superconducting states, we solve the Gor'kov equation

$$[i\omega_n-H(\boldsymbol{k})]\begin{bmatrix}\mathcal{G}(\boldsymbol{k},i\omega_n) & \mathcal{F}(\boldsymbol{k},i\omega_n)\\ -\underset{\sim}{\mathcal{F}}(\boldsymbol{k},i\omega_n) & -\underset{\sim}{\mathcal{G}}(\boldsymbol{k},i\omega_n)\end{bmatrix}=1, \tag{3.23}$$

where $\omega_n=(2n+1)\pi T$ is the fermionic Matsubara frequency with n being an integer, and $\underset{\sim}{X}(\boldsymbol{k},i\omega_n)\equiv X^{*}(-\boldsymbol{k},i\omega_n)$ represents the particle-hole conjugation of $X(\boldsymbol{k},i\omega_n)$. The Fermi-Dirac statistics of electrons gives the symmetry relation in the anomalous Green's function $\mathcal{F}^{\mathrm{T}}(-\boldsymbol{k},-i\omega_n)=-\mathcal{F}(\boldsymbol{k},i\omega_n)$. The GL free-energy functional per unit

cell is represented in terms of the Green's function [100, 101]

$$\Omega_{\rm SN}(\Delta) = a\Delta^2 + b\Delta^4 + c\Delta^6 + \text{h. o. t.}, \tag{3.24}$$

$$a\Delta^2 = \frac{\Delta^2}{\tilde{g}} + T\sum_{\omega_n}\frac{1}{N}\sum_{\boldsymbol{k}}\frac{1}{2}\mathrm{Tr}\left[\mathcal{F}_1(\boldsymbol{k}, i\omega_n)\Delta^\dagger(\boldsymbol{k})\right], \tag{3.25}$$

$$b\Delta^4 = T\sum_{\omega_n}\frac{1}{N}\sum_{\boldsymbol{k}}\frac{1}{4}\mathrm{Tr}\left[\mathcal{F}_1(\boldsymbol{k}, i\omega_n)\Delta^\dagger(\boldsymbol{k})\mathcal{F}_1(\boldsymbol{k}, i\omega_n)\Delta^\dagger(\boldsymbol{k})\right], \tag{3.26}$$

$$c\Delta^6 = T\sum_{\omega_n}\frac{1}{N}\sum_{\boldsymbol{k}}\frac{1}{6}\mathrm{Tr}\left[\mathcal{F}_1(\boldsymbol{k}, i\omega_n)\Delta^\dagger(\boldsymbol{k})\mathcal{F}_1(\boldsymbol{k}, i\omega_n)\Delta^\dagger(\boldsymbol{k})\mathcal{F}_1(\boldsymbol{k}, i\omega_n)\Delta^\dagger(\boldsymbol{k})\right], \tag{3.27}$$

where $\mathcal{F}_1(\boldsymbol{k}, i\omega_n) \equiv -\mathcal{G}_{\rm N}(\boldsymbol{k}, i\omega_n)\Delta(\boldsymbol{k})\underset{\sim}{\mathcal{G}}_{\rm N}(\boldsymbol{k}, i\omega_n)$ is the anomalous Green's function within the first order of Δ and $\mathcal{G}_{\rm N}$ is the Green's function in the normal state. The calculated results are given by

$$\mathcal{F}_1(\boldsymbol{k}, i\omega_n) = \frac{\Delta}{Z_0}\left(f_1^{\Delta}(\boldsymbol{k}, i\omega_n) + f_1^{\rm s}(\boldsymbol{k}, i\omega_n) + f_1^{\rm q}(\boldsymbol{k}, i\omega_n) + f_1^{\rm odd}(\boldsymbol{k}, i\omega_n)\right), \tag{3.28}$$

$$f_1^{\Delta}(\boldsymbol{k}, i\omega_n) = -(\omega_n^2 + \xi_{\boldsymbol{k}}^2)\vec{\eta}_{\boldsymbol{k}}\cdot\vec{\gamma}\, U_T, \tag{3.29}$$

$$f_1^{\rm s}(\boldsymbol{k}, i\omega_n) = 2\xi_{\boldsymbol{k}}\,\vec{\eta}_{\boldsymbol{k}}\cdot\vec{\epsilon}_{\boldsymbol{k}}\, U_T, \tag{3.30}$$

$$f_1^{\rm q}(\boldsymbol{k}, i\omega_n) = -\vec{\epsilon}_{\boldsymbol{k}}\cdot\vec{\gamma}\,\vec{\eta}_{\boldsymbol{k}}\cdot\vec{\gamma}\,\vec{\epsilon}_{\boldsymbol{k}}\cdot\vec{\gamma}\, U_T, \tag{3.31}$$

$$f_1^{\rm odd}(\boldsymbol{k}, i\omega_n) = -i\omega_n P_{\rm O}\, U_T, \tag{3.32}$$

$$P_{\rm O} = \left[\vec{\eta}_{\boldsymbol{k}}\cdot\vec{\gamma}\,,\, \vec{\epsilon}_{\boldsymbol{k}}\cdot\vec{\gamma}\right], \tag{3.33}$$

$$\begin{aligned} Z_0 &= (\omega_n^2 + \xi_{\boldsymbol{k}}^2 - \vec{\epsilon}_{\boldsymbol{k}}^2)^2 + 4\omega_n^2\vec{\epsilon}_{\boldsymbol{k}}^2 \\ &= \xi_{\boldsymbol{k}}^4 + 2\xi_{\boldsymbol{k}}^2(\omega_n^2 - \vec{\epsilon}_{\boldsymbol{k}}^2) + (\omega_n^2 + \vec{\epsilon}_{\boldsymbol{k}}^2)^2, \end{aligned} \tag{3.34}$$

with $[A\,,\, B] = AB - BA$. f_1^{Δ} in Eq. (3.28) belongs to pseudospin-quintet symmetry and is linked to the pair potential through the gap equation. The spin-orbit interactions $\vec{\epsilon}_{\boldsymbol{k}}$ induce a pseudospin-singlet correlation function $f_1^{\rm s}$ and another pseudospin-quintet correlation function $f_1^{\rm q}$. $f_1^{\rm odd}$ represents an induced pairing correlation belonging to the odd-frequency symmetry class and holds finite value for $P_{\rm O} \neq 0$ [102, 103]. The structure of $f_1^{\rm q}$ is modified by $f_1^{\rm odd}$ since both correlation functions are connected each other by the Gor'kov equation in Eq. (3.23). Therefore the total even-frequency components which are linked to the pair potential

$$\mathrm{Tr}\left[\mathcal{F}_1(\boldsymbol{k}, i\omega_n)\Delta^\dagger(\boldsymbol{k})\right] = \frac{\Delta}{Z_0}\mathrm{Tr}\left[\left(f_1^{\Delta} + f_1^{\rm q}\right)\Delta^\dagger(\boldsymbol{k})\right], \tag{3.35}$$

are indirectly affected by the odd-frequency correlation function $f_1^{\rm odd}$.

In the absence of the odd-frequency pairing correlations (i.e., $P_{\rm O}=0$), $f_1^{\rm q}$ and the coefficients in the free-energy functional are calculated to be

$$f_1^{\rm q}(\boldsymbol{k},i\omega_n) = -\vec{\epsilon}_{\boldsymbol{k}}^{\,2}\,\vec{\eta}_{\boldsymbol{k}}\cdot\vec{\gamma}\,U_T, \tag{3.36}$$

$$a = \frac{1}{\tilde{g}} + T\sum_{\omega_n}\frac{1}{N}\sum_{\boldsymbol{k}}\frac{-2}{Z_0}(\omega_n^2+\xi_{\boldsymbol{k}}^2+\vec{\epsilon}_{\boldsymbol{k}}^{\,2}), \tag{3.37}$$

$$b = T\sum_{\omega_n}\frac{1}{N}\sum_{\boldsymbol{k}}\frac{1}{Z_0^2}\left\{(\omega_n^2+\xi_{\boldsymbol{k}}^2+\vec{\epsilon}_{\boldsymbol{k}}^{\,2})^2+4\xi_{\boldsymbol{k}}^2\vec{\epsilon}_{\boldsymbol{k}}^{\,2}\right\}\left\{2-|\vec{\eta}_{\boldsymbol{k}}\cdot\vec{\eta}_{\boldsymbol{k}}|^2\right\}. \tag{3.38}$$

$\vec{\epsilon}_{\boldsymbol{k}}^{\,2}$ in the last term of the numerator of Eq. (3.37) originates from $f_1^{\rm q}$ and amplifies the integrand. The coefficient a changes the sign at $T=T_c$. The gap equation corresponding to $a=0$ has the same expression as that in the BCS theory [103]. In addition, b is always positive. This means that the transition to the superconducting state is a second-order and that the superconducting state is stable for $T<T_c$. Therefore, the equation $P_{\rm O}=0$ characterizes the perturbations that preserve the thermal properties of the superconducting states. That is, the thermal properties of superconducting states in the absence of odd-frequency Cooper pairs are identical to those in the BCS state. Similarly, thermal properties of pseudospin-singlet pairing states coincide with the BCS state since there are no odd-frequency Cooper pairs. Pseudospin-singlet pair potential in the $j=3/2$ model is described by

$$\Delta(\boldsymbol{k}) = \Delta\,U_T, \tag{3.39}$$

in the BdG Hamiltonian in Eq. (3.4) [63, 64]. Here, Δ is chosen to be real. The anomalous Green's function within the first order of Δ results in,

$$\mathcal{F}_1^{\rm singlet} = \frac{\Delta}{Z_0}\left[-(\omega_n^2+\xi_{\boldsymbol{k}}^2+\vec{\epsilon}_{\boldsymbol{k}}^{\,2})+2\xi_{\boldsymbol{k}}\vec{\epsilon}_{\boldsymbol{k}}\cdot\vec{\gamma}\right]U_T. \tag{3.40}$$

In this pairing order, the spin-orbit interaction does not induce odd-frequency pairing correlations but generate an even-frequency pseudospin-quintet pairing correlation described by the second term in Eq. (3.40). The coefficients in the GL free-energy functional are expressed as

$$a^{\rm singlet} = \frac{1}{\tilde{g}} + T\sum_{\omega_n}\frac{1}{N}\sum_{\boldsymbol{k}}\frac{-2}{Z_0}(\omega_n^2+\xi_{\boldsymbol{k}}^2+\vec{\epsilon}_{\boldsymbol{k}}^{\,2}), \tag{3.41}$$

$$b^{\rm singlet} = T\sum_{\omega_n}\frac{1}{N}\sum_{\boldsymbol{k}}\frac{1}{Z_0^2}\left\{(\omega_n^2+\xi_{\boldsymbol{k}}^2+\vec{\epsilon}_{\boldsymbol{k}}^{\,2})^2+4\xi_{\boldsymbol{k}}^2\vec{\epsilon}_{\boldsymbol{k}}^{\,2}\right\}, \tag{3.42}$$

where $a^{\rm singlet}$ and $b^{\rm singlet}$ represent second and fourth-order coefficients of the GL functional, respectively. Since there are no odd-frequency Cooper pairs, the expression of $a^{\rm singlet}$ is equivalent to a in Eq. (3.37) and $b^{\rm singlet} > 0$ holds true. Therefore, the thermal property of the pseudospin-singlet state is identical to that of the BCS state as well as the pseudospin-quintet states without odd-frequency Cooper pairs.

In the presence of odd-frequency pairing correlation (i.e., $P_{\rm O} \neq 0$), it is not easy to obtain analytical expression of the GL coefficients without further simplifications. To proceed discussions, we restrict ourselves to consider E_g pairing order $\vec{\eta}_{\boldsymbol{k}} = (0, 0, 0, \eta_{\boldsymbol{k},4}, \eta_{\boldsymbol{k},5})$ because there are only two components in the pair potential. This simplification enables us to get the following analytical expressions:

$$f_1^{\rm q}(\boldsymbol{k}, i\omega_n) = \vec{\epsilon}_{\boldsymbol{k}}^2\, \vec{\eta}_{\boldsymbol{k}} \cdot \vec{\gamma}\, U_T - 2\vec{\epsilon}_{\boldsymbol{k}} \cdot \vec{\eta}_{\boldsymbol{k}}\, \vec{\epsilon}_{\boldsymbol{k}} \cdot \vec{\gamma}\, U_T, \tag{3.43}$$

$$a = \frac{1}{\tilde{g}} + T \sum_{\omega_n} \frac{1}{N} \sum_{\boldsymbol{k}} \frac{-2}{Z_0} (\omega_n^2 + \xi_{\boldsymbol{k}}^2 + \vec{\epsilon}_{\boldsymbol{k}}^2 - 2A_0), \quad A_0 = \vec{\epsilon}_{\boldsymbol{k}}^2 - |\vec{\epsilon}_{\boldsymbol{k}} \cdot \vec{\eta}_{\boldsymbol{k}}|^2, \tag{3.44}$$

$$\begin{aligned} b = T \sum_{\omega_n} \frac{1}{N} \sum_{\boldsymbol{k}} \frac{1}{Z_0^2} \Bigg[& (\omega_n^2 + \xi_{\boldsymbol{k}}^2 - \vec{\epsilon}_{\boldsymbol{k}}^2)^2 - 4\omega_n^2 \vec{\epsilon}_{\boldsymbol{k}}^2 \\ & - \left\{ (\omega_n^2 + \xi_{\boldsymbol{k}}^2 - \vec{\epsilon}_{\boldsymbol{k}}^2)^2 - 4\omega_n^2 \left(\epsilon_{\boldsymbol{k},1}^2 + \epsilon_{\boldsymbol{k},2}^2 + \epsilon_{\boldsymbol{k},3}^2 - \epsilon_{\boldsymbol{k},4}^2 - \epsilon_{\boldsymbol{k},5}^2 \right) \right\} \eta_{\boldsymbol{k},4}^2 \left(\eta_{\boldsymbol{k},5} - \eta_{\boldsymbol{k},5}^* \right)^2 \\ & + 8 |\vec{\epsilon}_{\boldsymbol{k}} \cdot \vec{\eta}_{\boldsymbol{k}}|^2 \left(\omega_n^2 + \xi_{\boldsymbol{k}}^2 - \vec{\epsilon}_{\boldsymbol{k}}^2 + |\vec{\epsilon}_{\boldsymbol{k}} \cdot \vec{\eta}_{\boldsymbol{k}}|^2 \right) \Bigg], \end{aligned} \tag{3.45}$$

where we chose the common phase factor of the pair potential so that Δ and $\eta_{\boldsymbol{k},4}$ are real but $\eta_{\boldsymbol{k},5}$ is complex in general. We found that the expression of $f_1^{\rm q}$ and a in Eqs. (3.43) and (3.44) is also valid for the general case: $\vec{\eta}_{\boldsymbol{k}} = (\eta_{\boldsymbol{k},1}, \eta_{\boldsymbol{k},2}, \eta_{\boldsymbol{k},3}, \eta_{\boldsymbol{k},4}, \eta_{\boldsymbol{k},5})$. Only f_1^{Δ} and $f_1^{\rm q}$ in $\mathcal{F}_1(\boldsymbol{k}, i\omega_n)$ contribute to a because $a = 0$ corresponds to the gap equation at $T = T_c$. Comparing with Eq. (3.37), an additional term $-2A_0$ appears in the presence of odd-frequency pairs in Eq. (3.44). The third and fourth terms in Eq. (3.44) ($\vec{\epsilon}_{\boldsymbol{k}}^2$ and $-2A_0$) originates from $f_1^{\rm q}$, which is affected by $f_1^{\rm odd}$ through the Gor'kov equation. Comparing with Eq. (3.36), it is important that the sign of the first term in Eq. (3.43) is reversed due to $f_1^{\rm odd}$ although there is a correction from the second term. Since $A_0 \geqq 0$, $f_1^{\rm odd}$ suppresses the amplitude of the even-frequency correlation function which is linked to the pair potential and indirectly decrease T_c due to their paramagnetic property [67]. Similar arguments have also been presented in other papers [14, 58, 59]. Even under the simplifications, it is not easy to extract the physical meaning from the coefficient b due to its quite complicated structure as shown in Eq. (3.45). To obtain the physical insights from the analytical expression of b, we also assume $(\eta_{\boldsymbol{k},4}, \eta_{\boldsymbol{k},5}) = (1, 0)$, $(0, 1)$, $(1, 1)/\sqrt{2}$, and $(1, i)/\sqrt{2}$. The first,

second, and fourth ones are predicted to be stable states within the phenomenological GL theory [64, 98, 104]. $P_{\rm O}$ for each state is calculated as

$$P_{\rm O}^{(1,0)} = 2\gamma^4 \sum_{\rm i\neq 4} \epsilon_{\boldsymbol{k},\rm i}\gamma^{\rm i}, \quad P_{\rm O}^{(0,1)} = 2\gamma^5 \sum_{\rm i\neq 5} \epsilon_{\boldsymbol{k},\rm i}\gamma^{\rm i}, \tag{3.46}$$

$$P_{\rm O}^{(1,1)/\sqrt{2}} = \sqrt{2}\left((\gamma^4+\gamma^5)\sum_{\rm i=1}^{3}\epsilon_{\boldsymbol{k},\rm i}\gamma^{\rm i} + (\epsilon_{\boldsymbol{k},5}-\epsilon_{\boldsymbol{k},4})\gamma^4\gamma^5\right), \tag{3.47}$$

$$P_{\rm O}^{(1,i)/\sqrt{2}} = \sqrt{2}\left((\gamma^4+i\gamma^5)\sum_{\rm i=1}^{3}\epsilon_{\boldsymbol{k},\rm i}\gamma^{\rm i} + (\epsilon_{\boldsymbol{k},5}-i\epsilon_{\boldsymbol{k},4})\gamma^4\gamma^5\right). \tag{3.48}$$

The analytical expressions of b in each state are

$$b^{\rm TRS} = T\sum_{\omega_n}\frac{1}{N}\sum_{\boldsymbol{k}}\frac{1}{Z_0^2}\Big[(\omega_n^2+\xi_{\boldsymbol{k}}^2-\vec{\epsilon}_{\boldsymbol{k}}^2)^2 + 4|\vec{\epsilon}_{\boldsymbol{k}}\cdot\vec{\eta}_{\boldsymbol{k}}|^2\left(\omega_n^2+2\xi_{\boldsymbol{k}}^2-2A_0\right) - 4\omega_n^2A_0\Big], \tag{3.49}$$

$$b^{\rm TRSB} = T\sum_{\omega_n}\frac{1}{N}\sum_{\boldsymbol{k}}\frac{1}{Z_0^2}\Big[2(\omega_n^2+\xi_{\boldsymbol{k}}^2-A_0+|\vec{\epsilon}_{\boldsymbol{k}}\cdot\vec{\eta}_{\boldsymbol{k}}|^2)^2 - 8\omega_n^2(A_0-|\vec{\epsilon}_{\boldsymbol{k}}\cdot\vec{\eta}_{\boldsymbol{k}}|^2)\Big], \tag{3.50}$$

where $b^{\rm TRS}$ is valid for $(\eta_{\boldsymbol{k},4},\eta_{\boldsymbol{k},5}) = (1,0)$, $(0,1)$, and $(1,1)/\sqrt{2}$ and $b^{\rm TRSB}$ is valid for $(1,i)/\sqrt{2}$. The last terms which are proportional to ω_n^2 in Eqs. (3.49) and (3.50) originates from $f_1^{\rm odd}$. We found that these terms are always less than or equal to zero. Thus the existence of these terms implies the sign change of b when the amplitude of $f_1^{\rm odd}$ is large enough. The equation $P_{\rm O}\neq 0$ characterizes the perturbations that change the thermal properties of the superconducting states. In terms of thermodynamic properties of superconductors, perturbations are distinguished by whether or not they induce odd-frequency Cooper pairs.

The sixth and higher order terms in Eq. (3.24) are also affected by the odd-frequency correlation functions. However, we are not able to divide the contributions from even and odd-frequency correlation functions due to the presence of the cross terms composed of these functions. For example, we consider $(\eta_{\boldsymbol{k},4},\eta_{\boldsymbol{k},5}) = (1,0)$ and $t_2 = 0$ in Eq. (3.4) as we assumed in Sec. 3.4. In this case, the sixth-order coefficient of the GL functional results in,

$$c = T\sum_{\omega_n}\frac{1}{N}\sum_{\boldsymbol{k}}\frac{-2}{3Z_0^3}\left\{(\omega_n^2+\xi_{\boldsymbol{k}}^2-\vec{\epsilon}_{\boldsymbol{k}}^2)^3 - 12\omega_n^2\vec{\epsilon}_{\boldsymbol{k}}^2(\omega_n^2+\xi_{\boldsymbol{k}}^2-\vec{\epsilon}_{\boldsymbol{k}}^2)\right\}. \tag{3.51}$$

The first term in Eq. (3.51) originates from the even-frequency correlation function. On the other hand, the second term is composed of both even and odd-frequency

correlation function. Although eighth-order coefficients and above are also modified by odd-frequency correlation functions, it is difficult to extract the physical meaning from these coefficients due to the cross terms. Thus it is difficult to extract physical meaning from these coefficients.

3.4 Discontinuous transition

In the previous section, we obtained that odd-frequency pairing correlation functions have negative contribution to the fourth order coefficient of GL free-energy. It implies that the transition to the superconducting phase becomes discontinuous. To progress the argument, we consider a specific pair potential represented by $(\eta_{\boldsymbol{k},4}, \eta_{\boldsymbol{k},5}) = (1, 0)$. In addition, we choose $t_2 = 0$ in the normal state Hamiltonian $H_{\rm N}(\boldsymbol{k})$ to obtain simple analytical solutions of the Gor'kov equation with infinite order of Δ in Eq. (3.23). Even under these simplifications, the following discussion is valid also for $(\eta_{\boldsymbol{k},4}, \eta_{\boldsymbol{k},5}) = (0, 1)$, $(1, 1)/\sqrt{2}$, and $(1, i)/\sqrt{2}$. The existence of odd-frequency Cooper pairs is a common feature among these states. The anomalous Green's function results in

$$\mathcal{F}(\boldsymbol{k}, i\omega_n) = -\frac{\Delta}{Z}\left[W - 2i\omega_n \vec{\epsilon}_{\boldsymbol{k}} \cdot \vec{\gamma}\right] \vec{\eta}_{\boldsymbol{k}} \cdot \vec{\gamma} U_T, \tag{3.52}$$

$$Z = W^2 + 4\omega_n^2 \vec{\epsilon}_{\boldsymbol{k}}^2, \quad W = \omega_n^2 + \xi_{\boldsymbol{k}}^2 - \vec{\epsilon}_{\boldsymbol{k}}^2 + \Delta^2. \tag{3.53}$$

The second term in Eq. (3.52) is the pairing correlation belonging to the odd-frequency symmetry class, which is induced by the spin-orbit interaction $\vec{\epsilon}_{\boldsymbol{k}}$. The coefficient of the fourth-order term is calculated to be

$$b(T) = T \sum_{\omega_n} \frac{1}{N} \sum_{\boldsymbol{k}} \frac{1}{Z_0^2} \left[W_0^2 - 4\omega_n^2 \vec{\epsilon}_{\boldsymbol{k}}^2\right], \tag{3.54}$$

with $Z_0 = Z|_{\Delta=0}$ and $W_0 = W|_{\Delta=0}$. The last term in Eq. (3.54) is derived from the odd-frequency pairing correlation functions and contributes negatively to the coefficient b. The results indicate the instability of the superconducting phase due to odd-frequency Cooper pairs. The amplitude of the pair potential Δ is determined self-consistently from the thermodynamic potential in the superconducting state

$$\Omega_{\rm S}(\Delta) = \frac{\Delta^2}{\tilde{g}} - \frac{2T}{N} \sum_{\boldsymbol{k}, \lambda = {\rm S}\pm} \log\left[2\cosh\left(\frac{E_\lambda(\boldsymbol{k})}{2T}\right)\right], \tag{3.55}$$

where $E_{\rm S\pm}(\boldsymbol{k}) = \sqrt{\xi_{\boldsymbol{k}}^2 + \Delta^2} \pm |\vec{\epsilon}_{\boldsymbol{k}}|$ and irrelevant constants are neglected. The pair potential is determined by minimizing $\Omega_{\rm S}(\Delta)$ with respect to Δ. Thus, the solution in

the equilibrium state ($\Delta_{\rm eq}$) always satisfies

$$\Omega_{\rm SN}(\Delta_{\rm eq}) = \min_{\Delta} \{\Omega_{\rm SN}(\Delta) \,|\, \Delta \in \mathbb{R}\} \leqq 0, \tag{3.56}$$

with $\Omega_{\rm SN}(\Delta) \equiv \Omega_{\rm S}(\Delta) - \Omega_{\rm S}(0)$. The solution of $\Delta_{\rm eq}$ is plotted as a function of temperature in Fig. 3.1(a) for several choices of spin-orbit interaction t_3. Hereafter, the transition temperature at $t_3 = 0$ is denoted by T_0, and the pair potential at $T = 0$ and $t_3 = 0$ is denoted by Δ_0. In the numerical simulation, we chose $\mu = t_1$ and $\tilde{g} = 2.463t_1$ so that $T_0 = 0.05t_1$. We obtained $\Delta_0 = 0.0882t_1 \approx 1.76T_0$, which corresponds to BCS universal relation [68]. The transition temperature decreases monotonically with increasing t_3. Although $\Delta_{\rm eq}$ is insensitive to t_3 at very low temperature $T \ll T_0$, it abruptly vanishes for $t_3 \gtrsim 0.023t_1$. Uniform superconducting states are no longer stable under strong spin-orbit couplings. Furthermore, $\Delta_{\rm eq}$ shows the discontinuous behavior at T_c for $t_3 \gtrsim 0.0205t_1$. In Fig. 3.1(b), the coefficient $b(T_c)$ is plotted as a function of t_3. We obtained $b(T_0) = 1.237t_1^{-3}$ at $t_3 = 0$. As predicted in Eq. (3.54), the odd-frequency pairing correlations decrease the coefficient $b(T_c)$. As a result, the transition becomes discontinuous for $b(T_c) < 0$ as shown in Fig. 3.1(a) and (b). Thus, odd-frequency Cooper pairs are responsible for the discontinuous transition to the superconducting states.

3.5 Superfluid density

To understand why odd-frequency Cooper pairs cause the discontinuous transition, we discuss the relationship between the coefficient b and the response function to an electromagnetic field,

$$j_x(\boldsymbol{q}, \omega) = -K_{xx}(\boldsymbol{q}, \omega) A_x(\boldsymbol{q}, \omega), \tag{3.57}$$

where j_ν is the electric current and $A_\nu(\boldsymbol{q}, \omega)$ is the Fourier component of a vector potential. The derivation of the response kernel $K_{\nu\nu}$ is presented in Appendix A. The response kernel to a static transverse gauge potential is called the Meissner kernel or *superfluid density*

$$Q = \frac{K_{xx}(\boldsymbol{q} \to 0, \omega = 0)}{2e^2 t_1}, \tag{3.58}$$

where e is the charge of an electron and Q is dimensionless. In Fig. 3.1(c), the superfluid density Q is plotted as a function of temperature for several choices of t_3, where $Q_0 =$

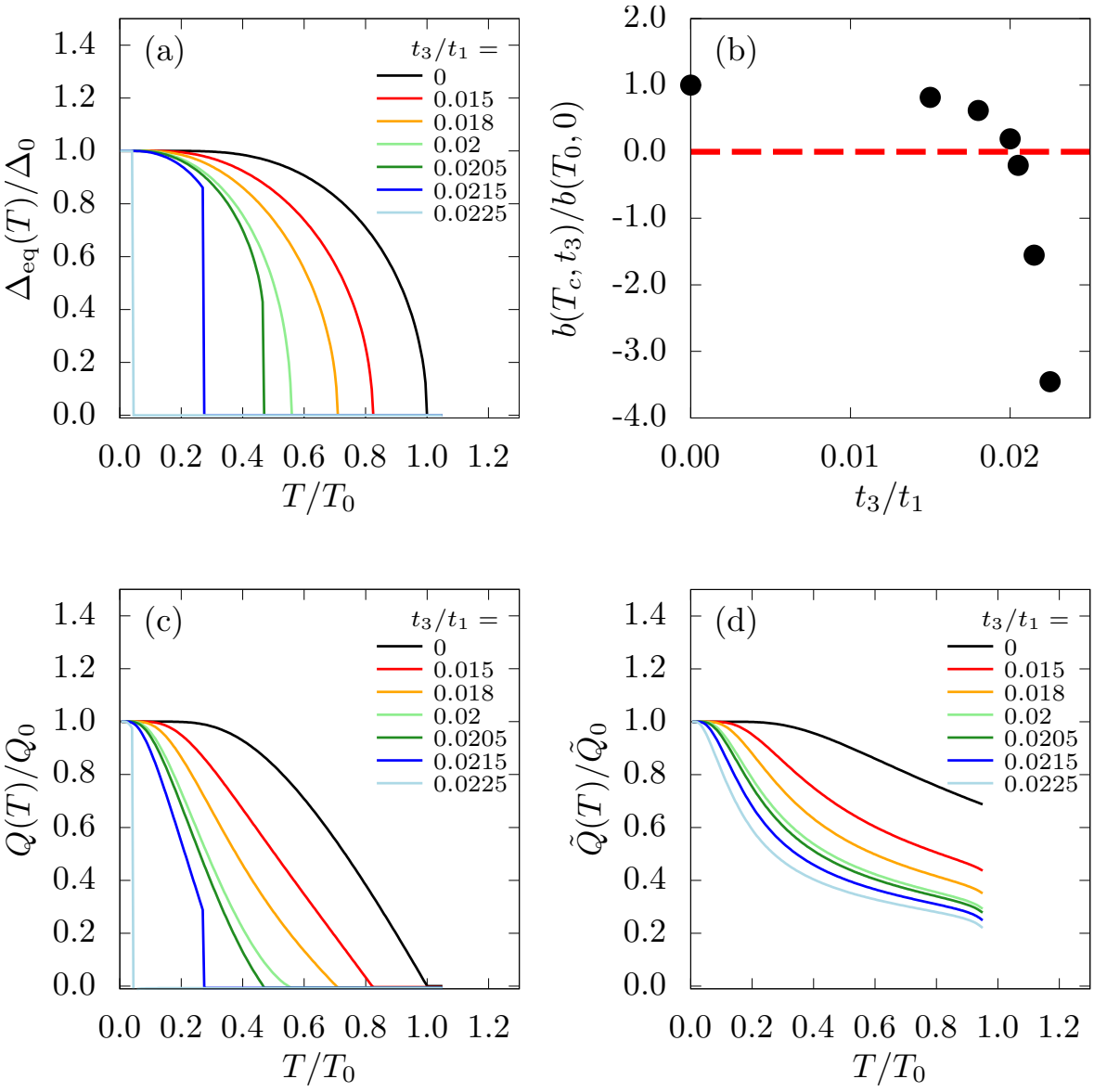

Figure 3.1: The self-consistent solution of the pair potential $\Delta_{\rm eq}(T)$ in a $j = 3/2$ superconductor is plotted as a function of temperature for several strengths of spin-orbit interaction t_3 in (a), where T_0 is the transition temperature at $t_3 = 0$ and Δ_0 is the amplitude of the pair potential at $T = 0$ and $t_3 = 0$. The coefficient b at $T = T_c$ is plotted as a function of t_3 in (b), where T_c is obtained from the results in (a). The temperature dependence of the superfluid density Q and $\tilde{Q}$ is shown in (c) and (d), respectively. Q_0 ($\tilde{Q}_0$) in (c) ((d)) represents Q ($\tilde{Q}$) at $T = 0$ and $t_3 = 0$.

0.0664 is the superfluid density at $T = 0$ and $t_3 = 0$ in our numerical simulation. At $T \approx 0$, the superfluid density is almost independent of t_3 for $t_3 \lesssim 0.0225 t_1$. However, the superfluid density decreases drastically at finite temperatures. To understand such characteristic features, we analyze the contribution of the anomalous Green's function in Eq. (3.52) to the superfluid density,

$$Q^{\mathcal{F}} = T \sum_{\omega_n} \frac{1}{N} \sum_{\boldsymbol{k}} 2t_1 \sin^2 k_x \frac{4\Delta^2}{Z^2} \left[W^2 - 4\omega_n^2 \vec{\epsilon}_{\boldsymbol{k}}^2 \right]. \tag{3.59}$$

The second term is derived from the odd-frequency pairing correlations and reduces the superfluid density. The dependence of Q on temperature in Fig. 3.1(c) is dominated mainly by that of $\Delta_{\rm eq}^2(T)$ because Q is proportional to $\Delta_{\rm eq}^2(T)$ as shown in Eq. (3.59). Thus, it is not easy to extract the effects of odd-frequency pairs on the superfluid density. To highlight a role of odd-frequency pairs in the discontinuous transition, we calculate

$$\tilde{Q}(T, t_3) = \frac{Q(T, t_3, \Delta_{\rm BCS}(T))}{\Delta_{\rm BCS}^2(T)}, \tag{3.60}$$

for $T < T_0$. Here we first replace $\Delta_{\rm eq}(T, t_3)$ by

$$\Delta_{\rm BCS}(T) = \Delta_{\rm eq}(T, t_3 = 0), \tag{3.61}$$

and divide the results by $\Delta_{\rm BCS}^2(T)$ to relax the influence of $\Delta_{\rm BCS}(T)$. $Q(T, t_3, \Delta_{\rm eq}(T, t_3))$ corresponds to $Q(T)$ shown in Fig. 3.1(c). In Fig. 3.1(d), $\tilde{Q}$ is plotted for several choices of t_3. The vertical axis is normalized to $\tilde{Q}_0 = \tilde{Q}(T = 0, t_3 = 0)$. The black line for $t_3 = 0$ almost corresponds to the results of BCS theory

$$\frac{\tilde{Q}(T, t_3 = 0)}{\tilde{Q}_0} \approx \Delta_0^2 \pi T \sum_{\omega_n} \frac{1}{(\omega_n^2 + \Delta_{\rm BCS}^2(T))^{3/2}}, \tag{3.62}$$

and decreases with increasing temperature almost linearly for $T \gtrsim 0.3 T_0$. $\tilde{Q}$ at $T = 0$ remains unchanged even in the presence of the spin-orbit interaction, whereas it at finite temperatures decreases with increasing t_3. The suppression from the black line is remarkable for $0.2 \lesssim T/T_0 \lesssim 0.5$. As a result, the curves for $t_3/t_1 = 0.018 - 0.0225$ are convex downward. The drastic suppression of the superfluid density in such finite temperatures is responsible for the suppression of T_c and the discontinuous transition finding at $t_3/t_1 \gtrsim 0.0205$. When we compare Eq. (3.54) with Eq. (3.59), the odd-frequency pairs decrease the coefficient b and the superfluid density $Q^{\mathcal{F}}$ in the same

manner. As shown in Eq. (3.52), the odd-frequency pairing correlation function is proportional to the Matsubara frequency, which is a common property of odd-frequency pairs in uniform superconductors [14, 67]. As a result, the effect of odd-frequency pairs on the instability is considerable at finite temperatures [105]. The temperature dependence of $\tilde{Q}$ and the discontinuous change of $\Delta_{\rm eq}$ and Q are the consequence of the presence of such odd-frequency Cooper pairs. We conclude that the discontinuous transition to the superconducting phase occurs because odd-frequency Cooper pairs reduce the superfluid density at finite temperatures.

3.6 Universality of phenomenon

The discontinuous transition due to odd-frequency Cooper pairs and the close relationship between b and Q are confirmed in other superconducting states. Indeed, the expression in Eqs. (3.54) and (3.59) can be applied also to $(\eta_{\boldsymbol{k},4}, \eta_{\boldsymbol{k},5}) = (0, 1)$ and $(1, 1)/\sqrt{2}$. The discontinuous transition in $j = 3/2$ superconductors has also been reported in T_{2g} pairing states at $T \geqq 0$ [70]. The authors of Ref. [70] found that the interband pairing is responsible for the discontinuous transition. Here, *band* means the diagonalized normal state band. Although there are some relations between interband pairing and odd-frequency Cooper pair, these are not equivalent concept. It can be the case that interband pairing corresponds to even-frequency Cooper pair and stabilizes the superconducting order. We present the examples in Appendix B. Odd-frequency Cooper pairs provide us clear insights to discuss the thermodynamic properties by their paramagnetic property. The instability at $T = 0$ for both T_{2g} and E_g pairing states has been also implied in Ref. [106]. The authors of Ref. [106] compared the free-energy among multiple superconducting states and concluded that the transition to another superconducting phase becomes first-order transition with changing the amplitude of the attractive interaction between the two electrons. If we assume that there are only one superconducting phase, the first-order transition from the normal state to the uniform superconducting state would relate to the discontinuous transition discussed in this study. Such abrupt change of the equilibrium state is similar to our results at $T = 0$. In addition to the studies in $j = 3/2$ superconductors, discontinuous transition was found in a two-band superconductor with interband pairing order when the band hybridization V is large enough [107]. In this model, V corresponds to the interaction which induces odd-frequency Cooper pairs and their paramagnetic property explains the mechanism of the discontinuous transition well. The detailed discussion about the interband superconductor considered in Ref. [107] is presented in Appendix B. The existence of odd-frequency Cooper pairs is a common feature among these supercon-

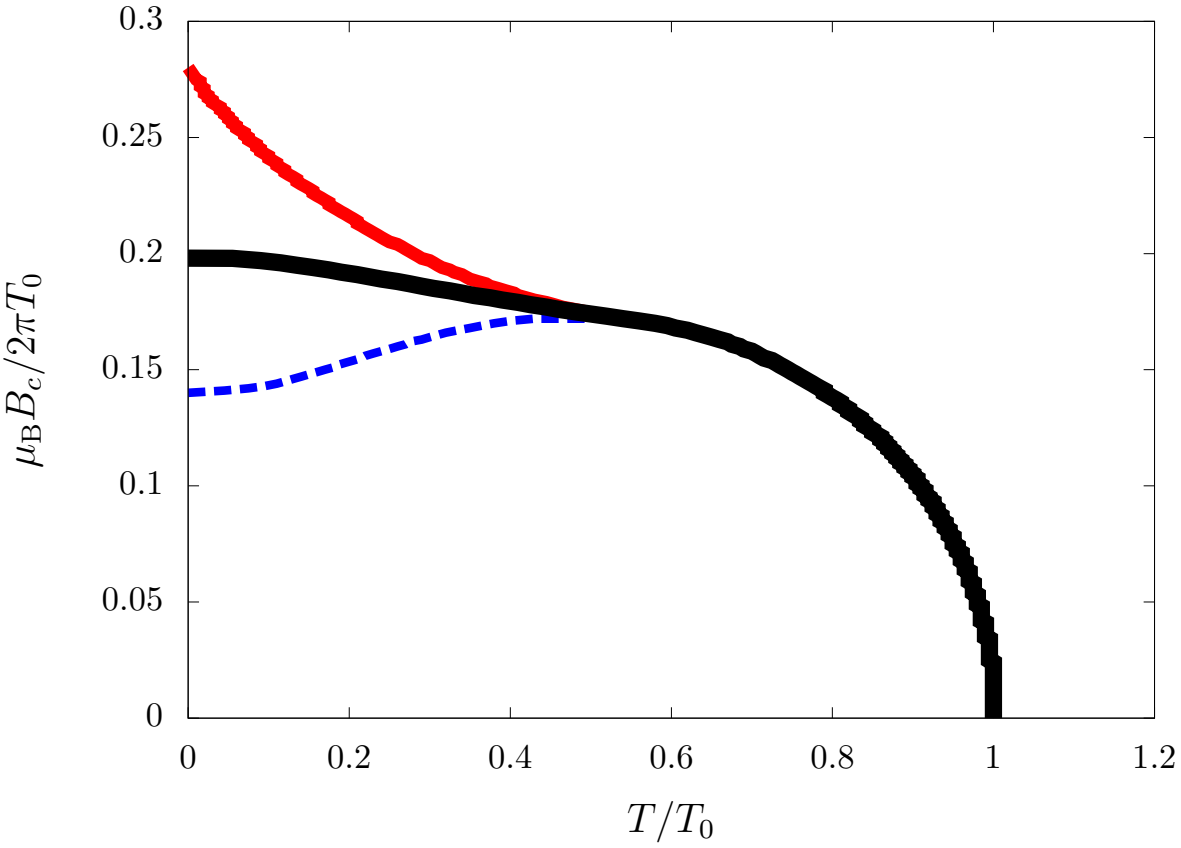

Figure 3.2: The critical value of the Zeeman fields B_c in a spin-singlet s-wave superconductor is plotted as a function of temperature, where T_0 is the transition temperature at $B = 0$. We reproduced the results obtained in Refs. [91, 92]. The black line is obtained by using the solutions giving the global minimum of the thermodynamic potential while the red (broken blue) line is obtained by using the solutions giving the local minimum (maximum) of the thermodynamic potential.

ducting states and is responsible for the discontinuous transition.

Finally, we emphasize the relevance of the conclusions in this chapter to an important open issue. The transition to the uniform spin-singlet s-wave superconducting state is known to be discontinuous under a Zeeman field B [91, 92, 108, 109]. Fig. 3.2 shows the temperature dependence of the critical field B_c. We showed that the critical field in the equilibrium state by the black line in Fig. 3.2. The critical field in the metastable state is represented by the red line. The broken blue line is obtained by using the solution giving the local maximum of the thermodynamic potential. Below the temperature at which the lines intersect ($T/T_0 \approx 0.56$), the transition becomes discontinuous [91, 92]. The calculated results for the coefficient b and the superfluid

density Q are given by

$$b = \frac{N_0}{4} Y(A_0, C_0), \tag{3.63}$$

$$Q = 2n\Delta^2 Y(A, C), \tag{3.64}$$

$$Y(A, C) = \sqrt{2}\pi T \sum_{\omega_n} \frac{A^3 + \sqrt{C}(A^2 - 2\omega_n^2 \mu_{\rm B}^2 B^2)}{[C(A + \sqrt{C})]^{3/2}}, \tag{3.65}$$

$$A = \Delta^2 + \omega_n^2 - \mu_{\rm B}^2 B^2,\ C = A^2 + 4\omega_n^2\, \mu_{\rm B}^2 B^2, \tag{3.66}$$

where $A_0 = A|_{\Delta=0}$, $C_0 = C|_{\Delta=0}$, $\mu_{\rm B}$ is Bohr's magneton, N_0 is the density of states at the Fermi level per spin in the normal state, and n is the electron density per spin. The derivations are given in Appendix. C. We also calculate

$$\begin{aligned} \tilde{Q}(T, B) &= \frac{Q(T, B, \Delta_{\rm BCS}(T))}{\Delta_{\rm BCS}^2(T)} \\ &= 2nY(A, C)|_{\Delta=\Delta_{\rm BCS}(T)}, \end{aligned} \tag{3.67}$$

where $\Delta_{\rm BCS}(T) = \Delta_{\rm eq}(T, B = 0)$ represents the pair potential of a BCS superconductor. The coefficient and the superfluid density share exactly the same expression for $\Delta \ll T$. The last term in Eq. (3.65) is derived from the odd-frequency pairing correlation, which is generated by a Zeeman field and is proportional to the Matsubara frequency. The self-consistent pair potential $\Delta_{\rm eq}$, the coefficient b at the transition temperature, the superfluid density Q, and $\tilde{Q}$ in the spin-singlet superconductor are plotted in Fig. 3.3(a), (b), (c), and (d), respectively. We denote the transition temperature at $B = 0$ by T_0 and the pair potential at $T = 0$ and $B = 0$ by $\Delta_0 \approx 1.76T_0$ [68]. The coefficient b at $T = T_0$ and $B = 0$ corresponds to the BCS results: $b_{\rm BCS}(T_0) = N_0 \frac{7\zeta(3)}{16(\pi T_0)^2}$. $Q_0 = 2n$ is the superfluid density at $T = 0$ and $B = 0$. $\tilde{Q}_0 = 2n/\Delta_0^2$ represents $\tilde{Q}$ at $T = 0$ and $B = 0$. The characteristic properties shown in Fig. 3.3 coincide with those in Fig. 3.1. The results suggest the universality of the phenomenon.

The discontinuous transition is caused by odd-frequency Cooper pair ($f^{\rm odd}$) and the reason is explained well by two basic properties of odd-frequency Cooper pair: *paramagnetism* and $f^{\rm odd} \propto \omega_n$. Therefore, we conclude a potential for the discontinuous transition is a common property among superconductors that contain subdominant odd-frequency Cooper pairs.

Fulde-Ferrell-Larkin-Ovchinnikov (FFLO) states can appear at high fields [110, 111]. For $\mu_{\rm B}B/2\pi T_0 \gtrsim 0.18$, such oscillating states become a stable solution [112]. Theoretical studies [113, 114] showed that the transition from the normal state to the FFLO state can be both first and second-order and it depends on the parameters.

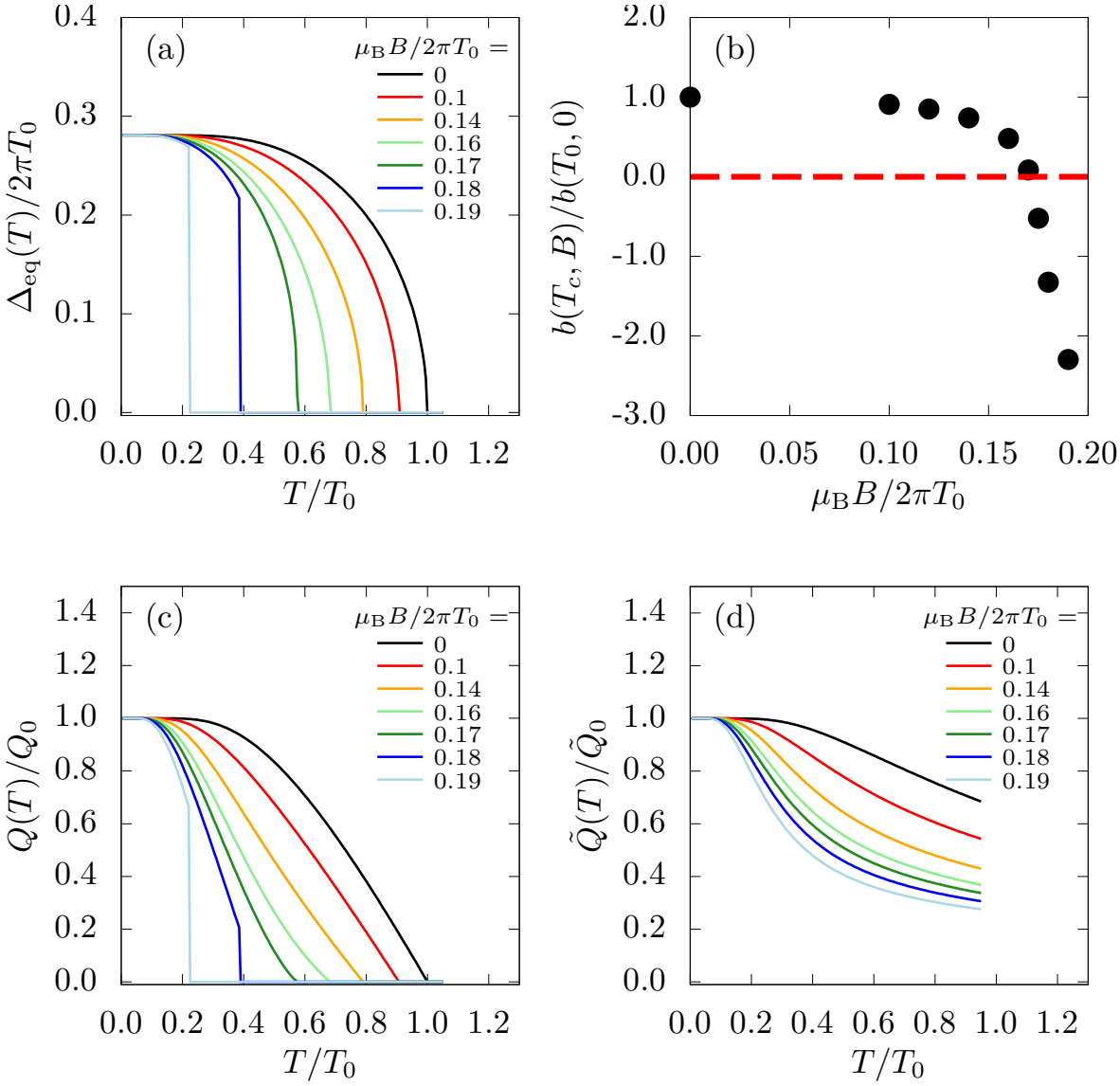

Figure 3.3: The self-consistent solution of the pair potential $\Delta_{\rm eq}(T)$ in a spin-singlet superconductor under a Zeeman field is plotted as a function of temperature for several strengths of Zeeman interaction B in (a), where T_0 is the transition temperature at $B = 0$ and Δ_0 is the amplitude of the pair potential at $T = 0$ and $B = 0$. The coefficient b at $T = T_c$ is plotted as a function of B in (b), where T_c is obtained from the results in (a). The temperature dependence of the superfluid density Q and $\tilde{Q}$ is shown in (c) and (d), respectively. Q_0 ($\tilde{Q}_0$) in (c) ((d)) represents Q ($\tilde{Q}$) at $T = 0$ and $B = 0$.

Since odd-frequency Cooper pairs also exist in such regime [80, 115], there might be nontrivial relationships between the non-uniform odd-frequency Cooper pairs and the order of the phase transition. However, the problem is beyond the scope of this study and is left for our future study.

3.7 Conclusion

We have theoretically studied the thermodynamic instability of uniform superconducting states including the subdominant pairing correlations belonging to the odd-frequency symmetry class. In $j = 3/2$ superconductors, we analyzed the contributions of the odd-frequency pairing correlations to the coefficients of Δ^4 term in Ginzburg-Landau (GL) free-energy, the pair potential, and the superfluid density. The odd-frequency pairing correlations decrease the coefficient and the superfluid density in the same manner. Since the effects are considerable at finite temperature, the transition to a superconducting phase becomes discontinuous. We conclude that a potential for the discontinuous transition to the superconducting state is a common feature of superconductors that accommodate odd-frequency Cooper pairs.

Chapter 4

Superconductivity in Cu-doped Bi_2Se_3 with potential disorder

4.1 Abstract

We study the effects of random nonmagnetic impurities on superconducting transition temperature T_c in a Cu-doped Bi_2Se_3, for which four types of pair potentials have been proposed. Although all the candidates belong to s-wave symmetry, two orbital degree of freedom in electronic structures enriches the symmetry variety of a Cooper pair such as even-orbital-parity and odd-orbital-parity. We consider realistic electronic structures of Cu-doped Bi_2Se_3 by using tight-binding Hamiltonian on a hexagonal lattice and consider effects of impurity scatterings through the self-energy of the Green's function within the Born approximation. We find that even-orbital-parity spin-singlet superconductivity is basically robust even in the presence of impurities. The degree of the robustness depends on the electronic structures in the normal state and on the pairing symmetry in orbital space. On the other hand, two odd-orbital-parity spin-triplet order parameters are always fragile in the presence of potential disorder.

4.2 Introduction

The robustness of superconductivity in the presence of nonmagnetic impurities depends on symmetry of the pair potential. The transition temperature T_c is insensitive to the impurity concentration in a spin-singlet s-wave superconductor [69, 116, 117]. In a cuprate superconductor, on the other hand, T_c of a spin-singlet d-wave superconductivity is suppressed drastically by the impurity scatterings [118]. The pair potential of an unconventional superconductor changes its sign on the Fermi surface depending

on the direction of a quasiparticle's momenta. The random impurity scatterings make the motion of a quasiparticle be isotropic in both real and momentum spaces. Such a diffused quasiparticle feels the pair potential averaged over the directions of momenta. The resulting pair potential is finite for an s-wave symmetry, whereas it is zero for unconventional pairing symmetries. Thus, unconventional superconductivity is fragile under the potential disorder.

Previous papers [71, 119–123] showed that s-wave superconductivity is not always robust against the nonmagnetic impurity scatterings in multiband (multiorbital) superconductors. The interorbital impurity scatterings decrease T_c, which is a common conclusion of all the theoretical studies. The two-band models considered in these papers, however, are too simple to discuss the effects of impurities on T_c in real materials such as iron pnictides [54, 124], MgB_2 [49, 50], and Cu-doped Bi_2Se_3 [56, 57]. The robustness of multiband superconductivity under the potential disorder may depend on electronic structures near the Fermi level. In iron pnictides and MgB_2, two electrons in the same conduction band form a Cooper pair [50, 124]. The impurity effect on such an intraband pair has been studied by taking realistic electronic structures into account [125]. In the case of Cu-doped Bi_2Se_3, four types of pair potentials $\Delta_1 - \Delta_4$ have been proposed as a promising candidate of order parameter [57]. Among them, an interorbital pairing order has attracted much attention as a topologically nontrivial superconductivity [57, 126]. Unfortunately, the possibility of such a topological superconductivity under the potential disorder has never been studied yet. We address this issue.

In this chapter, we study the effects of impurities on T_c of Cu-doped Bi_2Se_3. We describe electronic structures near the Fermi level by taking into account two p orbitals in Bi_2Se_3 and the hybridization between them [127, 128]. According to the theoretical proposal [57], we consider four types of s-wave pair potential on such orbital based electronic structures. The effects of impurities on T_c are estimated through the impurity self-energy within the Born approximation. The transition temperature is calculated by solving the gap equation numerically and is plotted as a function of impurity concentration $n_{\rm imp}$. We will show that the relation between T_c and $n_{\rm imp}$ depends sensitively on the types of pair potentials. Superconductivity with an intraorbital pair potential Δ_1 is robust even in the dirty regime. This conclusion is consistent with that at a limiting case of previous studies [71, 120–122]. There are two kinds of interorbital pairing order: even-orbital symmetry and odd-orbital symmetry. We find that T_c of an even-interorbital superconductivity Δ_3 decreases slowly with the increase of $n_{\rm imp}$ and vanishes in the dirty limit. The results for Δ_3 disagree with those in a simple two-band model [123] because the robustness of Δ_3 depends sensitively on electronic structures.

Finally, the odd-interorbital pairing orders (Δ_2 and Δ_4) vanish at a critical value of the impurity concentration, which agrees well with the results of a idealistic two-band model [123]. Thus we conclude that odd-orbital pair potential is fragile irrespective of electronic structures.

This chapter is organized as follows. In Sec. 4.3, we describe the effective Hamiltonian near the Fermi level in Cu-doped Bi_2Se_3 and four types of pair potentials in its superconducting state. The anomalous Green's function and the gap equation for each pair potential in the clean limit are obtained by solving the Gor'kov equation. In Sec. 4.4, we introduce the random impurity potential and discuss the effects of impurities on T_c within the Born approximation. The conclusion is given in Sec. 4.5. Throughout this chapter, we use the units of $k_{\rm B} = \hbar = 1$, where $k_{\rm B}$ is the Boltzmann constant. The symbol $\cdot\bar{\cdot}\cdot$, $\cdot\check{\cdot}\cdot$, and $\cdot\hat{\cdot}\cdot$ represent 8×8, 4×4, and 2×2 matrices, respectively.

4.3 Clean limit

4.3.1 Model

For constructing an effective model of the normal state, we start with the tight-binding Hamiltonian on a hexagonal lattice as shown in Fig. 4.1 [129]. Strictly speaking, the crystal structure of Bi_2Se_3 is rhombohedral [127, 128]. The simplification does not affect the low energy physics. We assume that an intercalated copper atom supplies electrons and makes a topological insulator Bi_2Se_3 be metallic [130]. In the hexagonal lattice, the primitive lattice vectors are $\left(\sqrt{3}a/2, a/2, 0\right)$, $(0, a, 0)$, $(0, 0, c)$ where a and c are the lattice constants in the xy plane and along the z axis, respectively. We define the nearest neighbor vectors $\boldsymbol{a}_1 = \left(\sqrt{3}a/2, a/2, 0\right)$, $\boldsymbol{a}_2 = (0, a, 0)$, $\boldsymbol{a}_3 = \left(-\sqrt{3}a/2, a/2, 0\right)$, and $\boldsymbol{a}_4 = (0, 0, c)$. The tight-binding Hamiltonian in real space can be written as [129, 131]

$$H_N = \sum_{\boldsymbol{R}} \boldsymbol{\psi}^\dagger_{\boldsymbol{R}} \check{\varepsilon} \boldsymbol{\psi}_{\boldsymbol{R}} + \sum_{\boldsymbol{R},i} \boldsymbol{\psi}^\dagger_{\boldsymbol{R}} \check{t}_{\boldsymbol{a}_i} \boldsymbol{\psi}_{\boldsymbol{R}+\boldsymbol{a}_i} + \text{H.c.}, \tag{4.1}$$

$$\boldsymbol{\psi}_{\boldsymbol{R}} = \left[\psi_{+,\uparrow}(\boldsymbol{R}), \psi_{-,\uparrow}(\boldsymbol{R}), \psi_{+,\downarrow}(\boldsymbol{R}), \psi_{-,\downarrow}(\boldsymbol{R})\right]^{\rm T}, \tag{4.2}$$

where $\psi^\dagger_{\sigma,s}$ ($\psi_{\sigma,s}$) is the creation (annihilation) operator of an electron at the orbital σ ($= +$ or $-$) with spin s ($=\uparrow$ or $\downarrow$). We consider only the nearest neighbor hopping on the hexagonal lattice in the xy plane and that along the z axis. An orbital $+$ ($-$) mainly consists of p_z orbital of a Bi (Se) atom. The matrix element of hopping $\check{t}_{\boldsymbol{a}_i}$

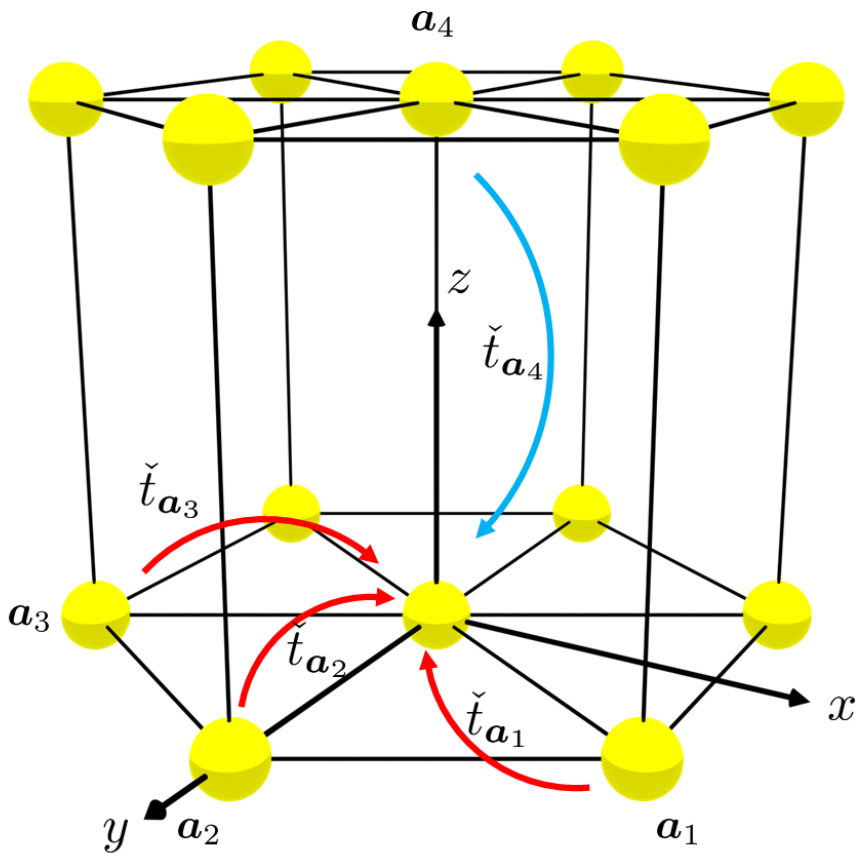

Figure 4.1: The simplified lattice structure of a Cu-doped Bi_2Se_3. The arrow indicates the hopping.

$(i = 1 - 4)$ is described as

$$\langle \boldsymbol{R}, \sigma, s | \, H \, | \boldsymbol{R} + \boldsymbol{a}_i, \sigma', s' \rangle \, . \tag{4.3}$$

The nearest neighbor hopping elements are illustrated in Fig. 4.1. In momentum space, the tight-binding Hamiltonian is described as

$$\check{H}_N(\boldsymbol{k}) = \check{\varepsilon} + \sum_i \check{t}_{\boldsymbol{a}_i} e^{i\boldsymbol{k}\cdot\boldsymbol{a}_i} + \text{H.c.}. \tag{4.4}$$

The matrix structures of $\check{t}_{\boldsymbol{a}_i}$ are given in Appendix D. The tight-binding Hamiltonian can be written as

$$\check{H}_N(\boldsymbol{k}) = c_{\boldsymbol{k}}\hat{s}_0\hat{\sigma}_0 + m_{\boldsymbol{k}}\hat{s}_0\hat{\sigma}_3 + V_z\hat{s}_0\hat{\sigma}_2 + (V_y\hat{s}_1 - V_x\hat{s}_2)\hat{\sigma}_1, \tag{4.5}$$

$$c_{\boldsymbol{k}} = -\mu + c_1\alpha_1(\boldsymbol{k}) + c_2\alpha_2(\boldsymbol{k}), \tag{4.6}$$

$$m_{\boldsymbol{k}} = m_0 + m_1\alpha_1(\boldsymbol{k}) + m_2\alpha_2(\boldsymbol{k}), \tag{4.7}$$

$$V_{x,y} = v\alpha_{x,y}(\boldsymbol{k}), \tag{4.8}$$

$$V_z = v_z\alpha_z(\boldsymbol{k}), \tag{4.9}$$

where $\alpha_i(\boldsymbol{k})$ $(i = 1, 2, x, y, z)$ is

$$\alpha_1(\boldsymbol{k}) = \frac{2}{c^2}\left(1 - \cos k_z c\right), \tag{4.10}$$

$$\alpha_2(\boldsymbol{k}) = \frac{4}{3a^2}\left(3 - 2\cos\frac{\sqrt{3}k_x a}{2}\cos\frac{k_y a}{2} - \cos k_y a\right), \tag{4.11}$$

$$\alpha_x(\boldsymbol{k}) = \frac{2}{\sqrt{3}a}\sin\frac{\sqrt{3}k_x a}{2}\cos\frac{k_y a}{2}, \tag{4.12}$$

$$\alpha_y(\boldsymbol{k}) = \frac{2}{3a}\left(\cos\frac{\sqrt{3}k_x a}{2}\sin\frac{k_y a}{2} + \sin k_y a\right), \tag{4.13}$$

$$\alpha_z(\boldsymbol{k}) = \frac{1}{c}\sin k_z c. \tag{4.14}$$

We define the Pauli matrices $\hat{s}_j$ in spin space, $\hat{\sigma}_j$ in orbital space, and $\hat{\tau}_j$ in particle-hole space for $j = 1 - 3$. The unit matrix in these spaces are $\hat{s}_0$, $\hat{\sigma}_0$, and $\hat{\tau}_0$. In Eq. (4.5), the hopping in the z direction ($\check{t}_{\boldsymbol{a}_4}$) causes the orbital hybridization term V_z and the hopping in the xy plane ($\check{t}_{\boldsymbol{a}_1}$, $\check{t}_{\boldsymbol{a}_2}$, $\check{t}_{\boldsymbol{a}_3}$) causes the spin-orbit interaction term $V_{x,y}$. When we expand the trigonometric functions around the Γ point, the tight-binding Hamiltonian $\check{H}_N(\boldsymbol{k})$ corresponds to $\boldsymbol{k}\cdot\boldsymbol{p}$ Hamiltonian of Bi_2Se_3 [127, 128].

The superconducting state in $Cu_xBi_2Se_3$ is described by a Hamiltonian

$$\mathcal{H}^{(0)} = \sum_{\boldsymbol{k}} \boldsymbol{\Psi}^\dagger(\boldsymbol{k}) \bar{H}_{\boldsymbol{k}}^{(0)} \boldsymbol{\Psi}(\boldsymbol{k}), \quad \boldsymbol{\Psi}(\boldsymbol{k}) = \begin{bmatrix} \boldsymbol{\psi}_e(\boldsymbol{k}) \\ \boldsymbol{\psi}_h(\boldsymbol{k}) \end{bmatrix}, \tag{4.15}$$

$$\boldsymbol{\psi}_e(\boldsymbol{k}) = \begin{bmatrix} \psi_{+,\uparrow}(\boldsymbol{k}) \\ \psi_{-,\uparrow}(\boldsymbol{k}) \\ \psi_{+,\downarrow}(\boldsymbol{k}) \\ \psi_{-,\downarrow}(\boldsymbol{k}) \end{bmatrix}, \ \boldsymbol{\psi}_h(\boldsymbol{k}) = \begin{bmatrix} \psi^\dagger_{+,\uparrow}(-\boldsymbol{k}) \\ \psi^\dagger_{-,\uparrow}(-\boldsymbol{k}) \\ \psi^\dagger_{+,\downarrow}(-\boldsymbol{k}) \\ \psi^\dagger_{-,\downarrow}(-\boldsymbol{k}) \end{bmatrix}, \tag{4.16}$$

$$\bar{H}_{\boldsymbol{k}}^{(0)} = \begin{pmatrix} \check{H}_N(\boldsymbol{k}) & \check{\Delta}_\lambda \\ \check{\Delta}_\lambda^\dagger & -\check{H}_N^*(-\boldsymbol{k}) \end{pmatrix}. \tag{4.17}$$

According to the previous proposal [57], we consider four types of momentum-independent pair potential defined by

$$\Delta_1 = \frac{g_1}{N} \sum_{\boldsymbol{k}} \langle \psi_{+,\uparrow}(\boldsymbol{k}) \psi_{+,\downarrow}(-\boldsymbol{k}) \rangle = \frac{g_1}{N} \sum_{\boldsymbol{k}} \langle \psi_{-,\uparrow}(\boldsymbol{k}) \psi_{-,\downarrow}(-\boldsymbol{k}) \rangle, \tag{4.18}$$

$$\Delta_2 = \frac{g_2}{N} \sum_{\boldsymbol{k}} \langle \psi_{+,\uparrow}(\boldsymbol{k}) \psi_{-,\downarrow}(-\boldsymbol{k}) \rangle = -\frac{g_2}{N} \sum_{\boldsymbol{k}} \langle \psi_{-,\uparrow}(\boldsymbol{k}) \psi_{+,\downarrow}(-\boldsymbol{k}) \rangle, \tag{4.19}$$

$$\Delta_3 = \frac{g_3}{N} \sum_{\boldsymbol{k}} \langle \psi_{+,\uparrow}(\boldsymbol{k}) \psi_{-,\downarrow}(-\boldsymbol{k}) \rangle = \frac{g_3}{N} \sum_{\boldsymbol{k}} \langle \psi_{-,\uparrow}(\boldsymbol{k}) \psi_{+,\downarrow}(-\boldsymbol{k}) \rangle, \tag{4.20}$$

$$\Delta_4 = \frac{g_4}{N} \sum_{\boldsymbol{k}} \langle \psi_{+,\uparrow}(\boldsymbol{k}) \psi_{-,\uparrow}(-\boldsymbol{k}) \rangle = -\frac{g_4}{N} \sum_{\boldsymbol{k}} \langle \psi_{-,\uparrow}(\boldsymbol{k}) \psi_{+,\uparrow}(-\boldsymbol{k}) \rangle, \tag{4.21}$$

where $g_\lambda > 0$ ($\lambda = 1 - 4$) represents the attractive interaction between two electrons. Generally speaking, the pair correlation function can be represented as

$$f_{s,\sigma;s',\sigma'}(\boldsymbol{k}) = \langle \psi_{s,\sigma}(\boldsymbol{k}) \, \psi_{s',\sigma'}(-\boldsymbol{k}) \rangle \, , \tag{4.22}$$

where we assume a spatially uniform equal-time Cooper pair. The momentum-symmetry is even-parity s-wave symmetry, which is a common property among the four candidates in a Cu-doped Bi_2Se_3. Because of the Fermi-Dirac statistics of electrons, the pairing correlation obeys

$$f_{s,\sigma;s',\sigma'}(\boldsymbol{k}) = -f_{s',\sigma';s,\sigma}(\boldsymbol{k}). \tag{4.23}$$

The remaining symmetry options of the pairing function are orbitals and spins of a Cooper pair. Therefore, the pairing function must be either antisymmetric under $s \leftrightarrow s'$ or antisymmetric under $\sigma \leftrightarrow \sigma'$.

Both Eqs. (4.18) and (4.20) belong to spin-singlet symmetry. Thus the pairing

functions belong to even-orbital parity. In Eq. (4.20), a Cooper pair consists of two electrons in the different orbitals (interorbital pair): one electron is in + orbital and the other is in − orbital. In Eq. (4.18), on the other hand, a Cooper pair consists of two electrons in the same orbital (intraorbital pair). The pair potential in the + orbital and that in the − orbital have the same amplitude and the same sign.

Both Eqs. (4.19) and (4.21) represent the spin-triplet interorbital pairing correlations. In these cases, the pair correlation belongs to odd-orbital-parity symmetry. In addition to the symmetry options for Cooper pairing, the pair potentials are classified by the irreducible representation of D_{3d} point group. Δ_2 and Δ_4 can be distinguished from each other by the irreducible representation. The matrix form of pair potentials, the irreducible representation, spin symmetry, and orbital-parity of the pair potentials are summarized in Table 4.1. Although Fu and Berg [57] proposed a pair potential of $\Delta(i\hat{s}_2)\hat{\sigma}_3$, it is unitary equivalent to Eq. (4.18) as long as the Hamiltonian $\bar{H}_{\boldsymbol{k}}^{(0)}$ preserves time-reversal symmetry [122]. (See Appendix E for details.) They also considered a pair potential of $\Delta\hat{s}_0(i\hat{\sigma}_2)$ independently of Eq. (4.21). However, the behavior of T_c under the potential disorder in the two pair potentials are the same with each other. Thus, in this study, we discuss effects of random impurity scatterings on superconducting states described by Eqs. (4.18)-(4.21). We note that the orbital parity and the momentum parity are independent symmetry options of each other. The former represents symmetry of correlation function under the commutation of two orbitals. The latter is derived from inversion symmetry of the lattice structure.

In addition to the pair potentials in Eqs. (4.18)-(4.21), generally speaking, the mean-field Hamiltonian contains the interorbital Cooper pair scattering terms described as

$$g'_\lambda \langle \psi^\dagger_{\sigma',s'}(-\boldsymbol{k}')\psi^\dagger_{\gamma',s}(\boldsymbol{k}')\rangle \psi_{\gamma,s}(\boldsymbol{k})\psi_{\sigma,s'}(-\boldsymbol{k}), \tag{4.24}$$

with $\gamma \neq \gamma'$ and $\sigma \neq \sigma'$ [132]. We do not consider these terms because they only renormalize the amplitude of the pair potential as

$$\Delta_\lambda \to \Delta_\lambda \left(1 + P\frac{g'_\lambda}{g_\lambda}\right), \tag{4.25}$$

and do not change main conclusions of this study, where P is 1 (-1) for the even-(odd-) orbital-parity superconductivity.

Table 4.1: Symmetry classification of pair potentials. Equal-time pairing order parameter belongs to even-frequency symmetry. A spin-singlet component is described by $i\hat{s}_2$. An opposite-spin-triplet and an equal-spin-triplet components are indicated by $\hat{s}_1$ and $\hat{s}_3$, respectively.

Matrix	Rep.	Frequency	Spin	Momentum parity	Orbital parity
$\Delta_1(i\hat{s}_2)\hat{\sigma}_0$	A_{1g}	Even	Singlet	Even	Even (Intra)
$\Delta_2\hat{s}_1(i\hat{\sigma}_2)$	A_{1u}	Even	Triplet	Even	Odd (Inter)
$\Delta_3(i\hat{s}_2)\hat{\sigma}_1$	A_{2u}	Even	Singlet	Even	Even (Inter)
$\Delta_4\hat{s}_3(i\hat{\sigma}_2)$	E_u	Even	Triplet	Even	Odd (Inter)

4.3.2 Gor'kov equation

The Matsubara Green's function is obtained by solving the Gor'kov equation,

$$\left[i\omega_n - \check{H}^{(0)}(\boldsymbol{k})\right]\bar{G}^{(0)}(\boldsymbol{k}, i\omega_n) = 1, \tag{4.26}$$

$$\bar{G}^{(0)}(\boldsymbol{k}, i\omega_n) = \begin{pmatrix} \check{\mathcal{G}}^{(0)}(\boldsymbol{k}, i\omega_n) & \check{\mathcal{F}}_\lambda^{(0)}(\boldsymbol{k}, i\omega_n) \\ -\check{\mathcal{F}}_\lambda^{(0)*}(-\boldsymbol{k}, i\omega_n) & -\check{\mathcal{G}}^{(0)*}(-\boldsymbol{k}, i\omega_n) \end{pmatrix}, \tag{4.27}$$

where $\omega_n = (2n+1)\pi T$ is a fermionic Matsubara frequency and T is a temperature. To discuss the transition temperature, we need to find the solutions of Eq. (4.26) within the first order of Δ. The results of the normal part

$$\check{\mathcal{G}}^{(0)}(\boldsymbol{k}, i\omega_n) = \frac{1}{X}\left[(i\omega_n - c_{\boldsymbol{k}})\ \hat{s}_0\hat{\sigma}_0 + m_{\boldsymbol{k}}\,\hat{s}_0\hat{\sigma}_3 + V_z\,\hat{s}_0\hat{\sigma}_2 + (V_y\hat{s}_1 - V_x\hat{s}_2)\,\hat{\sigma}_1\right], \tag{4.28}$$

$$X(\boldsymbol{k}, i\omega_n) = (i\omega_n - c_{\boldsymbol{k}})^2 - m_{\boldsymbol{k}}^2 - V_x^2 - V_y^2 - V_z^2, \tag{4.29}$$

are common for all the pair potentials because the normal Green's function does not include the pair potential at the lowest order. The results of anomalous Green's function

are given by,

$$\begin{aligned}
\check{\mathcal{F}}_1^{(0)}(\boldsymbol{k}, i\omega_n) = \frac{\Delta_1}{Z}\big[&-i\left(\omega_n^2 + c_{\boldsymbol{k}}^2 + m_{\boldsymbol{k}}^2 + V_x^2 + V_y^2 + V_z^2\right)\hat{s}_2\hat{\sigma}_0 \\
&+2ic_{\boldsymbol{k}}m_{\boldsymbol{k}}\,\hat{s}_2\hat{\sigma}_3 + 2ic_{\boldsymbol{k}}V_z\,\hat{s}_2\hat{\sigma}_2 - 2c_{\boldsymbol{k}}V_y\,\hat{s}_3\hat{\sigma}_1 - 2ic_{\boldsymbol{k}}V_x\,\hat{s}_0\hat{\sigma}_1\big], \qquad (4.30)\\
\check{\mathcal{F}}_2^{(0)}(\boldsymbol{k}, i\omega_n) = \frac{\Delta_2}{Z}\big[&-i\left(\omega_n^2 + c_{\boldsymbol{k}}^2 - m_{\boldsymbol{k}}^2 + V_x^2 + V_y^2 + V_z^2\right)\hat{s}_1\hat{\sigma}_2 \\
&+2m_{\boldsymbol{k}}V_y\,\hat{s}_0\hat{\sigma}_0 - 2c_{\boldsymbol{k}}V_y\,\hat{s}_0\hat{\sigma}_3 + 2im_{\boldsymbol{k}}V_x\,\hat{s}_3\hat{\sigma}_0 - 2ic_{\boldsymbol{k}}V_x\,\hat{s}_3\hat{\sigma}_3 \\
&+2ic_{\boldsymbol{k}}V_z\,\hat{s}_1\hat{\sigma}_0 - 2im_{\boldsymbol{k}}V_z\,\hat{s}_1\hat{\sigma}_3 + 2i\omega_n m_{\boldsymbol{k}}\,\hat{s}_1\hat{\sigma}_1\big], \qquad (4.31)\\
\check{\mathcal{F}}_3^{(0)}(\boldsymbol{k}, i\omega_n) = \frac{\Delta_3}{Z}\big[&-i\left(\omega_n^2 + c_{\boldsymbol{k}}^2 - m_{\boldsymbol{k}}^2 + V_x^2 + V_y^2 - V_z^2\right)\big)\,\hat{s}_2\hat{\sigma}_1 \\
&+2iV_xV_z\,\hat{s}_0\hat{\sigma}_2 + 2V_yV_z\,\hat{s}_3\hat{\sigma}_2 - 2ic_{\boldsymbol{k}}V_x\,\hat{s}_0\hat{\sigma}_0 + 2im_{\boldsymbol{k}}V_x\,\hat{s}_0\hat{\sigma}_3 \\
&-2c_{\boldsymbol{k}}V_y\,\hat{s}_3\hat{\sigma}_0 + 2m_{\boldsymbol{k}}V_y\,\hat{s}_3\hat{\sigma}_3 - 2i\omega_n m_{\boldsymbol{k}}\,\hat{s}_2\hat{\sigma}_2 + 2i\omega_n V_z\,\hat{s}_2\hat{\sigma}_3\big], \qquad (4.32)\\
\check{\mathcal{F}}_4^{(0)}(\boldsymbol{k}, i\omega_n) = \frac{\Delta_4}{Z}\big[&-i\left(\omega_n^2 + c_{\boldsymbol{k}}^2 - m_{\boldsymbol{k}}^2 + V_x^2 - V_y^2 + V_z^2\right)\,\hat{s}_3\hat{\sigma}_2 \\
&-2V_xV_y\,\hat{s}_0\hat{\sigma}_2 - 2im_{\boldsymbol{k}}\,V_x\hat{s}_1\hat{\sigma}_0 + 2ic_{\boldsymbol{k}}V_x\,\hat{s}_1\hat{\sigma}_3 + 2ic_{\boldsymbol{k}}V_z\,\hat{s}_3\hat{\sigma}_0 \\
&-2im_{\boldsymbol{k}}V_z\,\hat{s}_3\hat{\sigma}_3 - 2V_yV_z\,\hat{s}_2\hat{\sigma}_1 + 2i\omega_n m_{\boldsymbol{k}}\,\hat{s}_3\hat{\sigma}_1 - 2\omega_n V_y\,\hat{s}_2\hat{\sigma}_3\big], \qquad (4.33)
\end{aligned}$$

with $Z(\boldsymbol{k}, i\omega_n) = |X(\boldsymbol{k}, i\omega_n)|^2$. The $\hat{s}_2\hat{\sigma}_0$ component in Eq. (4.30), the $\hat{s}_1\hat{\sigma}_2$ component in Eq. (4.31), the $\hat{s}_2\hat{\sigma}_1$ component in Eq. (4.32), and the $\hat{s}_3\hat{\sigma}_2$ component in Eq. (4.33) are linked to the pair potentials Δ_1, Δ_2, Δ_3, and Δ_4, respectively. Therefore, the gap equations in the linear regime result in

$$\begin{aligned}
\Delta_1 &= -g_1 T \sum_{\omega_n} \frac{1}{N} \sum_{\boldsymbol{k}} \mathrm{Tr}\left[\check{\mathcal{F}}_1^{(0)}(\boldsymbol{k}, i\omega_n)\frac{(-i\hat{s}_2)\hat{\sigma}_0}{4}\right] \\
&= g_1 T \sum_{\omega_n} \frac{1}{N} \sum_{\boldsymbol{k}} \frac{\Delta_1}{Z(\boldsymbol{k}, i\omega_n)}\left[\omega_n^2 + c_{\boldsymbol{k}}^2 + m_{\boldsymbol{k}}^2 + V_x^2 + V_y^2 + V_z^2\right], \qquad (4.34)
\end{aligned}$$

$$\begin{aligned}
\Delta_2 &= -g_2 T \sum_{\omega_n} \frac{1}{N} \sum_{\boldsymbol{k}} \mathrm{Tr}\left[\check{\mathcal{F}}_2^{(0)}(\boldsymbol{k}, i\omega_n)\frac{\hat{s}_1(-i\hat{\sigma}_2)}{4}\right] \\
&= g_2 T \sum_{\omega_n} \frac{1}{N} \sum_{\boldsymbol{k}} \frac{\Delta_2}{Z(\boldsymbol{k}, i\omega_n)}\left[\omega_n^2 + c_{\boldsymbol{k}}^2 - m_{\boldsymbol{k}}^2 + V_x^2 + V_y^2 + V_z^2\right], \qquad (4.35)
\end{aligned}$$

$$\Delta_3 = -g_3 T \sum_{\omega_n} \frac{1}{N} \sum_{\boldsymbol{k}} \mathrm{Tr}\left[\check{\mathcal{F}}_3^{(0)}(\boldsymbol{k}, i\omega_n) \frac{(-i\hat{s}_2)\hat{\sigma}_1}{4}\right]$$
$$= g_3 T \sum_{\omega_n} \frac{1}{N} \sum_{\boldsymbol{k}} \frac{\Delta_3}{Z(\boldsymbol{k}, i\omega_n)} \left[\omega_n^2 + c_{\boldsymbol{k}}^2 - m_{\boldsymbol{k}}^2 + V_x^2 + V_y^2 - V_z^2\right], \tag{4.36}$$

$$\Delta_4 = -g_4 T \sum_{\omega_n} \frac{1}{N} \sum_{\boldsymbol{k}} \mathrm{Tr}\left[\check{\mathcal{F}}_4^{(0)}(\boldsymbol{k}, i\omega_n) \frac{\hat{s}_3(-i\hat{\sigma}_2)}{4}\right]$$
$$= g_4 T \sum_{\omega_n} \frac{1}{N} \sum_{\boldsymbol{k}} \frac{\Delta_4}{Z(\boldsymbol{k}, i\omega_n)} \left[\omega_n^2 + c_{\boldsymbol{k}}^2 - m_{\boldsymbol{k}}^2 + V_x^2 - V_y^2 + V_z^2\right]. \tag{4.37}$$

Eqs. (4.30), (4.31), (4.32), and (4.33) show that the orbital hybridization (V_z), the spin-orbit interaction ($V_{x,y}$), and the asymmetry between the two orbitals ($m_{\boldsymbol{k}}$) generate various paring correlations which belong to different symmetry classes from that of the pair potential [48, 67]. Especially, we discuss briefly a role of odd-frequency pairing correlation in the gap equation. For instance, the pairing correlation $\check{\mathcal{F}}_2^{(0)}$ includes $2i\omega_n m_{\boldsymbol{k}}\, \hat{s}_1\hat{\sigma}_1$ which describes a spin-triplet even-orbital-parity component. Such an component must be odd-frequency symmetry because the pairing correlation function must be antisymmetric under the permutation of two electrons. In the gap equation, the odd-frequency pairing component decreases the numerator as shown in $-m_{\boldsymbol{k}}^2$ in Eq. (4.35). It has been pointed out that an odd-frequency pair decreases the transition temperature [67]. If we would be able to tune the parameters to delete more the odd-frequency components, the gap equation results in higher T_c.

4.4 Effects of disorder

We consider the random nonmagnetic impurities described by

$$\bar{H}_{\mathrm{imp}}(\boldsymbol{R}) = V_{\mathrm{imp}}(\boldsymbol{R})\ \hat{\tau}_3\hat{s}_0(\hat{\sigma}_0 + \hat{\sigma}_1). \tag{4.38}$$

The schematic picture of potential disorder in a $Cu_xBi_2Se_3$ is shown in Fig. 4.2. We assume the impurity potential satisfies the following properties,

$$\overline{V_{\mathrm{imp}}(\boldsymbol{R})} = 0, \tag{4.39}$$
$$\overline{V_{\mathrm{imp}}(\boldsymbol{R})V_{\mathrm{imp}}(\boldsymbol{R}')} = n_{\mathrm{imp}} v_{\mathrm{imp}}^2 \delta_{\boldsymbol{R},\boldsymbol{R}'}, \tag{4.40}$$

where $\overline{\cdots}$ means the ensemble average, n_{imp} is the density of the impurities, and v_{imp} is the strength of the impurity potential. We also assume that the attractive interactions

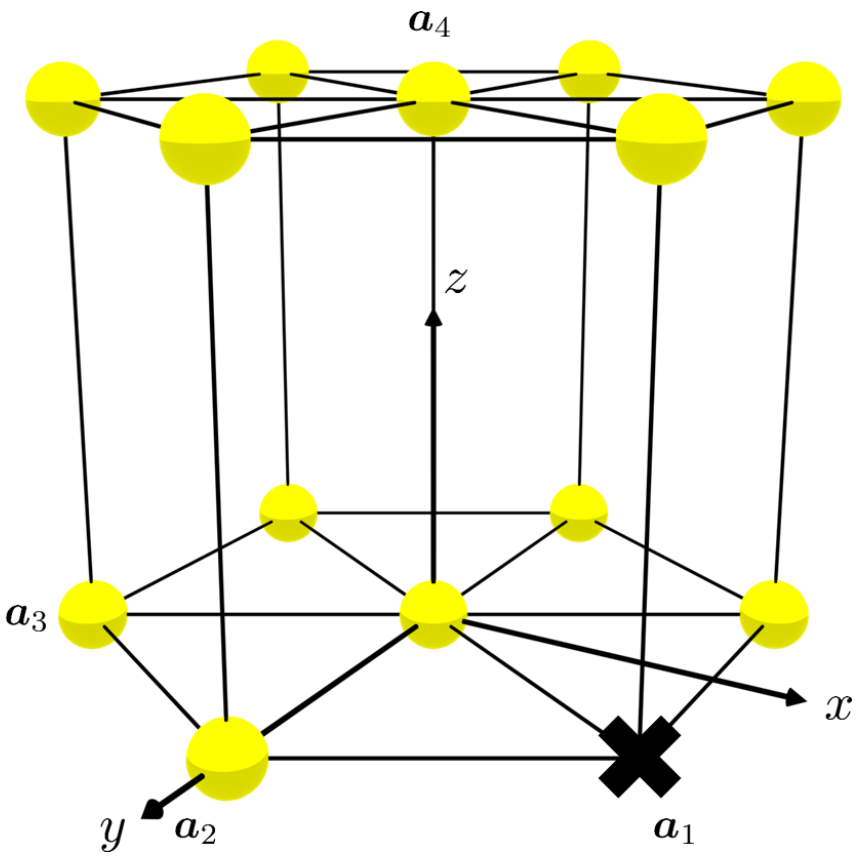

Figure 4.2: A model of the random potential in a $Cu_xBi_2Se_3$. The cross mark denotes an impurity.

between two electrons are insensitive to the impurity potentials [117]. We calculate the Green's function in the presence of the impurity potentials within the Born approximation. The Green's function is expanded up to the second order of the impurity

potential.

$$\begin{aligned}
&\bar{G}(\boldsymbol{R}-\boldsymbol{R}',\omega_n)\\
&\approx \bar{G}^{(0)}(\boldsymbol{R}-\boldsymbol{R}',\omega_n)+\sum_{\boldsymbol{R}_1}\bar{G}^{(0)}(\boldsymbol{R}-\boldsymbol{R}_1,\omega_n)\overline{\bar{H}_{\rm imp}(\boldsymbol{R}_1)}\bar{G}^{(0)}(\boldsymbol{R}_1-\boldsymbol{R}',\omega_n)\\
&+\sum_{\boldsymbol{R}_1,\boldsymbol{R}_2}\bar{G}^{(0)}(\boldsymbol{R}-\boldsymbol{R}_1,\omega_n)\overline{\bar{H}_{\rm imp}(\boldsymbol{R}_1)\bar{G}^{(0)}(\boldsymbol{R}_1-\boldsymbol{R}_2,\omega_n)\bar{H}_{\rm imp}(\boldsymbol{R}_2)}\bar{G}(\boldsymbol{R}_2-\boldsymbol{R}',\omega_n),
\end{aligned} \tag{4.41}$$

$$\begin{aligned}
&\approx \bar{G}^{(0)}(\boldsymbol{R}-\boldsymbol{R}',\omega_n)\\
&+n_{\rm imp}v_{\rm imp}^2\sum_{\boldsymbol{R}_1}\bar{G}^{(0)}(\boldsymbol{R}-\boldsymbol{R}_1,\omega_n)\,\hat{\tau}_3\,\hat{s}_0\,\hat{\sigma}_0\bar{G}^{(0)}(0,\omega_n)\,\hat{\tau}_3\,\hat{s}_0\,\hat{\sigma}_0\bar{G}(\boldsymbol{R}_1-\boldsymbol{R}',\omega_n)\\
&+n_{\rm imp}v_{\rm imp}^2\sum_{\boldsymbol{R}_1}\bar{G}^{(0)}(\boldsymbol{R}-\boldsymbol{R}_1,\omega_n)\,\hat{\tau}_3\,\hat{s}_0\,\hat{\sigma}_1\bar{G}^{(0)}(0,\omega_n)\,\hat{\tau}_3\,\hat{s}_0\,\hat{\sigma}_1\bar{G}(\boldsymbol{R}_1-\boldsymbol{R}',\omega_n).
\end{aligned} \tag{4.42}$$

We transform the Eq. (4.41) to (4.42) by using the properties in Eqs. (4.39) and (4.40). In momentum space, Eq. (4.42) becomes

$$\bar{G}(\boldsymbol{k},i\omega_n)=\bar{G}^{(0)}(\boldsymbol{k},i\omega_n)+\bar{G}^{(0)}(\boldsymbol{k},i\omega_n)\bar{\Sigma}_{\rm imp}\bar{G}(\boldsymbol{k},i\omega_n), \tag{4.43}$$

$$\bar{\Sigma}_{\rm imp}=\bar{\Sigma}_{\rm intra}+\bar{\Sigma}_{\rm inter}, \tag{4.44}$$

$$\bar{\Sigma}_{\rm intra}=n_{\rm imp}v_{\rm imp}^2\hat{\tau}_3\hat{s}_0\hat{\sigma}_0\frac{1}{N}\sum_{\boldsymbol{k}}\bar{G}^{(0)}(\boldsymbol{k},i\omega_n)\hat{\tau}_3\hat{s}_0\hat{\sigma}_0, \tag{4.45}$$

$$\bar{\Sigma}_{\rm inter}=n_{\rm imp}v_{\rm imp}^2\hat{\tau}_3\hat{s}_0\hat{\sigma}_1\frac{1}{N}\sum_{\boldsymbol{k}}\bar{G}^{(0)}(\boldsymbol{k},i\omega_n)\hat{\tau}_3\hat{s}_0\hat{\sigma}_1, \tag{4.46}$$

where $\bar{\Sigma}_{\rm intra}$ and $\bar{\Sigma}_{\rm inter}$ are the self-energy due to the intraorbital impurity scatterings and that of the interorbital impurity scatterings, respectively. We describe the total self-energy as follows.

$$\bar{\Sigma}_{\rm imp}=\bar{\Sigma}_{\rm intra}+\bar{\Sigma}_{\rm inter}=\begin{bmatrix}\check{\Sigma}_g & \check{\Sigma}_{f_\lambda}\\ -\check{\Sigma}^*_{f_\lambda} & -\check{\Sigma}^*_g\end{bmatrix}, \tag{4.47}$$

$$\check{\Sigma}_g=n_{\rm imp}v_{\rm imp}^2[\check{g}^{(0)}+\hat{s}_0\hat{\sigma}_1\check{g}^{(0)}\hat{s}_0\hat{\sigma}_1], \tag{4.48}$$

$$\check{\Sigma}_{f_\lambda}=-n_{\rm imp}v_{\rm imp}^2[\check{f}^{(0)}_\lambda+\hat{s}_0\hat{\sigma}_1\check{f}^{(0)}_\lambda\hat{s}_0\hat{\sigma}_1], \tag{4.49}$$

where we denote the momentum summation of the Green's function as $1/N\sum_{\boldsymbol{k}}\check{\mathcal{G}}^{(0)}(\boldsymbol{k},i\omega_n)=\check{g}^{(0)}$ and $1/N\sum_{\boldsymbol{k}}\check{\mathcal{F}}^{(0)}(\boldsymbol{k},i\omega_n)=\check{f}^{(0)}$. Therefore, the Gor'kov equation in the presence

of the impurity potential is described by

$$\left[i\omega_n - \bar{H}_0(\boldsymbol{k}) - \bar{\Sigma}_{\rm imp}\right] \bar{G}(\boldsymbol{k}, i\omega_n) = 1, \tag{4.50}$$

$$\bar{G}(\boldsymbol{k}, i\omega_n) = \begin{pmatrix} \check{\mathcal{G}}(\boldsymbol{k}, i\omega_n) & \check{\mathcal{F}}_\lambda(\boldsymbol{k}, i\omega_n) \\ -\check{\mathcal{F}}^*_\lambda(-\boldsymbol{k}, i\omega_n) & -\check{\mathcal{G}}^*(-\boldsymbol{k}, i\omega_n) \end{pmatrix}. \tag{4.51}$$

The normal part of self-energy ($\check{\Sigma}_g$) is calculated as follows.

$$\check{\Sigma}_g = \left[-i\omega_n\eta_n + I_n\right] \hat{s}_0\hat{\sigma}_0, \tag{4.52}$$

$$\eta_n = n_{\rm imp} v_{\rm imp}^2 \frac{1}{N}\sum_{\boldsymbol{k}} \frac{2}{Z}\left[\omega_n^2 + c_{\boldsymbol{k}}^2 + m_{\boldsymbol{k}}^2 + V_x^2 + V_y^2 + V_z^2\right], \tag{4.53}$$

$$I_n = n_{\rm imp} v_{\rm imp}^2 \frac{1}{N}\sum_{\boldsymbol{k}} \frac{-2c_{\boldsymbol{k}}}{Z}\left[\omega_n^2 + c_{\boldsymbol{k}}^2 - m_{\boldsymbol{k}}^2 - V_x^2 - V_y^2 - V_z^2\right]. \tag{4.54}$$

Within the first order of Δ, the normal Green's function becomes

$$\check{\mathcal{G}}(\boldsymbol{k}, i\omega_n) = \check{\mathcal{G}}^{(0)}(\boldsymbol{k}, i\tilde{\omega}_n)|_{\mu\to\tilde{\mu}}, \tag{4.55}$$

$$\tilde{\omega}_n = \omega_n(1+\eta_n), \tag{4.56}$$

$$\tilde{\mu} = \mu - I_n. \tag{4.57}$$

The imaginary (real) part of the self-energy renormalizes the Matsubara frequency (chemical potential). The anomalous Green's function after summing up the momenta is described as

$$\check{f}_1^{(0)} = \frac{1}{N}\sum_{\boldsymbol{k}} \frac{\Delta_1}{Z}\left[-i\left(\omega_n^2 + c_{\boldsymbol{k}}^2 + m_{\boldsymbol{k}}^2 + V_x^2 + V_y^2 + V_z^2\right) \hat{s}_2\hat{\sigma}_0 + 2icm\,\hat{s}_2\hat{\sigma}_3\right], \tag{4.58}$$

$$\check{f}_2^{(0)} = \frac{1}{N}\sum_{\boldsymbol{k}} \frac{\Delta_2}{Z}\left[-i\left(\omega_n^2 + c_{\boldsymbol{k}}^2 - m_{\boldsymbol{k}}^2 + V_x^2 + V_y^2 + V_z^2\right) \hat{s}_1\hat{\sigma}_2 + 2i\omega_n m_{\boldsymbol{k}}\,\hat{s}_1\hat{\sigma}_1\right], \tag{4.59}$$

$$\check{f}_3^{(0)} = \frac{1}{N}\sum_{\boldsymbol{k}} \frac{\Delta_3}{Z}\left[-i\left(\omega_n^2 + c_{\boldsymbol{k}}^2 - m_{\boldsymbol{k}}^2 + V_x^2 + V_y^2 - V_z^2\right) \hat{s}_2\hat{\sigma}_1 - 2i\omega_n m\,\hat{s}_2\hat{\sigma}_2\right], \tag{4.60}$$

$$\check{f}_4^{(0)} = \frac{1}{N}\sum_{\boldsymbol{k}} \frac{\Delta_4}{Z}\left[-i\left(\omega_n^2 + c_{\boldsymbol{k}}^2 - m_{\boldsymbol{k}}^2 + V_x^2 - V_y^2 + V_z^2\right) \hat{s}_3\hat{\sigma}_2 + 2i\omega_n m_{\boldsymbol{k}}\,\hat{s}_3\hat{\sigma}_1\right]. \tag{4.61}$$

By substituting these expressions into Eq. (4.49), we obtain the anomalous part of the self-energy for each pair potential.

$$\check{\Sigma}_{f_1} = \Delta_1(i\hat{s}_2)\hat{\sigma}_0 \cdot \eta_n, \tag{4.62}$$

$$\check{\Sigma}_{f_2} = \Delta_2\hat{s}_1\hat{\sigma}_1 \cdot (-i\omega_n)J_n, \tag{4.63}$$

$$\check{\Sigma}_{f_3} = \Delta_3(i\hat{s}_2)\hat{\sigma}_1 \cdot \eta'_n, \tag{4.64}$$

$$\check{\Sigma}_{f_4} = \Delta_4\hat{s}_3\hat{\sigma}_1 \cdot (-i\omega_n)J_n, \tag{4.65}$$

$$\eta'_n = n_{\rm imp}v_{\rm imp}^2\frac{1}{N}\sum_{\boldsymbol{k}}\frac{2}{Z}\left[\omega_n^2 + c_{\boldsymbol{k}}^2 - m_{\boldsymbol{k}}^2 + V_x^2 + V_y^2 - V_z^2\right], \tag{4.66}$$

$$J_n = n_{\rm imp}v_{\rm imp}^2\frac{1}{N}\sum_{\boldsymbol{k}}\frac{4m_{\boldsymbol{k}}}{Z}. \tag{4.67}$$

Before demonstrating T_c under the potential disorder, we briefly summarize a relation between the self-energy and the pair potential in the four cases. The results in Eq. (4.62) show that $\check{\Sigma}_{f_1}$ has the same matrix structure with the pair potential as shown in Table. 4.1. Namely, $\check{\Sigma}_{f_1}$ renormalizes the pair potential Δ_1 which belongs to even-frequency spin-singlet even-momentum-parity even-orbital-parity (ESEE) pairing symmetry. We will show that this fact explains the robustness of Δ_1 in the presence of impurity scatterings. The same feature can be seen in $\check{\Sigma}_{f_3}$ in Eq. (4.64), which implies the robustness of Δ_3. On the other hand, $\check{\Sigma}_{f_2}$ and $\check{\Sigma}_{f_4}$ have the different matrix structure from their pair potentials shown in Table. 4.1. In other words, the impurity self-energy leaves the pair potentials as they are. The previous studies suggested that the superconductivity in such cases can be fragile. We also note that $\check{\Sigma}_{f_2}$ and $\check{\Sigma}_{f_4}$ enhance the pair correlation belonging to odd-frequency spin-triplet even-momentum-parity even-orbital-parity (OTEE) symmetry. In what follows, we discuss characteristic behavior of T_c as a function of impurity concentration case by case.

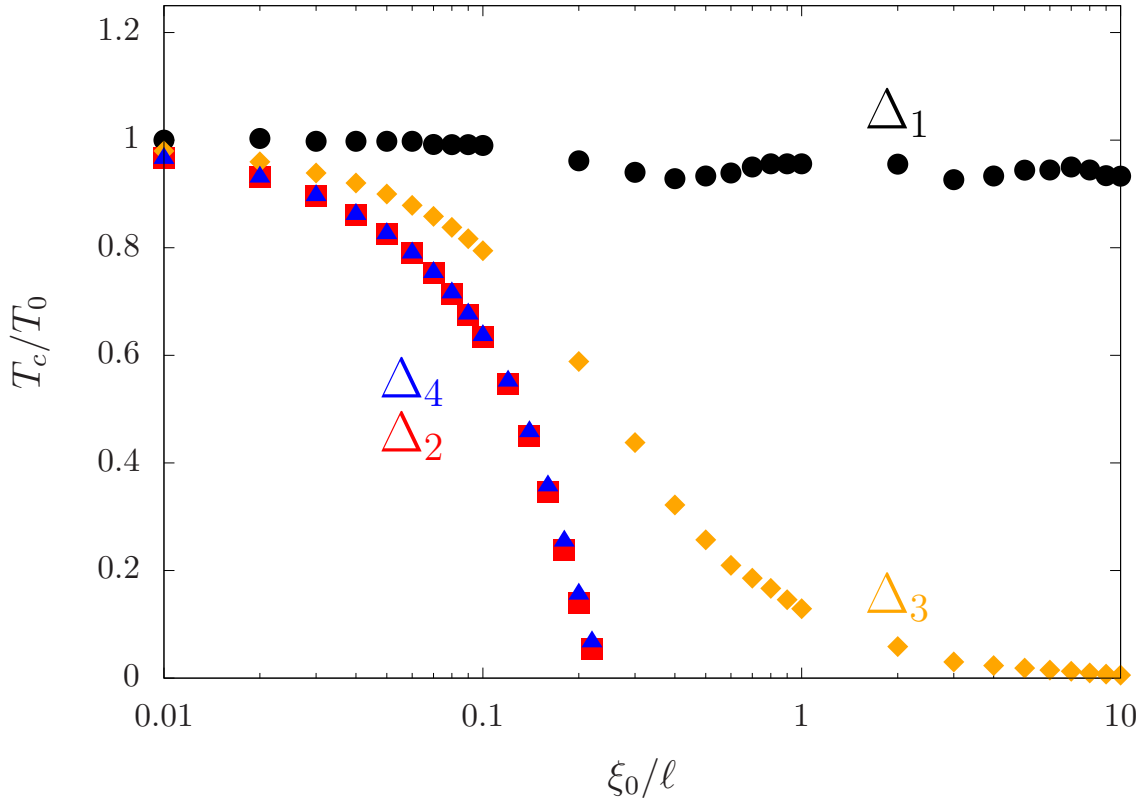

Figure 4.3: The superconducting transition temperature T_c is plotted as a function of ξ_0/ℓ. The vertical axis is normalized to the transition temperature in the clean limit T_0. We fix T_0 for all pair potentials.

4.4.1 Δ_1

The gap equation for Δ_1 results in

$$\Delta_1 = g_1 T \sum_{\omega_n} \frac{1}{N} \sum_{\boldsymbol{k}} \frac{\tilde{\Delta}_1}{\tilde{Z}} \left[\tilde{\omega}_n^2 + \tilde{c}_{\boldsymbol{k}}^2 + m_{\boldsymbol{k}}^2 + V_x^2 + V_y^2 + V_z^2 \right]. \tag{4.68}$$

By comparing with the gap equation in the clean limit in Eq. (4.34), the renormalized values are defined as

$$\tilde{\Delta}_1 = \Delta_1 (1 + \eta_n), \tag{4.69}$$

$$\tilde{Z}(\boldsymbol{k}, i\omega_n) = Z(\boldsymbol{k}, i\tilde{\omega}_n)|_{\mu \to \tilde{\mu}}, \tag{4.70}$$

$$\tilde{c}_{\boldsymbol{k}} = c_{\boldsymbol{k}}|_{\mu \to \tilde{\mu}}. \tag{4.71}$$

The impurity self-energy renormalizes the pair potential and the Matsubara frequency in the same manner as $\Delta_1 \to \tilde{\Delta}_1$ and $\omega_n \to \tilde{\omega}_n$ [69]. We solve the gap equation numerically and plot the transition temperature T_c of Δ_1 as a function of ξ_0/ℓ in Fig. 4.3. Here T_0 is the transition temperature in the clean limit, $\xi_0 = v_F/(2\pi T_0)$ is the superconducting coherence length, v_F is the Fermi velocity, $\ell = v_F \tau_{\rm imp}$ is the mean free path due to impurity scatterings, and $\tau_{\rm imp}$ is the lifetime of a quasiparticle. We found that the normal part of self-energy $\check{\Sigma}_g$ is nearly independent of the Matsubara frequency in the low energy region for $\omega_n \leq \omega_c$. Here $\omega_c = 10^3 T_0$ is the cut-off energy of the Matsubara frequency. Therefore, we estimate $\tau_{\rm imp}$ from the imaginary part of $\check{\Sigma}_g$ as

$$\frac{1}{\tau_{\rm imp}} = -2{\rm Tr} \left[\frac{1}{4} {\rm Im}\, \check{\Sigma}_g \right] \sim 2\pi \times n_{\rm imp} v_{\rm imp}^2 \times 10^{-2}\,[{\rm eV}]. \tag{4.72}$$

The horizontal axis ξ_0/ℓ in Fig. 4.3 is proportional to the impurity concentration $n_{\rm imp}$. The results in Fig. 4.3 show that T_c of Δ_1 is almost independent of the impurity concentration as shown with filled circles. Such behavior agrees well with T_c in a limiting case of idealistic models. The previous papers [71, 120–122] considered two-band superconductivity with the intraband pairing order parameters (say D_1 and D_2) on idealistic two-band electronic structures and demonstrated that T_c is independent of impurity concentration at $D_1 = D_2$. The interband impurity scatterings disappear in such a symmetric situation, which explains the unchanged T_c. The superconducting state in Cu-doped Bi_2Se_3 with Δ_1 corresponds to the symmetric intraband pairing state in the previous studies. In this study, we confirmed that the conclusions of the previous papers on idealistic band structures are valid even if we calculate T_c on a realistic

electronic structure. In Fig. 4.3, the results for Δ_1 show the oscillating behavior. Although it is not easy to specify the reasons of the oscillations, such behavior comes from a realistic band structure. In the Born approximation, we conclude that T_c of Δ_1 is insensitive to the impurity scatterings.

4.4.2 Δ_3

The gap equation for Δ_3 becomes

$$\Delta_3 = g_3 T \sum_{\omega_n} \frac{1}{N} \sum_{\boldsymbol{k}} \frac{\Delta_3'}{\tilde{Z}} \left[\tilde{\omega}_n^2 + \tilde{c}_{\boldsymbol{k}}^2 - m_{\boldsymbol{k}}^2 + V_x^2 + V_y^2 - V_z^2 \right], \tag{4.73}$$

$$\Delta_3' = \Delta_3 (1 + \eta_n'). \tag{4.74}$$

The pair potential is renormalized by the impurity self-energy as $\Delta_3 \to \Delta_3'$ in Eq. (4.73) in a slightly different way from the relation $\omega_n \to \tilde{\omega}_n$. By solving Eq. (4.73), we plot T_c of Δ_3 as a function of ξ_0/ℓ in Fig. 4.3. The results show that T_c of the spin-singlet interorbital pairing order is suppressed slowly with the increase of ξ_0/ℓ and goes to zero in the dirty limit. A previous paper [123], however, demonstrated on an idealistic two-band structure that T_c of a spin-singlet s-wave interband pairing order is independent of the impurity concentration. Thus Δ_3 in a Cu-doped Bi_2Se_3 is more fragile than that in an idealistic two-band model. The difference between the results in the two models can be explained by the enhancement of odd-frequency pairing components due to the realistic electronic structures. The odd-frequency pairing correlation is absent in an idealistic band structure [123]. As a result, the impurity self-energy renormalizes the pair potential and the Matsubara frequency in the same manner, which leads to unchanged T_c versus ξ_0/ℓ. In Cu-doped Bi_2Se_3, on the other hand, the asymmetry between two-orbitals ($m_{\boldsymbol{k}}$) and the orbital hybridization (V_z) generate the odd-frequency pairing correlations as described in Eq. (4.32). These correlations contribute negatively to the numerator of the renormalization factor of the pair potential $1 + \eta_n'$ as shown in $-m_{\boldsymbol{k}}^2$ and $-V_z^2$ in Eq. (4.66). As a consequence, the reduction of the pair potential by odd-frequency pairs causes the suppression of T_c in the dirty regime. We conclude that the robustness of the spin-singlet s-wave interorbital pairing order depends on band structures.

4.4.3 Δ_2 and Δ_4

The gap equations for Δ_2 and Δ_4 result in

$$\Delta_2 = g_2 T \sum_{\omega_n} \frac{1}{N} \sum_{\boldsymbol{k}} \frac{\Delta_2}{\tilde{Z}} \left[\tilde{\omega}_n^2 + \tilde{c}_{\boldsymbol{k}}^2 - m_{\boldsymbol{k}}^2 + V_x^2 + V_y^2 + V_z^2 - 2J_n \omega_n \tilde{\omega}_n m_{\boldsymbol{k}} \right], \tag{4.75}$$

$$\Delta_4 = g_4 T \sum_{\omega_n} \frac{1}{N} \sum_{\boldsymbol{k}} \frac{\Delta_4}{\tilde{Z}} \left[\tilde{\omega}_n^2 + \tilde{c}_{\boldsymbol{k}}^2 - m_{\boldsymbol{k}}^2 + V_x^2 - V_y^2 + V_z^2 - 2J_n \omega_n \tilde{\omega}_n m_{\boldsymbol{k}} \right]. \tag{4.76}$$

Both Δ_2 and Δ_4 represent spin-triplet interorbital pairing order antisymmetric under the permutation of two orbitals. The numerical results in Fig. 4.3 indicate that T_c of Δ_2 and that of Δ_4 decrease rapidly with the increase of ξ_0/ℓ and vanish around $\xi_0/\ell \approx 0.3$. The impurity self-energy renormalizes the Matsubara frequency as $\omega_n \to \tilde{\omega}_n$. However, it leaves the pair potentials unchanged as shown in Eqs. (4.75) and (4.76). Therefore, Δ_2 and Δ_4 are fragile in the presence of impurities. The obtained results of T_c for a Cu-doped Bi_2Se_3 agree even quantitatively with those calculated in an idealistic band structure [123]. The interorbital impurity scatterings mix the electronic states in the two orbitals and average the pair potentials over the two orbital degree of freedom. As a result, the impurity scatterings wash out the sign of the pair potential in Eq. (4.17), which leads to the suppression of odd-orbital symmetric superconductivity. We confirmed that this physical interpretation is valid independent of band structures.

Several experiments have indicated nematic superconductivity in Cu-doped Bi_2Se_3 [133–135]. Such superconductivity can be realized when the pair potential belongs to the E_u representation of the D_{3d} point group [136]. The corresponding pair potential is described as

$$\check{\Delta}_{\text{nematic}} = \Delta \left(A_x \hat{s}_3 (i\hat{\sigma}_2) + A_y \hat{s}_0 (i\hat{\sigma}_2) \right), \tag{4.77}$$

where coefficients $A_{x,y}$ determine a nematic direction. Δ_4 corresponds to the specific case ($(A_x, A_y) = (1, 0)$) of the nematic superconductivity. The nematic is considered to be fragile in the presence of potential disorder because the nematic order belongs to odd-orbital symmetry as well as Δ_2 and Δ_4.

Finally, we compare our results in this chapter with those in a recent study [137]. The authors of Ref. [137] formulated the random impurity scatterings based on the two-band picture in momentum space, which is obtained by diagonalizing the normal state Hamiltonian in the absence of impurities [138]. They mapped a Hamiltonian for an interorbital s-wave superconductor with random impurities to a Hamiltonian for a single-band unconventional superconductor with random impurities. As a result, they concluded that Δ_2, Δ_3, and Δ_4 are fragile under the potential disorder. Their conclu-

sion for Δ_3 does not agree with ours obtained by applying the standard method [69]. The difference in the theoretical methods causes the discrepancy. An earlier [139] and a recent [140] analysis also contradict our results. A key point might be the self-energy due to interorbital impurity scatterings. Actually all of the previous papers [71, 120–123] have suggested an importance of the interorbital/interband impurity scatterings on T_c. Refs. [137, 139, 140], on the other hand, does not consider the interorbital impurity scatterings.

4.5 Conclusion

We studied the effects of random nonmagnetic impurities on the superconducting transition temperature T_c in Cu-doped Bi_2Se_3. We consider four types of momentum-independent pair potentials, which include the intraorbital pairing (Δ_1), the interorbital-even-parity pairing (Δ_3), and the interorbital-odd-parity pairings (Δ_2 and Δ_4). The effects of the impurity scatterings are considered through the self-energy of the Green's function within the Born approximation. T_c of Δ_1 is insensitive to the impurity concentration, which is consistent with the previous theories. We find that Δ_1 with the electronic structure of a Cu-doped Bi_2Se_3 corresponds to a limiting case of idealistic models [71, 120–122]. T_c of Δ_3 decreases moderately with the increase of impurity concentration and vanishes in the dirty limit, which does not agree well with the results on an idealistic model [123]. The presence of the odd-frequency pairing correlations explain the discrepancy. T_c of Δ_2 and Δ_4 decrease rapidly with the increase of the impurity concentration. Superconductivity vanishes at a critical value of the impurity concentration. The results are consistent with those in an idealistic model even quantitatively [123].

We found that the robustness of the even-orbital-parity order parameters depends on the details of the band structures and that the odd-orbital-parity order parameters are fragile irrespective of the band structures.

Chapter 5

Conclusion

The dependency of the phenomena on the symmetry is a commonality in physics. From the establishment of the microscopic theory of superconductivity, the symmetry of Cooper pair has continued to play important roles. Various unique and interesting phenomena in non-uniform superconductors such as anomalous transport in junction systems have studied extensively by both theoretical and experimental researchers. Their numerous studies reveal that odd-frequency Cooper pairs, which are expressed by the anomalous Green's function of odd functions with respect to the Matsubara frequency, give us comprehensive explanations of the anomalous phenomena. The mechanism of the interesting phenomena is commonly attributed to the paramagnetic property of odd-frequency Cooper pairs. Odd-frequency Cooper pair is a reasonable concept to understand the underlying physics.

After the birth of the cocept of odd-frequency Cooper pairs by Berezinskii, it has been considered that the uniform odd-frequency pairing could not exist in the bulk of a superconductor because of the paramagnetic property. However, by the proposal of the various subdominant pairing correlations in multiband/orbital systems, it has been shown that the paramagnetic odd-frequency Cooper pairs are able to exist uniformly in such systems. Although there are nontrivial relationships between uniform odd-frequency Cooper pairs and exotic quantum states, such as quasiparticles on Bogoliubov Fermi surfaces in multiband/orbital systems, the physics originating from uniform odd-frequency Cooper pairs has been an open question.

In this thesis, we have theoretically studied the thermodynamic properties of uniform superconductors that accommodate subdominant odd-frequency Cooper pairs. We determined the amplitude of the order parameter in a $j = 3/2$ superconductor self-consistently and found the transition to the uniform superconducting phase becomes discontinuous when the amplitude of the odd-frequency pairing correlation function is

large enough. We also calculated the Ginzburg-Landau (GL) free-energy functional and found that the sign of the fourth-order term with respect to Δ becomes negative. It has been revealed that the odd-frequency pairing correlation functions make negative contributions to the GL coefficient, while those with even symmetry make positive contributions to the coefficient. We demonstrated that the superfluid density decreases greatly at finite temperarures due to the contributions of paramagnetic odd-frequency pairing correlation functions which are proportional to the Matsubara frequency. Existence of such odd-frequency pairing correlations explain the mechanism of the discontinuous transition well. We also addressed an important open issue: the discontinuous transition to uniform superconducting phase under Zeeman fields and obtained similar results as above. We conclude that a potential for the discontinuous transition is a common property of superconductors that include uniform odd-frequency Cooper pairs.

We have also discussed the effect of the potential disorder in a multiorbital superconductor. According to the conventional knowledge, known as Anderson's theorem, s-wave superconducting order is completely robust against nonmagnetic impurity scatterings. On the contrary, several previous studies pointed out that s-wave superconducting order in multiband/orbital metals is not necessarily robust against disorder. To make the comprehensive arguments about the nonmagnetic impurity effect in multiband/orbital superconductors, we discussed the robustness of several pairing orders against disorder. We calculated the superconducting transition temperature T_c as a function of impurity concentration within the Born approximation. We used the effective model of a multiorbital s-wave superconductor $Cu_xBi_2Se_3$, in which the various candidates of the order parameter has been proposed. Among the potential candidates of the superconducting order, we found that T_c of spin-triplet s-wave odd-orbital-parity pairing order is suppressed greatly by the impurity scatterings irrespective of the details of the eletronic structures. The homogenization of the two orbitals due to the interorbital impurity scattering, which is unique to multiorbital systems, explains the reason. We also found that the spin-singlet even-orbital-parity pairing order is basically robust but T_c within the Born approximation is gradually suppressed by the disorder when the odd-frequency Cooper pairs are present in the clean limit. Uniform odd-frequency Cooper pairs play an important role even in the impurity effect.

Throughout this study, we have discussed the stability of uniform superconducting order in multiband/orbital metals against thermal fluctuations and potential disorder. We have presented comprehensive arguments in terms of odd-frequency Cooper pairs and have found that anomalous properties of such superconductors could be explained well by this concept. Our conclusions established in this study could help to understand

anomalous phenomena found in various superconductors that contain uniform odd-frequency Cooper pairs.

Appendix A

Linear response to electromagnetic fields in a lattice model

The coupling between an electron and an electromagnetic field is considered through the Peierls phase in the kinetic energy [141, 142]:

$$\mathcal{H}_{\rm N}^{\rm kin} = -t_1 \sum_{j_z} \sum_{\langle \boldsymbol{r}_{\rm i}, \boldsymbol{r}_{\rm j} \rangle} e^{i\varphi_{\rm ij}} c^{\dagger}_{\boldsymbol{r}_{\rm i}, j_z} c_{\boldsymbol{r}_{\rm j}, j_z} + {\rm H.c.}, \quad \varphi_{\rm ij} = e \int_{\boldsymbol{r}_{\rm j}}^{\boldsymbol{r}_{\rm i}} d\boldsymbol{r} \cdot \boldsymbol{A}(\boldsymbol{r}), \tag{A.1}$$

where $c^{\dagger}_{\boldsymbol{r}, j_z}$ ($c_{\boldsymbol{r}, j_z}$) is the creation (annihilation) operator for the electron at $\boldsymbol{r}$ with pseudospin j_z. We neglect the correction to the weak spin-orbit interactions ($t_3 \ll t_1$). The current density operator $\boldsymbol{j}$ is defined from the variation of the Hamiltonian with respect to the vector potential:

$$\delta\mathcal{H}(t) = -\sum_{\boldsymbol{r}} \boldsymbol{j}(\boldsymbol{r}, t) \cdot \delta\boldsymbol{A}(\boldsymbol{r}, t). \tag{A.2}$$

Within the first order of the vector potential, the current can be decomposed into the paramagnetic and diamagnetic terms,

$$j_\mu(\boldsymbol{r}, t) = j_\mu^{\rm para}(\boldsymbol{r}) + j_\mu^{\rm dia}(\boldsymbol{r}, t) \quad (\mu = x,\, y,\, z), \tag{A.3}$$

$$j_\mu^{\rm para}(\boldsymbol{r}) = iet_1 \sum_{j_z} \left[c^{\dagger}_{\boldsymbol{r}+\hat{\boldsymbol{r}}_\mu, j_z} c_{\boldsymbol{r}, j_z} - {\rm H.c.} \right], \quad j_\mu^{\rm dia}(\boldsymbol{r}, t) = e^2 k_\mu(\boldsymbol{r}) A_\mu(\boldsymbol{r}, t), \tag{A.4}$$

where $\hat{\boldsymbol{r}}_\mu$ is the basic lattice vector along the μ-direction of a simple cubic lattice and $k_\mu(\boldsymbol{r})$ is local kinetic energy operator with respect to the μ-oriented links, which is

defined as

$$k_\mu(\boldsymbol{r}) = -t_1 \sum_{j_z} \left[c^\dagger_{\boldsymbol{r}+\hat{\boldsymbol{r}}_\mu, j_z} c_{\boldsymbol{r}, j_z} + \text{H.c.} \right]. \tag{A.5}$$

The perturbation Hamiltonian $\mathcal{H}'$ within the first order of the vector potential reads,

$$\mathcal{H}'(t) = -\sum_{\boldsymbol{r}} \boldsymbol{j}^{\text{para}}(\boldsymbol{r}) \cdot \boldsymbol{A}(\boldsymbol{r}, t). \tag{A.6}$$

In Sec. 3.5, we examine the linear response in the x-direction:

$$j_x(\boldsymbol{q}, \omega) = -K_{xx}(\boldsymbol{q}, \omega) A_x(\boldsymbol{q}, \omega). \tag{A.7}$$

The response kernel K_{xx} is calculated to be [143–145]

$$K_{xx}(\boldsymbol{q}, \omega) = e^2 \langle -k_x(\boldsymbol{r}) \rangle - \Lambda^{\text{R}}_{xx}(\boldsymbol{q}, \omega), \tag{A.8}$$

where $\langle -k_x(\boldsymbol{r}) \rangle$ represents the kinetic energy along the x-direction per unit cell and Λ^{R}_{xx} is the current-current correlation function expressed as

$$\Lambda^{\text{R}}_{xx}(\boldsymbol{q}, \omega) = \Lambda_{xx}(\boldsymbol{q}, i\nu_m \to \omega + i\delta), \tag{A.9}$$

$$\begin{aligned} \Lambda_{xx}(\boldsymbol{q}, i\nu_m) = -e^2 T \sum_{\omega_n} \frac{1}{N} \sum_{\boldsymbol{k}} 4t_1^2 \sin^2 \left(k_x + \frac{q_x}{2} \right) \\ \times \text{Tr} \left[\mathcal{G}(\boldsymbol{k}+\boldsymbol{q}, i\omega_n + i\nu_m) \mathcal{G}(\boldsymbol{k}, i\omega_n) - \underset{\sim}{\mathcal{F}}(\boldsymbol{k}+\boldsymbol{q}, i\omega_n + i\nu_m) \mathcal{F}(\boldsymbol{k}, i\omega_n) \right], \end{aligned} \tag{A.10}$$

where $\nu_m = 2m\pi T$ is a bosonic Matsubara frequency with m being an integer and δ is a small positive real value. The superfluid density is defined by

$$Q = \frac{K_{xx}(\boldsymbol{q} \to 0, \omega = 0)}{2e^2 t_1}. \tag{A.11}$$

The contribution of odd-frequency pairing correlations in Sec. 3.5 is described using

$$Q^{\mathcal{F}} = T \sum_{\omega_n} \frac{1}{N} \sum_{\boldsymbol{k}} 2t_1 \sin^2 k_x \text{Tr} \left[-\underset{\sim}{\mathcal{F}}(\boldsymbol{k}, i\omega_n) \mathcal{F}(\boldsymbol{k}, i\omega_n) \right]. \tag{A.12}$$

The summation over Matsubara frequencies can be carried out analytically, when we use the spectral representation of the Green's function,

$$G(\boldsymbol{k}, i\omega_n) = \sum_{\lambda} \frac{\vec{\phi}_{\boldsymbol{k},\lambda}\vec{\phi}^{\dagger}_{\boldsymbol{k},\lambda}}{i\omega_n - E_\lambda(\boldsymbol{k})}. \tag{A.13}$$

Here, the summation is taken over all eight indices of the eigenstates of the BdG Hamiltonian and $\vec{\phi}_{\boldsymbol{k},\lambda}$ is the eigenvector belonging to the eigenenergy $E_\lambda(\boldsymbol{k})$. After the summation over the Matsubara frequencies, we reach at

$$\langle -k_x(\boldsymbol{r})\rangle = \frac{1}{N}\sum_{\boldsymbol{k},\lambda=\mathrm{S}\pm} 2t_1 \cos k_x \left[u^2_{\boldsymbol{k}} f(E_\lambda) + v^2_{\boldsymbol{k}} f(-E_\lambda)\right], \tag{A.14}$$

with

$$u^2_{\boldsymbol{k}} = 1 + \frac{\xi_{\boldsymbol{k}}}{\sqrt{\xi^2_{\boldsymbol{k}} + \Delta^2}}, \quad v^2_{\boldsymbol{k}} = 1 - \frac{\xi_{\boldsymbol{k}}}{\sqrt{\xi^2_{\boldsymbol{k}} + \Delta^2}}, \tag{A.15}$$

and

$$\Lambda^{\mathrm{R}}_{xx}(\boldsymbol{q}\to 0, \omega = 0) = e^2 \frac{1}{N}\sum_{\boldsymbol{k},\lambda=\mathrm{S}\pm} 8t_1^2 \sin^2 k_x \left(-\frac{\partial f(E_\lambda)}{\partial E_\lambda}\right), \tag{A.16}$$

for $(\eta_{\boldsymbol{k},4}, \eta_{\boldsymbol{k},5}) = (1,0)$, $(0,1)$, and $(1,1)/\sqrt{2}$ states at $t_2 = 0$.

The Green's function for $(\eta_{\boldsymbol{k},4}, \eta_{\boldsymbol{k},5}) = (1,0)$, $(0,1)$, and $(1,1)/\sqrt{2}$ states at $t_2 = 0$ is calculated to be

$$\begin{aligned}\mathcal{G}(\boldsymbol{k}, i\omega_n) = -\frac{1}{Z}\big[&(\omega_n^2 + \xi^2_{\boldsymbol{k}} + \Delta^2)(i\omega_n + \xi_{\boldsymbol{k}}) + \vec{\epsilon}^{\,2}_{\boldsymbol{k}}(i\omega_n - \xi_{\boldsymbol{k}}) \\ &- \left\{(i\omega_n + \xi_{\boldsymbol{k}})^2 + \Delta^2 - \vec{\epsilon}^{\,2}_{\boldsymbol{k}}\right\}\vec{\epsilon}_{\boldsymbol{k}}\cdot\vec{\gamma}\big],\end{aligned} \tag{A.17}$$

$$\mathcal{F}(\boldsymbol{k}, i\omega_n) = -\frac{\Delta}{Z}\left[\omega_n^2 + \xi^2_{\boldsymbol{k}} + \Delta^2 - \vec{\epsilon}^{\,2}_{\boldsymbol{k}} - 2i\omega_n \vec{\epsilon}_{\boldsymbol{k}}\cdot\vec{\gamma}\right]\vec{\eta}_{\boldsymbol{k}}\cdot\vec{\gamma}U_T, \tag{A.18}$$

$$Z = (\omega_n^2 + \xi^2_{\boldsymbol{k}} + \Delta^2 - \vec{\epsilon}^{\,2}_{\boldsymbol{k}})^2 + 4\omega_n^2\vec{\epsilon}^{\,2}_{\boldsymbol{k}}. \tag{A.19}$$

The last term in Eq (A.18) represents the odd-frequency pairing correlation induced by the spin-orbit interaction.

Appendix B

Interband pairing and odd-frequency Cooper pair

We consider following mean-field Hamiltonian which describes the electronic states of interband pairing order in a two-band model,

$$\mathcal{H} = \sum_{\boldsymbol{k}} \left[a^\dagger_{\boldsymbol{k},\uparrow}\ a^\dagger_{\boldsymbol{k},\downarrow}\ b^\dagger_{\boldsymbol{k},\uparrow}\ b^\dagger_{\boldsymbol{k},\downarrow} a_{-\boldsymbol{k},\uparrow}\ a_{-\boldsymbol{k},\downarrow}\ b_{-\boldsymbol{k},\uparrow}\ b_{-\boldsymbol{k},\downarrow} \right] \times \left[\begin{array}{cccc|cccc} \varepsilon^{\mathrm{a}}_{\boldsymbol{k}} & & V & & & & & \Delta \\ & \varepsilon^{\mathrm{a}}_{\boldsymbol{k}} & & V & & & s\Delta & \\ V & & \varepsilon^{\mathrm{b}}_{\boldsymbol{k}} & & & -s\Delta & & \\ & V & & \varepsilon^{\mathrm{b}}_{\boldsymbol{k}} & -\Delta & & & \\ \hline & & & -\Delta & -\varepsilon^{\mathrm{a}}_{\boldsymbol{k}} & & -V & \\ & & -s\Delta & & & -\varepsilon^{\mathrm{a}}_{\boldsymbol{k}} & & -V \\ & s\Delta & & & -V & & -\varepsilon^{\mathrm{b}}_{\boldsymbol{k}} & \\ \Delta & & & & & -V & & -\varepsilon^{\mathrm{b}}_{\boldsymbol{k}} \end{array}\right] \left[\begin{array}{c} a_{\boldsymbol{k},\uparrow} \\ a_{\boldsymbol{k},\downarrow} \\ b_{\boldsymbol{k},\uparrow} \\ b_{\boldsymbol{k},\downarrow} \\ a^\dagger_{-\boldsymbol{k},\uparrow} \\ a^\dagger_{-\boldsymbol{k},\downarrow} \\ b^\dagger_{-\boldsymbol{k},\uparrow} \\ b^\dagger_{-\boldsymbol{k},\downarrow} \end{array}\right], \tag{B.1}$$

where $a^\dagger_{k\sigma}$ ($b^\dagger_{k\sigma}$) is a creation operator of an electron in band a (b) with momentum $\boldsymbol{k}$ and spin $\sigma\,(=\uparrow,\downarrow)$. $\varepsilon^{\mathrm{l}}_{\boldsymbol{k}}$ ($\mathrm{l}=\mathrm{a},\mathrm{b}$) is defined by $\varepsilon^{\mathrm{l}}_{\boldsymbol{k}} = \frac{\boldsymbol{k}^2}{2m_{\mathrm{l}}} - \mu_{\mathrm{l}}$ and V is the hybridization potential mixing the two bands. Δ represents interband pairing potential belonging to s-wave spin-triplet odd-band-parity (spin-singlet even-band-parity) symmetry class when we choose $s = +1\,(-1)$. Eq. (B.1) with $s = +1$ corresponds to the mean-field Hamiltonian considered in Ref. [107]. Eq. (B.1) can be block diagonalized and the

reduced Hamiltonian is represented by

$$\check{H}(\boldsymbol{k}) = \begin{bmatrix} \hat{H}_{\rm N} & \hat{\Delta} \\ \hat{\Delta}^\dagger & -\hat{H}_{\rm N} \end{bmatrix}, \quad \hat{H}_{\rm N} = \xi + \varepsilon\hat{\rho}_3 + V\hat{\rho}_1, \quad \hat{\Delta} = \begin{cases} \Delta(i\hat{\rho}_2) & (s=+1) \\ \Delta\hat{\rho}_1 & (s=-1) \end{cases}, \tag{B.2}$$

where $\xi = (\varepsilon^{\rm a}_{\boldsymbol{k}} + \varepsilon^{\rm b}_{\boldsymbol{k}})/2$, $\varepsilon = (\varepsilon^{\rm a}_{\boldsymbol{k}} - \varepsilon^{\rm b}_{\boldsymbol{k}})/2$, and $\hat{\rho}_j$ for $j = 1-3$ are Pauli matrices in the two-band space. The Matsubara Green's function is calculated by the Gor'kov equation,

$$\left[i\omega_n - \check{H}(\boldsymbol{k})\right] \begin{bmatrix} \hat{\mathcal{G}}(\boldsymbol{k}, i\omega_n) & \hat{\mathcal{F}}(\boldsymbol{k}, i\omega_n) \\ \underline{\hat{\mathcal{F}}}(\boldsymbol{k}, i\omega_n) & \underline{\hat{\mathcal{G}}}(\boldsymbol{k}, i\omega_n) \end{bmatrix} = 1. \tag{B.3}$$

The anomalous Green's function $\hat{\mathcal{F}}$ is calculated as

$$\hat{\mathcal{F}}(\boldsymbol{k}, i\omega_n) = \begin{cases} \frac{-1}{Z_{+1}}\left[\omega_n^2 + \xi^2 - \varepsilon^2 - V^2 + \Delta^2 - 2i\omega_n(\varepsilon\hat{\rho}_3 + V\hat{\rho}_1)\right]\Delta(i\hat{\rho}_2) & (s=+1) \\ \frac{-1}{Z_{-1}}\left[\omega_n^2 + \xi^2 - \varepsilon^2 + V^2 + \Delta^2 - 2V\xi\hat{\rho}_1 + 2iV\varepsilon\hat{\rho}_2 - 2i\omega_n\varepsilon\hat{\rho}_3\right]\Delta\hat{\rho}_1 & (s=-1) \end{cases}, \tag{B.4}$$

$$Z_{+1} = (\omega_n^2 + \xi^2 - \varepsilon^2 - V^2 + \Delta^2)^2 + 4\omega_n^2(\varepsilon^2 + V^2), \tag{B.5}$$

$$Z_{-1} = (\omega_n^2 + \xi^2 - \varepsilon^2 + V^2 + \Delta^2)^2 - 4(V^2\xi^2 - V^2\varepsilon^2 - \omega_n^2\varepsilon^2). \tag{B.6}$$

$-2i\omega_n\varepsilon\hat{\rho}_3\Delta(i\hat{\rho}_2)$ and $-2i\omega_n V\hat{\rho}_1\Delta(i\hat{\rho}_2)$ in the numerator for $s=+1$ and $-2i\omega_n\varepsilon\hat{\rho}_3\Delta\hat{\rho}_1$ in that for $s=-1$ represent odd-frequency pairing correlations. When the band hybridization is absent (i.e., $V=0$), the Hamiltonian in Eq. (B.1) describes a pure interband pairing state even considering in the basis that diagonalizes the normal state Hamiltonian. The interband pairing does not correspond to odd-frequency Cooper pair because the even-frequency pairing correlations in Eq. (B.4) are also interband pairings.

The authors of Ref. [107] found that the transition from the normal state to the superconducting state described by $\mathcal{H}$ in Eq. (B.1) with $s=+1$ with changing the temperature becomes first-order when the band hybridization V is large enough. The mechanism is explained well by the paramagnetic property of the odd-frequency Cooper pairs induced by V as well as we discussed in this study. Moreover, we can expect the discontinuous transition also occur even when the asymmetry between the two bands ε is increased because an odd-frequency pairing correlation is induced by ε. This expectation is easily confirmed since $\check{H}(\boldsymbol{k})$ in Eq. (B.2) for $s=+1$ is equivalent to the Hamiltonian of a spin-singlet superconductor under Zeeman fields. We obtain the fourth-order coefficient of the GL free-energy $b \propto Y_{\rm inter}(A_0, C_0)$ and the superfluid

density $Q \propto Y_{\rm inter}(A, C)$ with $Y_{\rm inter} = Y|_{\mu_{\rm B}B \to \sqrt{\epsilon^2+V^2}}$ in Eq. (3.65) when we consider a simple band structure $m_{\rm a} = m_{\rm b}$ [67].

Appendix C

A spin-singlet superconductor under spin-dependent potentials

We consider a spatially uniform spin-singlet s-wave superconducting state under spin-dependent potentials. The Gor'kov equation reads,

$$\left[i\omega_n - \check{H}_{\rm BdG}\right] \left[\begin{array}{cc} \mathcal{G} & \mathcal{F} \\ -\underset{\sim}{\mathcal{F}} & -\underset{\sim}{\mathcal{G}} \end{array} \right]_{(\boldsymbol{k},i\omega_n)} = \check{1}, \quad \check{H}_{\rm BdG} = \left[\begin{array}{cc} \hat{H}_{\rm N} & \hat{\Delta} \\ -\underset{\sim}{\hat{\Delta}} & -\underset{\sim}{\hat{H}}_{\rm N} \end{array} \right]. \tag{C.1}$$

The anomalous Green's function is represented as

$$\mathcal{F}(\boldsymbol{k}, i\omega_n) = \left[\hat{\Delta}\,\underset{\sim}{\hat{\Delta}} - \omega_n^2 - \hat{\Delta}\,\underset{\sim}{\hat{H}}_{\rm N}\,\hat{\Delta}^{-1}\,\hat{H}_{\rm N} + i\omega_n\,P\right]^{-1}\hat{\Delta}, \tag{C.2}$$

$$P = (\hat{\Delta}\,\underset{\sim}{\hat{H}}_{\rm N} - \hat{H}_{\rm N}\,\hat{\Delta})\,\hat{\Delta}^{-1}, \quad \hat{\Delta} = \Delta\, i\hat{\sigma}_2, \tag{C.3}$$

where $\hat{\sigma}_{\rm j}$ for ${\rm j} = 1-3$ are Pauli matrices in the spin space. The odd-frequency pairing correlations appear for $P \neq 0$ [14]. The coefficients in the GL free-energy functional are calculated by

$$a\Delta^2 = \frac{\Delta^2}{g} + T\sum_{\omega_n}\frac{1}{V_{\rm vol}}\sum_{\boldsymbol{k}}\frac{1}{2}{\rm Tr}\left[\mathcal{F}_1(\boldsymbol{k}, i\omega_n)\hat{\Delta}^\dagger\right], \tag{C.4}$$

$$b\Delta^4 = T\sum_{\omega_n}\frac{1}{V_{\rm vol}}\sum_{\boldsymbol{k}}\frac{1}{4}{\rm Tr}\left[\mathcal{F}_1(\boldsymbol{k}, i\omega_n)\,\hat{\Delta}^\dagger\,\mathcal{F}_1(\boldsymbol{k}, i\omega_n)\,\hat{\Delta}^\dagger\right]. \tag{C.5}$$

The electric current $\boldsymbol{j}$ within the linear response to a vector potential $\boldsymbol{A}$ is described by [69]

$$\boldsymbol{j} = -\frac{e^2}{mc}\, Q\, \boldsymbol{A}, \tag{C.6}$$

$$Q = n\, T \sum_{\omega_n} \int d\xi \, \langle \mathrm{Tr} \left[\mathcal{G}\, \mathcal{G} - \underset{\sim}{\mathcal{F}}\, \mathcal{F} - \mathcal{G}_{\mathrm{N}}\, \mathcal{G}_{\mathrm{N}} \right]_{(\boldsymbol{k}, \omega_n)} \rangle_{\mathrm{FS}}, \tag{C.7}$$

where n is the electron density per spin and $\langle \cdots \rangle_{\mathrm{FS}} \equiv \int \frac{d\Omega}{4\pi} \cdots$ is the Fermi surface average. Q is referred to as superfluid density.

Firstly, we consider the normal state Hamiltonian including an antisymmetric spin-orbit interaction,

$$\hat{H}_{\mathrm{N}}(\boldsymbol{k}) = \xi_{\boldsymbol{k}} - \boldsymbol{\alpha}_{\boldsymbol{k}} \cdot \hat{\boldsymbol{\sigma}}, \quad \xi_{\boldsymbol{k}} = \frac{\hbar^2 \boldsymbol{k}^2}{2m} - \mu, \quad \boldsymbol{\alpha}_{-\boldsymbol{k}} = -\boldsymbol{\alpha}_{\boldsymbol{k}}. \tag{C.8}$$

The Fermi surface is split into two due to the spin-orbit interaction in the normal state. The Green's functions are calculated to be

$$\mathcal{G}(\boldsymbol{k}, i\omega_n) = -\frac{(i\omega_n + \xi_{\boldsymbol{k}})(\omega_n^2 + \xi_{\boldsymbol{k}}^2 + \Delta^2) + (i\omega_n - \xi_{\boldsymbol{k}})\boldsymbol{\alpha}_{\boldsymbol{k}}^2 + \{(i\omega_n + \xi_{\boldsymbol{k}})^2 - \boldsymbol{\alpha}_{\boldsymbol{k}}^2 - \Delta^2\}\, \boldsymbol{\alpha}_{\boldsymbol{k}} \cdot \hat{\boldsymbol{\sigma}}}{\left\{\omega_n^2 + \xi_{\boldsymbol{k}}^2 + \Delta^2 + \boldsymbol{\alpha}_{\boldsymbol{k}}^2\right\}^2 - 4\xi_{\boldsymbol{k}}^2\, \boldsymbol{\alpha}_{\boldsymbol{k}}^2}, \tag{C.9}$$

$$\mathcal{F}(\boldsymbol{k}, i\omega_n) = -\frac{\omega_n^2 + \xi_{\boldsymbol{k}}^2 + \Delta^2 + \boldsymbol{\alpha}_{\boldsymbol{k}}^2 + 2\, \xi_{\boldsymbol{k}}\, \boldsymbol{\alpha}_{\boldsymbol{k}} \cdot \hat{\boldsymbol{\sigma}}}{\left\{\omega_n^2 + \xi_{\boldsymbol{k}}^2 + \Delta^2 + \boldsymbol{\alpha}_{\boldsymbol{k}}^2\right\}^2 - 4\xi_{\boldsymbol{k}}^2\, \boldsymbol{\alpha}_{\boldsymbol{k}}^2} \Delta\, i\hat{\sigma}_2. \tag{C.10}$$

The last term in the numerator of $\mathcal{F}$ represents the spin-triplet odd-parity pairing correlation induced by the spin-orbit interaction. Since $P = 0$, the odd-frequency component is absent. The gap equation becomes

$$\Delta = g\, T \sum_{\omega_n} \frac{1}{V_{\mathrm{vol}}} \sum_{\boldsymbol{k}} \frac{1}{2} \mathrm{Tr} \left[\mathcal{F}(\boldsymbol{k}, i\omega_n)\, i\hat{\sigma}_2 \right] = g\, N_0 \pi T \sum_{\omega_n} \frac{\Delta}{\sqrt{\omega_n^2 + \Delta^2}}, \tag{C.11}$$

which is identical to that in the BCS theory, where N_0 is the density of states at the Fermi level per spin. It is possible to show that the superfluid density and the

coefficients of the GL free-energy are identical to those in the BCS theory,

$$Q_{\rm BCS} = 2n\pi T \sum_{\omega_n} \frac{\Delta^2}{(\omega_n^2+\Delta^2)^{3/2}}, \tag{C.12}$$

$$a_{\rm BCS} = \frac{1}{g} - N_0 \pi T \sum_{\omega_n} \frac{1}{|\omega_n|}, \tag{C.13}$$

$$b_{\rm BCS} = \frac{N_0\pi}{4} T \sum_{\omega_n} \frac{1}{|\omega_n|^3} = N_0 \frac{7\zeta(3)}{16(\pi T)^2}, \tag{C.14}$$

where $\zeta(n)$ is Riemann zeta function. Therefore, the spin-orbit interactions do not change any thermal properties of a spin-singlet superconductor [90].

Secondly, we consider the normal state Hamiltonian including the Zeeman potential,

$$\hat{H}_{\rm N}(\boldsymbol{k}) = \xi_{\boldsymbol{k}} - \mu_{\rm B} \boldsymbol{B}\cdot\hat{\boldsymbol{\sigma}}, \tag{C.15}$$

where $\mu_{\rm B}$ is Bohr's magneton and $\boldsymbol{B}$ is a Zeeman field. The odd-frequency pairing correlation appears because $P = 2\,\mu_{\rm B}\,\boldsymbol{B}\cdot\hat{\boldsymbol{\sigma}}$ remains finite. The Green's functions are calculated as

$$\begin{aligned}\mathcal{G}(\boldsymbol{k}, i\omega_n) = \frac{-1}{Z_{\rm z}} \big[&(i\omega_n + \xi_{\boldsymbol{k}})(\omega_n^2 + \xi_{\boldsymbol{k}}^2 + \Delta^2) + (i\omega_n - \xi_{\boldsymbol{k}})\mu_{\rm B}^2 B^2 \\ &+ \left\{ (i\omega_n + \xi_{\boldsymbol{k}})^2 + \Delta^2 - \mu_{\rm B}^2 B^2 \right\} \mu_{\rm B} \boldsymbol{B}\cdot\hat{\boldsymbol{\sigma}} \big],\end{aligned} \tag{C.16}$$

$$\mathcal{F}(\boldsymbol{k}, i\omega_n) = \frac{-1}{Z_{\rm z}} \left[\omega_n^2 + \xi_{\boldsymbol{k}}^2 + \Delta^2 - \mu_{\rm B}^2 \boldsymbol{B}^2 + 2i\omega_n\,\mu_{\rm B}\,\boldsymbol{B}\cdot\hat{\boldsymbol{\sigma}} \right] \Delta i\hat{\sigma}_2, \tag{C.17}$$

$$Z_{\rm z} = \xi_{\boldsymbol{k}}^4 + 2\,\xi_{\boldsymbol{k}}^2\,A + C, \quad A = \Delta^2 + \omega_n^2 - \mu_{\rm B}^2 B^2, \quad C = A^2 + 4\omega_n^2\,\mu_{\rm B}^2 B^2. \tag{C.18}$$

The last term in $\mathcal{F}$ represents the pairing correlation belonging to odd-frequency spin-triplet s-wave symmetry class. The gap equation becomes

$$\Delta = g\,N_0 \pi T \sum_{\omega_n} \frac{\Delta\sqrt{A+\sqrt{C}}}{\sqrt{2C}}. \tag{C.19}$$

The self-consistent pair potential $\Delta_{\rm eq}$ not only satisfies Eq. (C.19), but also minimize

the thermodynamic potential. The coefficients in the free-energy result in

$$a = \frac{1}{g} - N_0 \pi T \sum_{\omega_n} \frac{\omega_n^2}{|\omega_n|(\omega_n^2 + \mu_{\rm B}^2 B^2)}, \tag{C.20}$$

$$b = \frac{\sqrt{2}}{4} N_0 \pi T \sum_{\omega_n} \frac{A_0^3 + \sqrt{C_0}(A_0^2 - 2\omega_n^2 \mu_{\rm B}^2 B^2)}{[C_0(A_0 + \sqrt{C_0})]^{3/2}}, \tag{C.21}$$

$$A_0 = A|_{\Delta=0}, \quad C_0 = C|_{\Delta=0}. \tag{C.22}$$

The second term in Eq. (C.20) becomes smaller than that in Eq. (C.13), which leads to the suppression of T_c. The last term in Eq. (C.21) is derived from the odd-frequency pairing correlation function and decreases the coefficient b. The superfluid density is calculated to be

$$Q = 2\sqrt{2} n \pi T \sum_{\omega_n} \frac{\Delta^2 \left\{ A^3 + \sqrt{C}(A^2 - 2\omega_n^2 \mu_{\rm B}^2 B^2) \right\}}{[C(A + \sqrt{C})]^{3/2}}. \tag{C.23}$$

The comparison between the expression of the superfluid density in Eq. (C.23) and that of the coefficient b in Eq. (C.21) shows that the odd-frequency pairing correlation decreases Q and b in exactly the same manner.

Appendix D

Restriction of hopping matrix in tight-binding Hamiltonian

The crystal structure of Bi_2Se_3 preserves discrete symmetries [127, 128] such as threefold rotation R_3 along the z direction, twofold rotation R_2 along the x direction, and inversion P. In addition, both the normal and superconducting states preserve time-reversal T symmetry. With the basis of $(|+,\uparrow\rangle, |-,\uparrow\rangle, |+,\downarrow\rangle, |-,\downarrow\rangle)$, these symmetry operations can be represented as $R_3 = \exp(i\frac{\pi}{3}s_3\sigma_0)$, $R_2 = is_1\sigma_3$, $P = s_0\sigma_3$, and $T = is_2\sigma_0\mathcal{K}$, respectively. Here $\mathcal{K}$ represents the complex conjugation.

Under threefold rotation symmetry, the relation

$$\langle \boldsymbol{R}, \sigma, s| H |\boldsymbol{R} + \boldsymbol{a}_i, \sigma', s'\rangle = \exp\left(i\frac{\pi}{3}(s_3' - s_3)\right) \langle \boldsymbol{R}, \sigma, s| H |\boldsymbol{R} + \boldsymbol{a}_j, \sigma', s'\rangle , \tag{D.1}$$

is satisfied for $(\boldsymbol{a}_i, \boldsymbol{a}_j) = (\boldsymbol{a}_1, -\boldsymbol{a}_2)$, $(\boldsymbol{a}_2, -\boldsymbol{a}_3)$, and $(\boldsymbol{a}_3, \boldsymbol{a}_1)$. Under twofold rotation symmetry, the relation

$$\langle \boldsymbol{R}, \sigma, s| H |\boldsymbol{R} + \boldsymbol{a}_i, \sigma', s'\rangle = \sigma_3'\sigma_3 \langle \boldsymbol{R}, \sigma, \overline{s}| H |\boldsymbol{R} + \boldsymbol{a}_j, \sigma', \overline{s'}\rangle , \tag{D.2}$$

holds true for $(\boldsymbol{a}_i, \boldsymbol{a}_j) = (\boldsymbol{a}_1, -\boldsymbol{a}_3)$, $(\boldsymbol{a}_2, -\boldsymbol{a}_2)$, and $(\boldsymbol{a}_3, -\boldsymbol{a}_1)$. As a results of inversion symmetry, we find the relation of

$$\langle \boldsymbol{R}, \sigma, s| H |\boldsymbol{R} + \boldsymbol{a}_i, \sigma', s'\rangle = \sigma_3'\sigma_3 \langle \boldsymbol{R}, \sigma, s| H |\boldsymbol{R} - \boldsymbol{a}_i, \sigma', s'\rangle . \tag{D.3}$$

Finally, time-reversal symmetry is described as

$$\langle \boldsymbol{R}, \sigma, s| H |\boldsymbol{R} + \boldsymbol{a}_i, \sigma', s'\rangle = s_3's_3 \langle \boldsymbol{R}, \sigma', \overline{s'}| H |\boldsymbol{R} - \boldsymbol{a}_i, \sigma, \overline{s}\rangle . \tag{D.4}$$

We have used the notation of

$$\sigma_3 = \begin{cases} +1 & (\sigma = +) \\ -1 & (\sigma = -) \end{cases}, \quad s_3 = \begin{cases} +1 & (s = \uparrow) \\ -1 & (s = \downarrow) \end{cases}, \tag{D.5}$$

$$\overline{\sigma} = \begin{cases} - & (\sigma = +) \\ + & (\sigma = -) \end{cases}, \quad \overline{s} = \begin{cases} \downarrow & (s = \uparrow) \\ \uparrow & (s = \downarrow) \end{cases}. \tag{D.6}$$

According to the conditions in Eqs. (D.1), (D.2), (D.3), and (D.4), the hopping matrices can be reduced as [129, 131]

$$\check{t}_{\boldsymbol{a}_1} = \begin{pmatrix} t_{11} & t_{12} & 0 & t_{14} \\ -t_{12} & t_{22} & t_{14} & 0 \\ 0 & -t_{14}^* & t_{11} & t_{12} \\ -t_{14}^* & 0 & -t_{12} & t_{22} \end{pmatrix}, \tag{D.7}$$

$$\check{t}_{-\boldsymbol{a}_1} = \begin{pmatrix} t_{11} & -t_{12} & 0 & -t_{14} \\ t_{12} & t_{22} & -t_{14} & 0 \\ 0 & t_{14}^* & t_{11} & -t_{12} \\ t_{14}^* & 0 & t_{12} & t_{22} \end{pmatrix}, \tag{D.8}$$

$$\check{t}_{\boldsymbol{a}_2} = \begin{pmatrix} t_{11} & -t_{12} & 0 & -e^{i2\pi/3}t_{14} \\ t_{12} & t_{22} & -e^{i2\pi/3}t_{14} & 0 \\ 0 & -e^{i2\pi/3}t_{14} & t_{11} & -t_{12} \\ -e^{i2\pi/3}t_{14} & 0 & t_{12} & t_{22} \end{pmatrix}, \tag{D.9}$$

$$\check{t}_{-\boldsymbol{a}_2} = \begin{pmatrix} t_{11} & t_{12} & 0 & e^{i2\pi/3}t_{14} \\ -t_{12} & t_{22} & e^{i2\pi/3}t_{14} & 0 \\ 0 & e^{i2\pi/3}t_{14} & t_{11} & t_{12} \\ e^{i2\pi/3}t_{14} & 0 & -t_{12} & t_{22} \end{pmatrix}, \tag{D.10}$$

$$\check{t}_{\boldsymbol{a}_3} = \begin{pmatrix} t_{11} & t_{12} & 0 & -t_{14}^* \\ -t_{12} & t_{22} & -t_{14}^* & 0 \\ 0 & t_{14} & t_{11} & t_{12} \\ t_{14} & 0 & -t_{12} & t_{22} \end{pmatrix}, \tag{D.11}$$

$$\check{t}_{-\boldsymbol{a}_3} = \begin{pmatrix} t_{11} & -t_{12} & 0 & t_{14}^* \\ t_{12} & t_{22} & t_{14}^* & 0 \\ 0 & -t_{14} & t_{11} & -t_{12} \\ -t_{14} & 0 & t_{12} & t_{22} \end{pmatrix}, \tag{D.12}$$

$$\check{t}_{\boldsymbol{a}_4} = \begin{pmatrix} t'_{11} & t'_{12} & 0 & 0 \\ -t'_{12} & t'_{22} & 0 & 0 \\ 0 & 0 & t'_{11} & t'_{12} \\ 0 & 0 & -t'_{12} & t'_{22} \end{pmatrix}, \tag{D.13}$$

$$\check{t}_{-\boldsymbol{a}_4} = \begin{pmatrix} t'_{11} & -t'_{12} & 0 & 0 \\ t'_{12} & t'_{22} & 0 & 0 \\ 0 & 0 & t'_{11} & -t'_{12} \\ 0 & 0 & t'_{12} & t'_{22} \end{pmatrix}. \tag{D.14}$$

In momentum space, the tight-binding Hamiltonian becomes

$$\check{H}_N(\boldsymbol{k}) = \begin{pmatrix} c+m & -i(v_3\alpha_3 + v_z\alpha_z & 0 & v(\alpha_y + i\alpha_x) \\ i(v_3\alpha_3 + v_z\alpha_z) & c-m & v(\alpha_y + i\alpha_x) & 0 \\ 0 & v(\alpha_y - i\alpha_x) & c+m & -i(v_3\alpha_3 + v_z\alpha_z) \\ v(\alpha_y - i\alpha_x) & 0 & i(v_3\alpha_3 + v_z\alpha_z) & c-m \end{pmatrix}, \tag{D.15}$$

with

$$c_{\boldsymbol{k}} = -\mu + c_1\alpha_1(\boldsymbol{k}) + c_2\alpha_2(\boldsymbol{k}), \tag{D.16}$$

$$m_{\boldsymbol{k}} = m_0 + m_1\alpha_1(\boldsymbol{k}) + m_2\alpha_2(\boldsymbol{k}), \tag{D.17}$$

$$c_1 = -\frac{c^2}{2}(t'_{11} + t'_{22}), \tag{D.18}$$

$$c_2 = -\frac{3a^2}{4}(t_{11} + t_{22}), \tag{D.19}$$

$$\mu = -3(t_{11} + t_{22}) - (t'_{11} + t'_{22}) - \varepsilon, \tag{D.20}$$

$$m_1 = -\frac{c^2}{2}(t'_{11} - t'_{22}), \tag{D.21}$$

$$m_2 = -\frac{3a^2}{4}(t_{11} - t_{22}), \tag{D.22}$$

$$m_0 = 3(t_{11} - t_{22}) + t'_{11} - t'_{22}, \tag{D.23}$$

$$v = -3ie^{i2\pi/3}at_{14}, \tag{D.24}$$

$$v_z = -2ct'_{12}, \tag{D.25}$$

$$v_3 = \frac{3a^3}{4}t_{12}. \tag{D.26}$$

Here $\alpha_1(\boldsymbol{k})$, $\alpha_2(\boldsymbol{k})$, $\alpha_x(\boldsymbol{k})$, $\alpha_y(\boldsymbol{k})$, and $\alpha_z(\boldsymbol{k})$, are defined in Eqs. (4.10)-(4.14). We also define $\alpha_3(\boldsymbol{k}) = -\frac{8}{3a^3}(2\cos\frac{\sqrt{3}}{2}k_xa\sin\frac{1}{2}k_ya - \sin k_ya)$. In this study, we set the parameters as follows [129, 146]: $a = 4.14$ Å, $c = 28.7$ Å, $\mu = 0.5$ eV, $c_2 = 30.4$ eVÅ^2, $m_0 = -0.28$ eV, $m_2 = 44.5$ eVÅ^2, $v = 3.33$ eVÅ, $c_1/c^2 = 0.024$ eV, $m_1/c^2 = 0.20$ eV, and $v_z/c = 0.32$ eV. We choose $v_3 = 0$ for simplicity [127, 128].

Appendix E

Unitary equivalence of the Hamiltonian with intraorbital pairing order

The superconducting state with s-wave spin-singlet intraorbital pairing order is described by a following Bogoliubov-de Gennes Hamiltonian [122].

$$\bar{H}^{(0)}_{\boldsymbol{k}}(\theta,\varphi_1,\varphi_2)=\begin{bmatrix} \xi_1 & -iV_ze^{i\theta} & 0 & Ve^{i\theta} & 0 & 0 & \Delta_+ & 0 \\ iV_ze^{-i\theta} & \xi_2 & Ve^{-i\theta} & 0 & 0 & 0 & 0 & \Delta_- \\ 0 & V^*e^{i\theta} & \xi_1 & -iV_ze^{i\theta} & -\Delta_+ & 0 & 0 & 0 \\ V^*e^{-i\theta} & 0 & iV_ze^{-i\theta} & \xi_2 & 0 & -\Delta_- & 0 & 0 \\ 0 & 0 & -\Delta_+^* & 0 & -\xi_1 & iV_ze^{-i\theta} & 0 & V^*e^{-i\theta} \\ 0 & 0 & 0 & -\Delta_-^* & -iV_ze^{i\theta} & -\xi_2 & V^*e^{i\theta} & 0 \\ \Delta_+^* & 0 & 0 & 0 & 0 & Ve^{-i\theta} & -\xi_1 & iV_ze^{-i\theta} \\ 0 & \Delta_-^* & 0 & 0 & Ve^{i\theta} & 0 & -iV_ze^{i\theta} & -\xi_2 \end{bmatrix}, \tag{E.1}$$

$$\xi_1=c_{\boldsymbol{k}}+m_{\boldsymbol{k}},\quad \xi_2=c_{\boldsymbol{k}}-m_{\boldsymbol{k}},\quad V=v(\alpha_y(\boldsymbol{k})+i\alpha_x(\boldsymbol{k})),\quad V_z=v_z\alpha_z(\boldsymbol{k}), \tag{E.2}$$

$$\Delta_+=\frac{g_+}{N}\sum_{\boldsymbol{k}}\langle\psi_{+,\uparrow}(\boldsymbol{k})\psi_{+,\downarrow}(-\boldsymbol{k})\rangle=|\Delta_+|e^{i\varphi_1}, \tag{E.3}$$

$$\Delta_-=\frac{g_-}{N}\sum_{\boldsymbol{k}}\langle\psi_{-,\uparrow}(\boldsymbol{k})\psi_{-,\downarrow}(-\boldsymbol{k})\rangle=|\Delta_-|e^{i\varphi_2}, \tag{E.4}$$

where $g_\sigma>0$ represents the attractive interaction between two electrons in the orbital σ and θ denotes the phase of the hybridization in the normal state. We obtain the normal part of $\bar{H}^{(0)}_{\boldsymbol{k}}(\theta,\varphi_1,\varphi_2)$ from Eq. (4.5) by choosing $\psi_{+,s}\to\psi_{+,s}e^{i\theta/2}$ and $\psi_{-,s}\to\psi_{-,s}e^{-i\theta/2}$. Although the phase factor $e^{i\theta}$ does not affect the physics in the normal

state, such a gauge transformation affects the relative phase difference between the order parameters $\varphi_1 - \varphi_2$ [122].

Time-reversal symmetry of $\bar{H}^{(0)}_{\boldsymbol{k}}$ is represented by

$$\mathcal{T}\bar{H}^{(0)}_{\boldsymbol{k}}\mathcal{T}^{-1} = \bar{H}^{(0)}_{-\boldsymbol{k}}, \quad \mathcal{T} = \hat{\tau}_0(i\hat{s}_2)\hat{\sigma}_0\mathcal{K}. \tag{E.5}$$

If we find a transformation $\bar{U}$ which eliminates all the phase factors in Eq. (E.1), it is possible to show time-reversal symmetry of $\bar{H}^{(0)}_{\boldsymbol{k}}$ [122]. By applying the unitary transformation,

$$\bar{U} = \mathrm{diag}[e^{-i\varphi_1/2}, e^{-i\varphi_2/2}, e^{-i\varphi_1/2}, e^{-i\varphi_2/2}, e^{i\varphi_1/2}, e^{i\varphi_2/2}, e^{i\varphi_1/2}, e^{i\varphi_2/2}], \tag{E.6}$$

the Hamiltonian is transformed into

$$\bar{U}\bar{H}^{(0)}_{\boldsymbol{k}}(\theta, \varphi_1, \varphi_2)\bar{U}^\dagger = \bar{H}^{(0)}_{\boldsymbol{k}}(\theta - \frac{\varphi_1 - \varphi_2}{2}, 0, 0). \tag{E.7}$$

Therefore, the three phases must satisfy a relation

$$2\theta - \varphi_1 + \varphi_2 = 2\pi n, \tag{E.8}$$

with n being an integer for the Hamiltonian to preserve time-reversal symmetry. By tuning $\theta = 0$ at $n = 0$, the two pair potentials have the same sign with each other because of $\varphi_1 - \varphi_2 = 0$. By tuning $\theta = \pi/2$, on the other hand, $\bar{H}^{(0)}_{\boldsymbol{k}}(\pi/2, 0, \pi)$ describes a state where two pair potentials have the opposite sign to each other. It is easy to show that $\bar{H}^{(0)}_{\boldsymbol{k}}(\pi/2, 0, \pi)$ and $\bar{H}^{(0)}_{\boldsymbol{k}}(0, 0, 0)$ are unitary equivalent to each other. We set $g_+ = g_- = g_1$ and $\Delta_+ = \Delta_- = \Delta_1$ in section 4.3. Under the condition, $\Delta_1(i\hat{s}_2)\hat{\sigma}_3$ is unitary equivalent to $\check{\Delta}_1 = \Delta_1(i\hat{s}_2)\hat{\sigma}_0$.

Bibliography

[1] H. Kamerlingh Onnes, Further experiments with liquid helium. C. On the change of electric resistance of pure metals at very low temperatures, etc. IV. The resistance of pure mercury at helium temperatures, Comm. Phys. Lab. Univ. Leiden **120** (1911).

[2] J. Bardeen, L. N. Cooper, and J. R. Schrieffer, Theory of Superconductivity, Phys. Rev. **108**, 1175 (1957).

[3] W. Meissner and R. Ochsenfeld, Ein neuer Effekt bei Eintritt der Supraleitfähigkeit, Naturwissenschaften **21**, 787 (1933).

[4] C. C. Tsuei and J. R. Kirtley, Pairing symmetry in cuprate superconductors, Rev. Mod. Phys. **72**, 969 (2000).

[5] J. A. Sauls, A theory for the superconducting phases of UPt3, J. Low Temp. Phys. **95**, 153 (1994).

[6] H. Tou, Y. Kitaoka, K. Ishida, K. Asayama, N. Kimura, Y. O¯nuki, E. Yamamoto, Y. Haga, and K. Maezawa, Nonunitary Spin-Triplet Superconductivity in UPt_3: Evidence from ^{195}Pt Knight Shift Study, Phys. Rev. Lett. **80**, 3129 (1998).

[7] M. J. Graf, S.-K. Yip, and J. A. Sauls, Identification of the orbital pairing symmetry in UPt_3, Phys. Rev. B **62**, 14393 (2000).

[8] Y. Machida, A. Itoh, Y. So, K. Izawa, Y. Haga, E. Yamamoto, N. Kimura, Y. Onuki, Y. Tsutsumi, and K. Machida, Twofold Spontaneous Symmetry Breaking in the Heavy-Fermion Superconductor UPt_3, Phys. Rev. Lett. **108**, 157002 (2012).

[9] D. Vollhardt and P. Wölfle, *The Superfluid Phases Of Helium 3* (Taylor & Francis, London, 1990).

[10] V. L. Berezinskii, New model of the anisotropic phase of superfluid He^3, JETP Lett. **20**, 287 (1974).

[11] F. S. Bergeret, A. F. Volkov, and K. B. Efetov, Odd triplet superconductivity and related phenomena in superconductor-ferromagnet structures, Rev. Mod. Phys. **77**, 1321 (2005).

[12] Y. Tanaka, M. Sato, and N. Nagaosa, Symmetry and Topology in Superconductors -Odd-Frequency Pairing and Edge States-, Journal of the Physical Society of Japan **81**, 011013 (2012).

[13] J. Linder and A. V. Balatsky, Odd-frequency superconductivity, Rev. Mod. Phys. **91**, 045005 (2019).

[14] C. Triola, J. Cayao, and A. M. Black-Schaffer, The Role of Odd-Frequency Pairing in Multiband Superconductors, Annalen der Physik **532**, 1900298 (2020), https://onlinelibrary.wiley.com/doi/pdf/10.1002/andp.201900298 .

[15] J. Cayao, C. Triola, and A. M. Black-Schaffer, Odd-frequency superconducting pairing in one-dimensional systems, The European Physical Journal Special Topics **229**, 545 (2020).

[16] Y. Tanuma, N. Hayashi, Y. Tanaka, and A. A. Golubov, Model for Vortex-Core Tunneling Spectroscopy of Chiral p-Wave Superconductors via Odd-Frequency Pairing States, Phys. Rev. Lett. **102**, 117003 (2009).

[17] D. Kuzmanovski, R. S. Souto, and A. V. Balatsky, Odd-frequency superconductivity near a magnetic impurity in a conventional superconductor, Phys. Rev. B **101**, 094505 (2020).

[18] V. Perrin, F. L. N. Santos, G. C. Ménard, C. Brun, T. Cren, M. Civelli, and P. Simon, Unveiling Odd-Frequency Pairing around a Magnetic Impurity in a Superconductor, Phys. Rev. Lett. **125**, 117003 (2020).

[19] Y. Tanaka and A. A. Golubov, Theory of the Proximity Effect in Junctions with Unconventional Superconductors, Phys. Rev. Lett. **98**, 037003 (2007).

[20] Y. Asano and Y. Tanaka, Majorana fermions and odd-frequency Cooper pairs in a normal-metal nanowire proximity-coupled to a topological superconductor, Phys. Rev. B **87**, 104513 (2013).

[21] Y. Asano, A. A. Golubov, Y. V. Fominov, and Y. Tanaka, Unconventional Surface Impedance of a Normal-Metal Film Covering a Spin-Triplet Superconductor Due to Odd-Frequency Cooper Pairs, Phys. Rev. Lett. **107**, 087001 (2011).

[22] F. S. Bergeret, A. F. Volkov, and K. B. Efetov, Long-Range Proximity Effects in Superconductor-Ferromagnet Structures, Phys. Rev. Lett. **86**, 4096 (2001).

[23] Y. Tanaka and S. Kashiwaya, Anomalous charge transport in triplet superconductor junctions, Phys. Rev. B **70**, 012507 (2004).

[24] R. Heid, On the thermodynamic stability of odd-frequency superconductors, Z. Phys. B - Condensed Matter **99**, 15 (1995).

[25] Y. Asano, Y. V. Fominov, and Y. Tanaka, Consequences of bulk odd-frequency superconducting states for the classification of Cooper pairs, Phys. Rev. B **90**, 094512 (2014).

[26] Y. V. Fominov, Y. Tanaka, Y. Asano, and M. Eschrig, Odd-frequency superconducting states with different types of Meissner response: Problem of coexistence, Phys. Rev. B **91**, 144514 (2015).

[27] A. Balatsky and E. Abrahams, New class of singlet superconductors which break the time reversal and parity, Phys. Rev. B **45**, 13125 (1992).

[28] V. J. Emery and S. Kivelson, Mapping of the two-channel Kondo problem to a resonant-level model, Phys. Rev. B **46**, 10812 (1992).

[29] V. J. Emery and S. A. Kivelson, Solution of an orbital Kondo array, Phys. Rev. Lett. **71**, 3701 (1993).

[30] M. Vojta and E. Dagotto, Indications of unconventional superconductivity in doped and undoped triangular antiferromagnets, Phys. Rev. B **59**, R713 (1999).

[31] P. Coleman, E. Miranda, and A. Tsvelik, Possible realization of odd-frequency pairing in heavy fermion compounds, Phys. Rev. Lett. **70**, 2960 (1993).

[32] O. Zachar, S. A. Kivelson, and V. J. Emery, Exact Results for a 1D Kondo Lattice from Bosonization, Phys. Rev. Lett. **77**, 1342 (1996).

[33] P. Coleman, A. Georges, and A. M. Tsvelik, Reflections on the one-dimensional realization of odd-frequency pairing, Journal of Physics: Condensed Matter **9**, 345 (1997).

[34] F. B. Anders, Composite spin and orbital triplet superconductivity formed out of a non-Fermi-liquid phase, Phys. Rev. B **66**, 020504 (2002).

[35] R. Flint, A. H. Nevidomskyy, and P. Coleman, Composite pairing in a mixed-valent two-channel Anderson model, Phys. Rev. B **84**, 064514 (2011).

[36] Y. Fuseya, H. Kohno, and K. Miyake, Realization of Odd-Frequency p-Wave Spin-Singlet Superconductivity Coexisting with Antiferromagnetic Order near Quantum Critical Point, Journal of the Physical Society of Japan **72**, 2914 (2003), https://doi.org/10.1143/JPSJ.72.2914 .

[37] T. Hotta, Double-Exchange Ferromagnetism and Orbital-Fluctuation-Induced Superconductivity in Cubic Uranium Compounds, Journal of the Physical Society of Japan **78**, 123710 (2009), https://doi.org/10.1143/JPSJ.78.123710 .

[38] J. Otsuki, Competing d-Wave and p-Wave Spin-Singlet Superconductivities in the Two-Dimensional Kondo Lattice, Phys. Rev. Lett. **115**, 036404 (2015).

[39] K. Shigeta, S. Onari, K. Yada, and Y. Tanaka, Theory of odd-frequency pairings on a quasi-one-dimensional lattice in the Hubbard model, Phys. Rev. B **79**, 174507 (2009).

[40] K. Shigeta, Y. Tanaka, K. Kuroki, S. Onari, and H. Aizawa, Competition of pairing symmetries and a mechanism for Berezinskii pairing in quasi-one-dimensional systems, Phys. Rev. B **83**, 140509 (2011).

[41] Y. Yanagi, Y. Yamashita, and K. Ueda, Dimensional Reduction and Odd-Frequency Pairing of the Checkerboard-Lattice Hubbard Model at 1/4-Filling, Journal of the Physical Society of Japan **81**, 123701 (2012), https://doi.org/10.1143/JPSJ.81.123701 .

[42] K. Shigeta, S. Onari, and Y. Tanaka, Possible Odd-Frequency Pairing in Quasi-One-Dimensional Organic Superconductors (TMTSF)2X, Journal of the Physical Society of Japan **82**, 104702 (2013), https://doi.org/10.7566/JPSJ.82.104702 .

[43] T. R. Kirkpatrick and D. Belitz, Disorder-induced triplet superconductivity, Phys. Rev. Lett. **66**, 1533 (1991).

[44] D. Belitz and T. R. Kirkpatrick, Even-parity spin-triplet superconductivity in disordered electronic systems, Phys. Rev. B **46**, 8393 (1992).

[45] E. Abrahams, A. Balatsky, J. R. Schrieffer, and P. B. Allen, Interactions for odd-ω-gap singlet superconductors, Phys. Rev. B **47**, 513 (1993).

[46] E. Abrahams, A. Balatsky, D. J. Scalapino, and J. R. Schrieffer, Properties of odd-gap superconductors, Phys. Rev. B **52**, 1271 (1995).

[47] A. M. Black-Schaffer and A. V. Balatsky, Proximity-induced unconventional superconductivity in topological insulators, Phys. Rev. B **87**, 220506 (2013).

[48] A. M. Black-Schaffer and A. V. Balatsky, Odd-frequency superconducting pairing in multiband superconductors, Phys. Rev. B **88**, 104514 (2013).

[49] J. Nagamatsu, N. Nakagawa, T. Muranaka, Y. Zenitani, and J. Akimitsu, Nature (London) **410**, 63 (2001).

[50] H. J. Choi, D. Roundy, H. Sun, M. L. Cohen, and S. G. Louie, Nature (London) **418**, 758 (2002).

[51] V. Moshchalkov, M. Menghini, T. Nishio, Q. H. Chen, A. V. Silhanek, V. H. Dao, L. F. Chibotaru, N. D. Zhigadlo, and J. Karpinski, Type-1.5 Superconductivity, Phys. Rev. Lett. **102**, 117001 (2009).

[52] P. M. C. Rourke, M. A. Tanatar, C. S. Turel, J. Berdeklis, C. Petrovic, and J. Y. T. Wei, Spectroscopic Evidence for Multiple Order Parameter Components in the Heavy Fermion Superconductor $CeCoIn_5$, Phys. Rev. Lett. **94**, 107005 (2005).

[53] G. Seyfarth, J. P. Brison, M.-A. Méasson, J. Flouquet, K. Izawa, Y. Matsuda, H. Sugawara, and H. Sato, Multiband Superconductivity in the Heavy Fermion Compound $PrOs_4Sb_{12}$, Phys. Rev. Lett. **95**, 107004 (2005).

[54] Y. Kamihara, T. Watanabe, M. Hirano, and H. Hosono, J. Am. Chem. Soc. **130**, 3296 (2008).

[55] G. R. Stewart, Superconductivity in iron compounds, Rev. Mod. Phys. **83**, 1589 (2011).

[56] Y. S. Hor, A. J. Williams, J. G. Checkelsky, P. Roushan, J. Seo, Q. Xu, H. W. Zandbergen, A. Yazdani, N. P. Ong, and R. J. Cava, Superconductivity in $Cu_xBi_2Se_3$ and its Implications for Pairing in the Undoped Topological Insulator, Phys. Rev. Lett. **104**, 057001 (2010).

[57] L. Fu and E. Berg, Odd-Parity Topological Superconductors: Theory and Application to $Cu_xBi_2Se_3$, Phys. Rev. Lett. **105**, 097001 (2010).

[58] A. Ramires and M. Sigrist, Identifying detrimental effects for multiorbital superconductivity: Application to Sr_2RuO_4, Phys. Rev. B **94**, 104501 (2016).

[59] A. Ramires, D. F. Agterberg, and M. Sigrist, Tailoring T_c by symmetry principles: The concept of superconducting fitness, Phys. Rev. B **98**, 024501 (2018).

[60] N. N. Bogoliubov, Sov. Phys. JETP **7**, 41 (1958).

[61] N. N. Bogoliubov, Sov. Phys. JETP **7**, 51 (1958).

[62] G. Volovik, Zeroes in the energy gap in superconductors with high transition temperature, Physics Letters A **142**, 282 (1989).

[63] D. F. Agterberg, P. M. R. Brydon, and C. Timm, Bogoliubov Fermi Surfaces in Superconductors with Broken Time-Reversal Symmetry, Phys. Rev. Lett. **118**, 127001 (2017).

[64] P. M. R. Brydon, D. F. Agterberg, H. Menke, and C. Timm, Bogoliubov Fermi surfaces: General theory, magnetic order, and topology, Phys. Rev. B **98**, 224509 (2018).

[65] D. Kim, S. Kobayashi, and Y. Asano, Quasiparticle on Bogoliubov Fermi Surface and Odd-Frequency Cooper Pair, Journal of the Physical Society of Japan **90**, 104708 (2021).

[66] P. Dutta, F. Parhizgar, and A. M. Black-Schaffer, Superconductivity in spin-3/2 systems: Symmetry classification, odd-frequency pairs, and Bogoliubov Fermi surfaces, Phys. Rev. Res. **3**, 033255 (2021).

[67] Y. Asano and A. Sasaki, Odd-frequency Cooper pairs in two-band superconductors and their magnetic response, Phys. Rev. B **92**, 224508 (2015).

[68] M. Tinkham, *Introduction to Superconductivity* (McGraw-Hill, New York, 1996).

[69] A. A. Abrikosov, L. P. Gor'kov, and I. E. Dzyaloshinski, *Methods of Quantum Field Theory in Statistical Physics* (Dover Publications, New York, 1975).

[70] H. Menke, C. Timm, and P. M. R. Brydon, Bogoliubov Fermi surfaces stabilized by spin-orbit coupling, Phys. Rev. B **100**, 224505 (2019).

[71] M. M. Korshunov, Y. N. Togushova, and O. V. Dolgov, Impurities in multiband superconductors, Physics-Uspekhi **59**, 1211 (2016).

[72] G. D. Mahan, *Many-Particle Physics* (Plenum Press, New York, 1990).

[73] A. L. Fetter and J. D. Walecka, *Quantum Theory of Many-Particle Systems* (McGraw-Hill, New York, 1971).

[74] L. J. Buchholtz and G. Zwicknagl, Identification of p-wave superconductors, Phys. Rev. B **23**, 5788 (1981).

[75] J. Hara and K. Nagai, A Polar State in a Slab as a Soluble Model of p-Wave Fermi Superfluid in Finite Geometry, Progress of Theoretical Physics **76**, 1237 (1986).

[76] C.-R. Hu, Midgap surface states as a novel signature for d_{xa}^2-x_b^2-wave superconductivity, Phys. Rev. Lett. **72**, 1526 (1994).

[77] Y. Tanaka and S. Kashiwaya, Theory of Tunneling Spectroscopy of d-Wave Superconductors, Phys. Rev. Lett. **74**, 3451 (1995).

[78] T. Yokoyama, Y. Tanaka, and A. A. Golubov, Theory of pairing symmetry inside the Abrikosov vortex core, Phys. Rev. B **78**, 012508 (2008).

[79] S.-I. Suzuki, T. Sato, and Y. Asano, Odd-frequency Cooper pair around a magnetic impurity, Phys. Rev. B **106**, 104518 (2022).

[80] S.-I. Suzuki, T. Sato, A. A. Golubov, and Y. Asano, Fulde-Ferrell-Larkin-Ovchinnikov state in a superconducting thin film attached to a ferromagnetic cluster, Phys. Rev. B **108**, 064509 (2023).

[81] Y. Tanaka, Y. Asano, A. A. Golubov, and S. Kashiwaya, Anomalous features of the proximity effect in triplet superconductors, Phys. Rev. B **72**, 140503 (2005).

[82] S.-I. Suzuki and Y. Asano, Paramagnetic instability of small topological superconductors, Phys. Rev. B **89**, 184508 (2014).

[83] S. Higashitani, Odd-frequency pairing effect on the superfluid density and the Pauli spin susceptibility in spatially nonuniform spin-singlet superconductors, Phys. Rev. B **89**, 184505 (2014).

[84] N. Schopohl, Transformation of the Eilenberger Equations of Superconductivity to a Scalar Riccati Equation, arXiv:cond-mat , 9804064 (1998).

[85] S. Higashitani, Mechanism of Paramagnetic Meissner Effect in High-Temperature Superconductors, Journal of the Physical Society of Japan **66**, 2556 (1997).

[86] H. Walter, W. Prusseit, R. Semerad, H. Kinder, W. Assmann, H. Huber, H. Burkhardt, D. Rainer, and J. A. Sauls, Low-Temperature Anomaly in the Penetration Depth of $YBa_2Cu_3O_7$ Films: Evidence for Andreev Bound States at Surfaces, Phys. Rev. Lett. **80**, 3598 (1998).

[87] S.-I. Suzuki and Y. Asano, Effects of surface roughness on the paramagnetic response of small unconventional superconductors, Phys. Rev. B **91**, 214510 (2015).

[88] J. Schmidt, F. Parhizgar, and A. M. Black-Schaffer, Odd-frequency superconductivity and Meissner effect in the doped topological insulator Bi_2Se_3, Phys. Rev. B **101**, 180512(R) (2020).

[89] F. Parhizgar and A. M. Black-Schaffer, Diamagnetic and paramagnetic Meissner effect from odd-frequency pairing in multiorbital superconductors, Phys. Rev. B **104**, 054507 (2021).

[90] P. A. Frigeri, D. F. Agterberg, A. Koga, and M. Sigrist, Superconductivity without Inversion Symmetry: MnSi versus $CePt_3Si$, Phys. Rev. Lett. **92**, 097001 (2004).

[91] G. Sarma, On the influence of a uniform exchange field acting on the spins of the conduction electrons in a superconductor, Journal of Physics and Chemistry of Solids **24**, 1029 (1963).

[92] K. Maki and T. Tsuneto, Pauli Paramagnetism and Superconducting State, Progress of Theoretical Physics **31**, 945 (1964), https://academic.oup.com/ptp/article-pdf/31/6/945/5271369/31-6-945.pdf
.

[93] A. Bianchi, R. Movshovich, N. Oeschler, P. Gegenwart, F. Steglich, J. D. Thompson, P. G. Pagliuso, and J. L. Sarrao, First-Order Superconducting Phase Transition in $CeCoIn_5$, Phys. Rev. Lett. **89**, 137002 (2002).

[94] H. A. Radovan, N. A. Fortune, T. P. Murphy, S. T. Hannahs, E. C. Palm, S. W. Tozer, and D. Hall, Magnetic enhancement of superconductivity from electron spin domains, Nature **425**, 51 (2003).

[95] R. Lortz, Y. Wang, A. Demuer, P. H. M. Böttger, B. Bergk, G. Zwicknagl, Y. Nakazawa, and J. Wosnitza, Calorimetric Evidence for a Fulde-Ferrell-Larkin-Ovchinnikov Superconducting State in the Layered Organic Superconductor $\kappa-(\mathrm{BEDT-TTF})_2\mathrm{Cu(NCS)}_2$, Phys. Rev. Lett. **99**, 187002 (2007).

[96] D. C. Cavanagh, D. F. Agterberg, and P. M. R. Brydon, Pair breaking in superconductors with strong spin-orbit coupling, Phys. Rev. B **107**, L060504 (2023).

[97] J. M. Luttinger and W. Kohn, Motion of Electrons and Holes in Perturbed Periodic Fields, Phys. Rev. **97**, 869 (1955).

[98] P. M. R. Brydon, L. Wang, M. Weinert, and D. F. Agterberg, Pairing of $j = 3/2$ Fermions in Half-Heusler Superconductors, Phys. Rev. Lett. **116**, 177001 (2016).

[99] B. Roy, S. A. A. Ghorashi, M. S. Foster, and A. H. Nevidomskyy, Topological superconductivity of spin-3/2 carriers in a three-dimensional doped Luttinger semimetal, Phys. Rev. B **99**, 054505 (2019).

[100] G. Eilenberger, General approximation method for the free energy functional of superconducting alloys, Zeitschrift für Physik **190**, 142 (1966).

[101] H. G. Suh, H. Menke, P. M. R. Brydon, C. Timm, A. Ramires, and D. F. Agterberg, Stabilizing even-parity chiral superconductivity in Sr_2RuO_4 , Phys. Rev. Res. **2**, 032023(R) (2020).

[102] D. Kim, S. Kobayashi, and Y. Asano, Josephson effect of superconductors with $J = \frac{3}{2}$ electrons, Phys. Rev. B **103**, 184516 (2021).

[103] D. Kim, T. Sato, S. Kobayashi, and Y. Asano, Spin Susceptibility of a J = 3/2 Superconductor, Journal of the Physical Society of Japan **92**, 054703 (2023), https://doi.org/10.7566/JPSJ.92.054703 .

[104] M. Sigrist and K. Ueda, Phenomenological theory of unconventional superconductivity, Rev. Mod. Phys. **63**, 239 (1991).

[105] A. Sasaki, S. Ikegaya, T. Habe, A. A. Golubov, and Y. Asano, Josephson effect in two-band superconductors, Phys. Rev. B **101**, 184501 (2020).

[106] A. Bhattacharya and C. Timm, Stability of Bogoliubov Fermi surfaces within BCS theory, Phys. Rev. B **107**, L220501 (2023).

[107] M. Gomes da Silva, F. Dinóla Neto, I. Padilha, J. Ricardo de Sousa, and M. Continentino, First-order superconducting transition in the inter-band model, Physics Letters A **378**, 1396 (2014).

[108] B. S. Chandrasekhar, A NOTE ON THE MAXIMUM CRITICAL FIELD OF HIGH - FIELD SUPERCONDUCTORS, Applied Physics Letters **1**, 7 (1962), https://doi.org/10.1063/1.1777362 .

[109] A. M. Clogston, Upper Limit for the Critical Field in Hard Superconductors, Phys. Rev. Lett. **9**, 266 (1962).

[110] P. Fulde and R. A. Ferrell, Superconductivity in a Strong Spin-Exchange Field, Phys. Rev. **135**, A550 (1964).

[111] A. I. Larkin and Y. N. Ovchinnikov, Sov. Phys. JETP **20**, 762 (1965).

[112] Y. Matsuda and H. Shimahara, Fulde-Ferrell-Larkin-Ovchinnikov State in Heavy Fermion Superconductors, Journal of the Physical Society of Japan **76**, 051005 (2007), https://doi.org/10.1143/JPSJ.76.051005 .

[113] H. Burkhardt and D. Rainer, Fulde-Ferrell-Larkin-Ovchinnikov state in layered superconductors, Annalen der Physik **506**, 181 (1994).

[114] S. Matsuo, S. Higashitani, Y. Nagato, and K. Nagai, Phase Diagram of the Fulde-Ferrell-Larkin-Ovchinnikov State in a Three-Dimensional Superconductor, Journal of the Physical Society of Japan **67**, 280 (1998).

[115] D. Chakraborty and A. M. Black-Schaffer, Interplay of finite-energy and finite-momentum superconducting pairing, Phys. Rev. B **106**, 024511 (2022).

[116] A. A. Abrikosov and L. P. Gor'kov, Superconducting alloys at finite temperatures, Sov. Phys. JETP **9**, 220 (1959).

[117] P. Anderson, Theory of dirty superconductors, Journal of Physics and Chemistry of Solids **11**, 26 (1959).

[118] Y. Sun and K. Maki, Impurity effects in d-wave superconductors, Phys. Rev. B **51**, 6059 (1995).

[119] P. B. Allen and B. Mitrovic, Theory of superconducting tc (Academic Press, 1983) pp. 1 – 92.

[120] A. A. Golubov and I. I. Mazin, Effect of magnetic and nonmagnetic impurities on highly anisotropic superconductivity, Phys. Rev. B **55**, 15146 (1997).

[121] D. V. Efremov, M. M. Korshunov, O. V. Dolgov, A. A. Golubov, and P. J. Hirschfeld, Disorder-induced transition between $s_{\pm}$ and s_{++} states in two-band superconductors, Phys. Rev. B **84**, 180512(R) (2011).

[122] Y. Asano and A. A. Golubov, Green's-function theory of dirty two-band superconductivity, Phys. Rev. B **97**, 214508 (2018).

[123] Y. Asano, A. Sasaki, and A. A. Golubov, Dirty two-band superconductivity with interband pairing order, New Journal of Physics **20**, 043020 (2018).

[124] K. Kuroki, S. Onari, R. Arita, H. Usui, Y. Tanaka, H. Kontani, and H. Aoki, Unconventional Pairing Originating from the Disconnected Fermi Surfaces of Superconducting $LaFeAsO_{1-x}F_x$, Phys. Rev. Lett. **101**, 087004 (2008).

[125] S. Onari and H. Kontani, Violation of Anderson's Theorem for the Sign-Reversing s-Wave State of Iron-Pnictide Superconductors, Phys. Rev. Lett. **103**, 177001 (2009).

[126] S. Sasaki, M. Kriener, K. Segawa, K. Yada, Y. Tanaka, M. Sato, and Y. Ando, Topological Superconductivity in $Cu_xBi_2Se_3$, Phys. Rev. Lett. **107**, 217001 (2011).

[127] H. Zhang, C.-X. Liu, X.-L. Qi, X. Dai, Z. Fang, and S.-C. Zhang, Topological insulators in Bi2Se3, Bi2Te3 and Sb2Te3 with a single Dirac cone on the surface, Nat. Phys. **5**, 438 (2009).

[128] C.-X. Liu, X.-L. Qi, H. J. Zhang, X. Dai, Z. Fang, and S.-C. Zhang, Model Hamiltonian for topological insulators, Phys. Rev. B **82**, 045122 (2010).

[129] T. Hashimoto, K. Yada, A. Yamakage, M. Sato, and Y. Tanaka, Bulk Electronic State of Superconducting Topological Insulator, J. Phys. Soc. Jpn. **82**, 044704 (2013).

[130] L. A. Wray, S.-Y. Xu, Y. Xia, Y. S. Hor, D. Qian, A. V. Fedorov, H. Lin, A. Bansil, R. J. Cava, and M. Z. Hasan, Observation of topological order in a superconducting doped topological insulator, Nat. Phys. **6**, 855 (2010).

[131] S. Mao, A. Yamakage, and Y. Kuramoto, Tight-binding model for topological insulators: Analysis of helical surface modes over the whole Brillouin zone, Phys. Rev. B **84**, 115413 (2011).

[132] A. J. Leggett, Number-Phase Fluctuations in Two-Band Superconductors, Progress of Theoretical Physics **36**, 901 (1966).

[133] K. Matano, M. Kriener, K. Segawa, Y. Ando, and G.-q. Zheng, Spin-rotation symmetry breaking in the superconducting state of CuxBi2Se3, Nat. Phys. **12**, 852 (2016).

[134] S. Yonezawa, K. Tajiri, S. Nakata, Y. Nagai, Z. Wang, K. Segawa, Y. Ando, and Y. Maeno, Thermodynamic evidence for nematic superconductivity in CuxBi2Se3, Nat. Phys. **13**, 123 (2017).

[135] R. Tao, Y.-J. Yan, X. Liu, Z.-W. Wang, Y. Ando, Q.-H. Wang, T. Zhang, and D.-L. Feng, Direct Visualization of the Nematic Superconductivity in $Cu_xBi_2Se_3$, Phys. Rev. X **8**, 041024 (2018).

[136] L. Fu, Odd-parity topological superconductor with nematic order: Application to $Cu_xBi_2Se_3$, Phys. Rev. B **90**, 100509(R) (2014).

[137] D. C. Cavanagh and P. M. R. Brydon, Robustness of unconventional s-wave superconducting states against disorder, Phys. Rev. B **101**, 054509 (2020).

[138] K. Michaeli and L. Fu, Spin-Orbit Locking as a Protection Mechanism of the Odd-Parity Superconducting State against Disorder, Phys. Rev. Lett. **109**, 187003 (2012).

[139] Y. Nagai, Robust superconductivity with nodes in the superconducting topological insulator $Cu_xBi_2Se_3$: Zeeman orbital field and nonmagnetic impurities, Phys. Rev. B **91**, 060502(R) (2015).

[140] L. Andersen, A. Ramires, Z. Wang, T. Lorenz, and Y. Ando, Generalized Anderson ' s theorem for superconductors derived from topological insulators, Sci. Adv. **6**, eaay6502 (2020).

[141] R. Peierls, Zur Theorie des Diamagnetismus von Leitungselektronen., Z. Physik **80**, 763 (1933).

[142] J. M. Luttinger, The Effect of a Magnetic Field on Electrons in a Periodic Potential, Phys. Rev. **84**, 814 (1951).

[143] D. J. Scalapino, S. R. White, and S. C. Zhang, Superfluid density and the Drude weight of the Hubbard model, Phys. Rev. Lett. **68**, 2830 (1992).

[144] D. J. Scalapino, S. R. White, and S. Zhang, Insulator, metal, or superconductor: The criteria, Phys. Rev. B **47**, 7995 (1993).

[145] T. Kostyrko, R. Micnas, and K. A. Chao, Gauge-invariant theory of the Meissner effect in the lattice model of a superconductor with local pairing, Phys. Rev. B **49**, 6158 (1994).

[146] T. Mizushima, A. Yamakage, M. Sato, and Y. Tanaka, Dirac-fermion-induced parity mixing in superconducting topological insulators, Phys. Rev. B **90**, 184516 (2014).